

**Impact of Atmospheric Cycling on the Release of Iron and Manganese  
into Seawater from Saharan Soil Particles**

Alexandra Xylouri

Submitted in accordance with the requirements for the degree of  
Doctor of Philosophy

The University of Leeds  
School of Earth and Environment

October, 2009

The candidate confirms that the work submitted is his/her own and that appropriate credit has been given where reference has been made to the work of others.

This copy has been supplied on the understanding that it is copyright material and that no quotation from the thesis may be published without proper acknowledgement.

# ***BIOTRACS***

***Bio-transformations of trace elements in  
aquatic systems***



***THIS THESIS WAS COMPLETED USING FRAMEWORK 6  
FUNDING FROM THE EUROPEAN UNION.***

***RESEARCH DG HUMAN RESOURCES AND MOBILITY  
PROJECT NO: 514262***

To Kate, Panos and my family,

*“Wisdom is, knowing how little we know”  
Socrates*

## Acknowledgements

*My journey began when I was given the opportunity back in 2005 by Professor Mike D. Krom, Professor Peter J. Statham and Professor Liane G. Benning, to come over to a very different country than the one I grew up. And it was a beautiful journey indeed, full of experiences, memories and hard times. So how can I not be extremely grateful to Mike Krom, who with his intense and rigorous efforts helped me become an independent researcher. His continuous guidance and pressure helped me progress and provide serious work. I also would like to thank Professor Peter Statham not only because he was always there to help me with my work, or for all the endless discussions on my subject that helped me expand my view, but more importantly for the moral support that I needed when I was ready to give up that encouraged me to keep going.*

*Professor Liane Benning was someone who just had answer to all my questions and at the same time made me ask myself twice as many. She used the ‘Socrates’ method, asking you so many questions and pressuring you so that in the end you would find the answer, a really amazing experience.*

*The best and most exciting time during my PhD was my participation in the SOLAS Cruise D326 and I really have to thank Professor Eric Achterberg for that but also for reminding me that science is also fun. During that cruise there is not a person I can not thank either researcher or member of the crew because without them it would have been impossible to make it through. However special thanks have to go to Dr Micha Rijkenberg for all the help with the Fe analysis and for all our discussions that made time in the container quite bearable. I also would like to thank Dr Duncan Purdie, Dr Claire Mahaffey, Dr Mark Moore for letting me part of their team in the Bioassays Experiments and providing me with their results.*

*I would also like to thank everyone who helped during my long hours in the laboratory either by showing something or just coming to greet me like Matt Patey, Sergio Balzano, Sebastian Steigenberger, Helen Planquette, Dave Hattfield, Vu Hong Phuc and Mike Ward who helped me with the FEGTEM and probably others that I am forgetting.*

*Special thanks to my dear friend Loredana Brinza who helped me so much in many levels of my life, career and personal.*

*I also want to thank my angel Dr Kate Furneax who is not with us today but managed in her short time on earth to change my life for ever.*

*Lastly I must thank my family. They gave me everything and more importantly freedom and support to follow my dreams. And I need to thank my partner, Panos, who never lost faith in me and made me believe in myself.*

## Abstract

Atmospheric transported dust is a major source of iron, manganese and other nutrients to the ocean. During atmospheric transport, dust containing iron and manganese undergoes cloud processes that can increase the reactivity and solubility of iron and manganese species when they enter into seawater.

Saharan sieved soils were artificially atmospherically weathered with different low pH treatments, using simple dilute acids and also cycling through a typical cloud pH range. Formation of nano-particulate iron (ferrihydrite) occurred, and was identified using high-resolution microscopy, together with a measured increase in the fraction of amorphous iron species that were leachable from the processed soil. Both treated and untreated soils were then mixed with filtered stored North Atlantic seawater in the laboratory and also with freshly collected seawater from the NE Atlantic whilst at sea. Initial release of iron from artificially treated Niger soil reached 6 nM and from artificially treated Niger Mali soil reached 3.5-10 nM (depending on the different experimental variables). This was significantly greater than from un-weathered particles ~1-1.5 nM at the soil concentrations used (10 mg).

For Mn all the dissolvable metal was removed during the cloud pH cycling and was not retained on the particles due to slower oxidation and scavenging than with the Fe. However, significantly more manganese ~ 60 nM from acid treated Mali soil and ~30 nM from acid treated Niger soil was released into seawater compared to the manganese released from the untreated soil (30 nM and 22 nM for Mali and Niger soil respectively). Low pH soil treatment led to increased release of Mn in the cloud water that stayed in solution for at least 5 days. This cloud-released Mn will therefore enter the ocean surface in a soluble form.

These data show the major impact of atmospheric processing on dissolution of Fe and particularly Mn from Saharan sieved soils that are transported through the troposphere to the surface ocean.

## Contents

<b>Acknowledgements</b> .....	iii
<b>Abstract</b> .....	v
<b>Contents</b> .....	vi
<b>Figures</b> .....	viii
<b>Tables</b> .....	xii
<b>Chapter 1</b> .....	1
Introduction .....	1
1.1 Iron and Manganese in the Ocean .....	1
1.2 Aims and Objectives .....	22
<b>Chapter 2</b> .....	24
Methods .....	24
2.0 Introduction .....	24
2.1 Sample Preparation .....	24
2.2 Atmospheric Processing Simulation .....	25
2.2.1 The Spokes and Jickells Approach .....	26
2.2.2 Acid Treatment .....	27
2.3 Seawater Dissolution Experiments .....	28
2.3.0 Cleaning Bottles Procedures .....	28
2.3.1 Seawater Dissolution Experiments in the Laboratory .....	28
2.3.2 Seawater Dissolution Experiments on Aboard Ship .....	29
2.4 Iron Analysis .....	32
2.4.1 Laboratory Incubations .....	33
2.4.2 Shipboard Incubations .....	35
2.5 Manganese Analysis .....	38
2.6 Iron and Manganese Extractions .....	40
2.7 Field Emission Gun Scanning Electron Microscopy FEGSEM .....	41
2.8 Field Emission Gun Transmission Electron Microscopy FEGTEM .....	42
2.9 X-ray Diffraction Analysis (XRD) .....	43
<b>Chapter 3</b> .....	44
Particulate Iron and Manganese .....	44
3.1 Introduction .....	44
3.2 Atmospheric Processes .....	47
3.2.1 Assessment of processes .....	48
3.3 Iron Sequential Leaches .....	54
3.4 Manganese Sequential Leaches .....	58
3.5 Microscopy .....	61
3.5.1 XRD Data .....	61
3.5.2 Electron Microscopy .....	63
3.6 Conclusions .....	70
<b>Chapter 4</b> .....	71
Dissolution Experiments with Saharan soil .....	71
4.1 Introduction .....	71
4.2 Results .....	73
4.2.1 <i>Iron</i> .....	73

4.2.2	<i>Manganese</i> .....	78
4.3	Discussion .....	82
	<i>Iron</i> .....	82
4.3.1	Comparison of Mali and Niger Soil .....	85
4.3.2	Comparison of Laboratory and Aboard Incubations .....	86
4.3.3	Comparison with Other Studies .....	86
4.3.4	Ligands .....	88
4.3.5	Carbonate.....	90
4.3.6	Removal of Iron from Solution .....	91
4.3.7	Implications for cloud processing .....	94
	<i>Manganese</i> .....	95
4.4	Conclusions .....	98
Chapter 5	.....	101
Bioassays	.....	101
5.1	Introduction .....	101
5.2	Description of the Bioassay Experiments .....	102
5.3	Results .....	105
5.3.1	Chlorophyll A.....	105
5.3.2	Alkaline Phosphatase Activity .....	107
5.4	Discussion .....	109
Chapter 6	.....	112
Conclusions	.....	112
<b>Bibliography</b>	.....	116

## Figures

Figure 1.1 Schematic model illustrating the biochemical processes of phytoplankton. The schematic is given only as a guide to the importance of Fe to organisms (Shi et al., 2007).....	2
Figure 1.2 Typical profile of dissolved iron in the North Pacific (data replotted from Moss Landing Marine Laboratories iron database, <a href="http://www.mlml.calstate.edu/data/irondata.htm">http://www.mlml.calstate.edu/data/irondata.htm</a> , cruise VERTEX VII, station 7.....	3
Figure 1.3 Typical profile of dissolved manganese in Atlantic surface (Shiller, 1997)...	4
Figure 1.4 (a) Global annual minimum distribution of surface concentrations of nitrate $\text{mmol m}^{-3}$ , one of the principal macronutrients limiting primary production (Levitus world ocean atlas 1994), (b) net primary productivity of $\text{grams C m}^{-2} \text{ year}^{-1}$ and (c) chlorophyll a $\text{mg m}^{-2}$ ( <a href="http://earthobservatory.nasa.gov/Newsroom/view.php?id=23717">http://earthobservatory.nasa.gov/Newsroom/view.php?id=23717</a> ). .....	6
Figure 1.5 The marine biogeochemical cycle of iron. Blue arrows: resuspension, Purple arrows: sedimentation: Black compartment: dissolved iron. Brown compartment: particulate iron. Units: $10^{12} \text{ g yr}^{-1}$ . 1 Goudie (2008), 2 Jickells and Spokes (2001), 3 Chester (2000), 4 de Baar and de Jong (2001) (Seguret, 2009) .....	9
Figure 1.6 Various chemical forms and species of iron which can exist in dissolved and particulate phase (Bruland K. W., 2001).....	10
Figure 1.7 Atmospheric Iron flux $\text{mg/m}^2/\text{month}$ (Gao et al., 2001) .....	15
Figure 1.8 Schematic showing the iron pathway when it is uplifted from the soil [1] to the atmosphere, where it can form clouds [2] and be wet [5] or dry [6] precipitated to the oceans or continue the cycling in clouds [4] (Mackie et al., 2005).....	17
Figure 2.1 Location of the two sampling sites in Mali and Niger that were used for this project and in circles the major dust sources (Stuut et al., 2009).....	25
Figure 2.2 Incubators on board of the RRS Discovery during the SOLAS D326 Cruise. ....	31
Figure 2.3 Schematic of the sequence of the experiments. ....	32
Figure 2.4 Manifold configuration for rinse, preconcentration and determination of total dissolved iron in seawater (Planquette et al., 2007). ....	34
Figure 2.5 Photograph of the iron analyzer that was used for the laboratory analysis. ...	35
Figure 2.6 Design of the flow injection analysis system for the measurement of total Fe(II).....	36

Figure 2.7 Picture of the Iron FI-Cl Analyzer system used during the cruise(Lohan et al., 2006).....	37
Figure 2.8 Schematic diagram of the FIA colorimetric Mn system based on that Mallini and Schiller (1993). .....	39
Figure 2.9 Photograph of the manganese analyser used during the cruise.....	40
Figure 3.1 Schematic representation of the possible wind induced entrainment processes to move, emit, and transport mineral dust particles from the source into the troposphere (Usher et al., 2003). .....	45
Figure 3.2 Schematic of the journey of mineral particle in the atmosphere and deposition in the seawater. ....	47
Figure 3.3 Possible main processes impacting aerosol particles within the cloud droplet .....	48
Figure 3.4 Schematic picture presenting the hypothesis of the alteration in the mineralogy of iron oxides that have been cloud processed.....	49
Figure 3.5 Representation of the reaction mode for the dissolution of Fe(III) (hydr)oxides by protons. Surface coordination controls the dissolution process (Sulzberger et al., 1995; Sulzberger et al., 1989; Sunda et al., 2003)).....	50
Figure 3.6 Minteq geochemical bench graphs of iron concentration versus pH for a) hematite and b) goethite(Stumm et al., 1981) minerals.....	51
Figure 3.7 a) Percentages of Fe (w/w) in total iron content of Niger soil: easily reducible iron species, FeH, amorphous iron oxides (ferrihydrite, lepidocrocite) and reducible iron species, FeD, crystalline iron oxides (goethite, hematite) (n=4; NS = not treated dust, NB= acid treated dust, NSJ = low pH acid cycled in MQ water), b) zoomed in the percentages of FeH.....	56
Figure 3.8 a) Percentages of leached Fe (w/w) in total iron content of Mali soil: easily reducible iron species, FeH; amorphous iron oxides (ferrihydrite, lepidocrocite) and reducible iron species, FeD; crystalline iron oxides (goethite, hematite) (n=3; MS = not treated dust, MB= acid treated soil, MSJ = low pH acid cycled soil, b) zoomed in the percentages of FeH. ....	57
Figure 3.9 The percentage of leached Mn (w/w) in total Mn content of soil from the two leaches in Niger samples (n=3; NS: not treated soil, NB: acid treated soil). ....	59
Figure 3.10 The percentage of Mn (w/w) from the two leaches in Mali samples (n=3; MS = not treated dust, MB= acid treated dust.....	60
Figure 3.11 X-Ray Diffraction pattern for the a) Niger, b) Mali soil and c) the 2-Theta values for the various minerals.....	62
Figure 3.12 FEGSEM image of synthetic ferrihydrite nanoparticles.....	63

Figure 3.13 SEM images of the non treated a) Niger (NS) and c) Mali (MS) soil with corresponding XRD spectrums b) Niger and d) Mali soil respectively. ....	64
Figure 3.14 SEM images of the a) acid treated Niger soil (NB) with b) corresponding EDX spectrum showing an Fe peak and of the c) acid treated Mali soil (MB) with d) corresponding spectrum EDX showing an intense Fe peak. ....	65
Figure 3.15 SEM images of the a) low pH cycled Niger soil (NSJ) with b) corresponding EDX spectrum and of the c) low pH cycled Mali soil (MSJ) with d) corresponding XRD spectrum. ....	66
Figure 3.16 FEGTEM image of low pH cycled Mali soil (MSJ) of the a) greater area of interest in 50nm scale, b) area in 20nm scale, c) zoom in the marked square given in image (b) in 5nm scale, showing details of lattice fringe geometries, d) SAED ion pattern of specific area, e) EDX spectrum showing the metals present in the area and f) EELS spectrum. ....	68
Figure 3.17 FEGTEM image of acid treated Niger soil a) greater area of interest, b) zoom in 20nm showing details of lattice fringe geometries, c) corresponding XRD spectrum and d) SAED pattern of the aggregate with indexed Bragg distances corresponding to 2-line ferrihydrite. ....	69
Figure 4.1 Dissolved Fe (DFe) versus log time for (a) Mali soil, (b) Niger soil during the laboratory experiments and percentage of dissolved Fe for (c) Mali and (d) Niger soil respectively (particle concentration $10\text{mg L}^{-1}$ , $20^{\circ}\text{C}$ ). ....	74
Figure 4.2 Dissolved nM Fe (DFe) versus log time for Mali soil during the abiotic, dark experiment, conducted during SOLAS cruise D326. ....	75
Figure 4.3 Dissolved iron DFe (nM) versus time (hour) for the three dissolution experiments for (A) Mali Soil MS, (B) Mali soil, low pH cycled MSJ and (C) Mali soil, acid treated (MB) during the on board experiments. ....	77
Figure 4.5 Dissolved Manganese [Mn] (nM) versus time (hours) (A) Abiotic Dark, (B) Abiotic Light and (C) Biotic Light experiments during on board incubations. ....	81
Figure 4.6 Schematic representation of what happens to the mineralogy of Saharan dust particles after cloud processing. ....	83
Figure 4.7 Schematic of how siderophores are bound to iron in seawater ( <a href="http://www.nsf.gov/od/lpa/news/press/images/fridaygraphicnature.jpg">http://www.nsf.gov/od/lpa/news/press/images/fridaygraphicnature.jpg</a> ). ....	89
Figure 4.8 Dissolved Fe concentrations in the control experiments A during the cruise, B in the laboratory. ....	92
Figure 5.1 Map of the location of the Bioassays 1, 2, 3, and 4. ....	103
Figure 5.2 Abundance and distribution of (a) heterotrophic bacteria, (b) synechococcus, (c) nanophytoplankton, (d) picophytoplankton. ....	104
Figure 5.3 Concentration of Chlorophyll ( $\mu\text{g/L}$ ) in Bioassays 1 and 2 (MS:Mali soil)	105

Figure 5.4 Concentration of Chlorophyll ( $\mu\text{g/L}$ ) in Bioassays 3 and 4 (MS:Mali soil, MB:acid treated processed soil) .....	106
Figure 5.5 (a) Alkaline Phosphatase Activity $\text{nmoles P } \mu\text{g}^{-1} \text{ Chl day}^{-1}$ for Bioassays 2 .....	107
Figure 5.5 (b) Alkaline Phosphatase Activity $\text{nmoles P } \mu\text{g}^{-1} \text{ Chl day}^{-1}$ for Bioassays 3 .....	108
Figure 5.5 (c) Alkaline Phosphatase Activity $\text{nmoles P } \mu\text{g}^{-1} \text{ Chl day}^{-1}$ for Bioassays 4 .....	109

## Tables

Table 1.1 A summary of studies investigating the solubility of aerosol iron including the matrix and filters used, parameters considered and the adopted analytical technique. CRM: certified reference material, PC: polycarbonate membrane, PP: polypropylene filter, What.: Whatman fibrous cellulose acetate filter (Seguret, 2009).....	12
Table 3.1 The percentage of Fe (% w/w) in total Fe content in soil, in Niger and Mali soil samples processed and non- processed (n=3).....	54
Table 4.1 Leachable Percentage (%) of Iron Seawater Solubilities.....	87

## Chapter 1

### Introduction

#### 1.1 Iron and Manganese in the Ocean

A variety of nutrients are essential for the growth of phytoplankton (Arrigo 2005). These can be divided into macronutrients such as nitrate and phosphate that are required in relatively high concentrations and micronutrients. Micronutrients such as trace metals iron (Fe) and manganese (Mn) have a high impact upon the primary productivity of the ocean (Turner et al., 2001). Dry deposition is a substantial source of both Fe and Mn to the surface ocean (Duce et al., 1991; Guieu et al., 1994). However, how much dissolved metal can be released from the particles is still a topic of debate, and kinetic and thermodynamic values for the release of metals from dust are needed for computer models which incorporate dust as part of their ocean system. Both Fe and Mn are essential for marine phytoplankton.

Iron is essential for the growth and metabolism of all marine organisms. It occurs in cytochromes and FeS redox proteins involved in key metabolic processes; photosynthetic and respiratory electron transport, nitrate and nitrite reduction, N<sub>2</sub> fixation and sulphate reduction (Geider et al., 1994; Jickells et al., 2005). It is also present in catalase and peroxidases and in some superoxide dismutases and it thus important in the detoxification of reactive oxygen species (O<sub>2</sub><sup>-</sup> and H<sub>2</sub>O<sub>2</sub>). Also, because it primarily functions in electron transport and redox catalysis rather than in structural components of cells, it is more important in controlling rates of metabolism and growth than cell yields (Sunda et al., 1997).

Iron is of particular relevance to marine phototrophs due to its central role in photosynthesis and nitrogen assimilation illustrated in Figure 1.1. Reductions in photosynthetic efficiency often accompany nutrient limitation. Many catalysts involved in electron transfer and reductive biosyntheses contain iron, and the abundances of most

of these catalysts decline under iron-limited conditions. Reductions of ferredoxin or cytochrome *f* content, nitrate assimilation rates, and dinitrogen fixation rates are amongst the diagnostics that have been used to infer iron limitation in some marine systems (Geider et al., 1994). A typical dissolved iron profile, showing surface depletion and deep water regeneration is presented in Figure 1.2. This data was obtained by the Moss Landing Marine Laboratories and published in Martin et al. (1989).

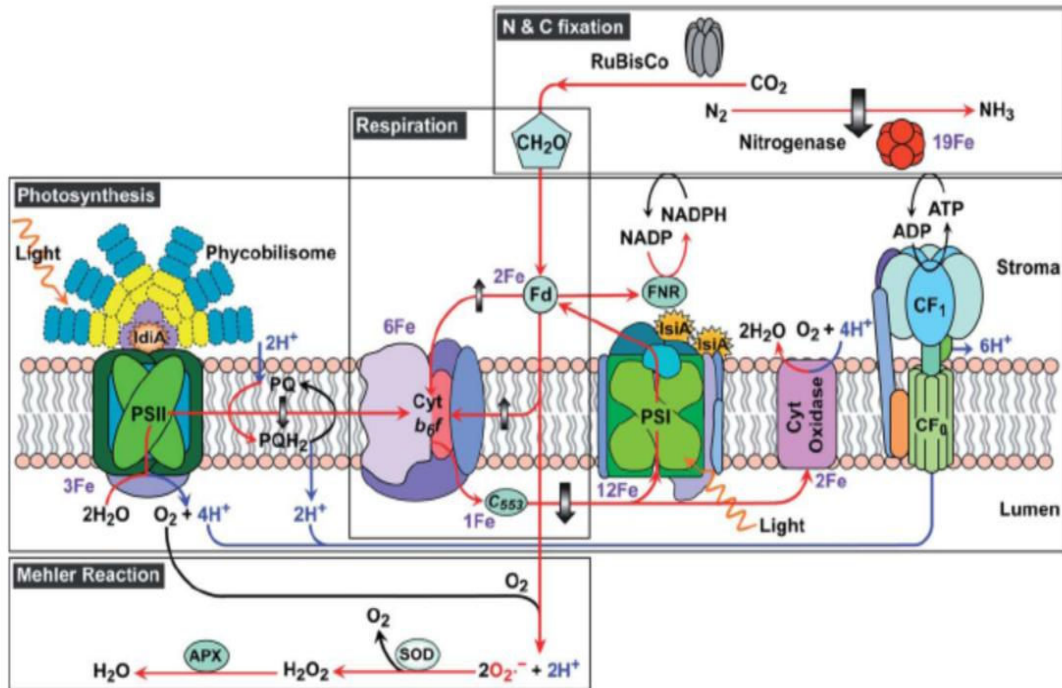
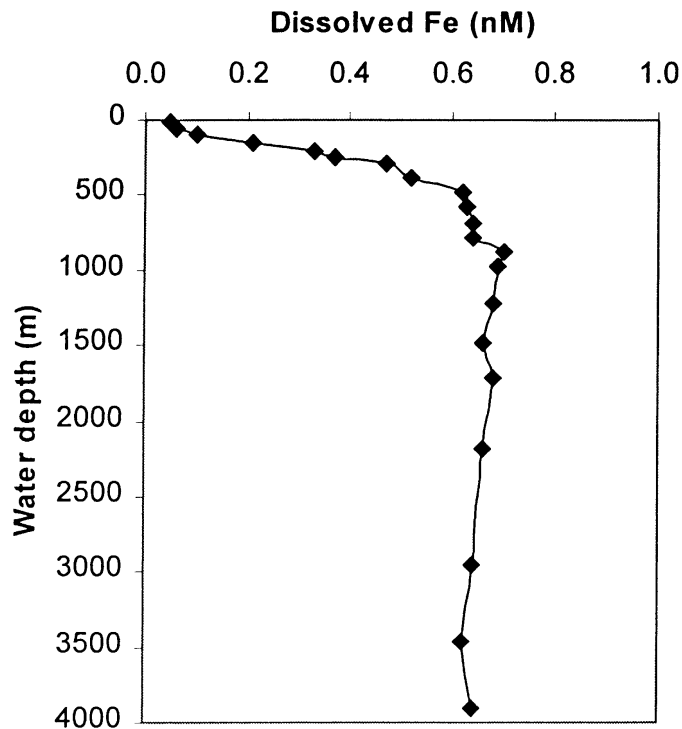


Figure 1.1 Schematic model illustrating the biochemical processes of phytoplankton. The schematic is given only as a guide to the importance of Fe to organisms (Shi et al., 2007).



**Figure 1.2** Typical profile of dissolved iron in the North Pacific (data replotted from Moss Landing Marine Laboratories iron database, <http://www.mlml.calstate.edu/data/irondata.htm>, cruise VERTEX VII, station 7).

Manganese is specifically important for photosynthetic and radical scavenging enzymes (Horsburgh et al., 2002; Kernen, 2002). Thermodynamically, Mn in fully oxygenated waters at natural pH is Mn(IV) and precipitates out of the water in the form  $\text{MnO}_2$ . However, dissolved Mn ocean profiles reveal that the surface waters contain high levels of soluble Mn(II). A portion of this soluble Mn is from direct atmospheric deposition (Statham and Chester 1988; Guieu et al., 1994; Siefert et al., 1998), and while slow oxidation to the +3 or +4 forms allow Mn to stay dissolved on the order of days, Mn should oxidize over time and precipitate from the surface ocean (Stumm et al., 1996). Oxidation does occur, but the build up of oxidized Mn is prevented by organic material (Sunda et al., 1993). Light in the surface ocean can promote an electron transfer between organic compounds, such as humic material, and Mn, resulting in the photoreduction of Mn to the +2 oxidation state. This results in a large concentration of soluble Mn (Statham et al., 1986) as high as 30 nM after rain events (Mendez, 2008) in the surface waters, available for biological use. The soluble fraction of manganese in Atlantic surface waters is presented in Figure 1.3 taken from the study of Shiller A. M. (1997).

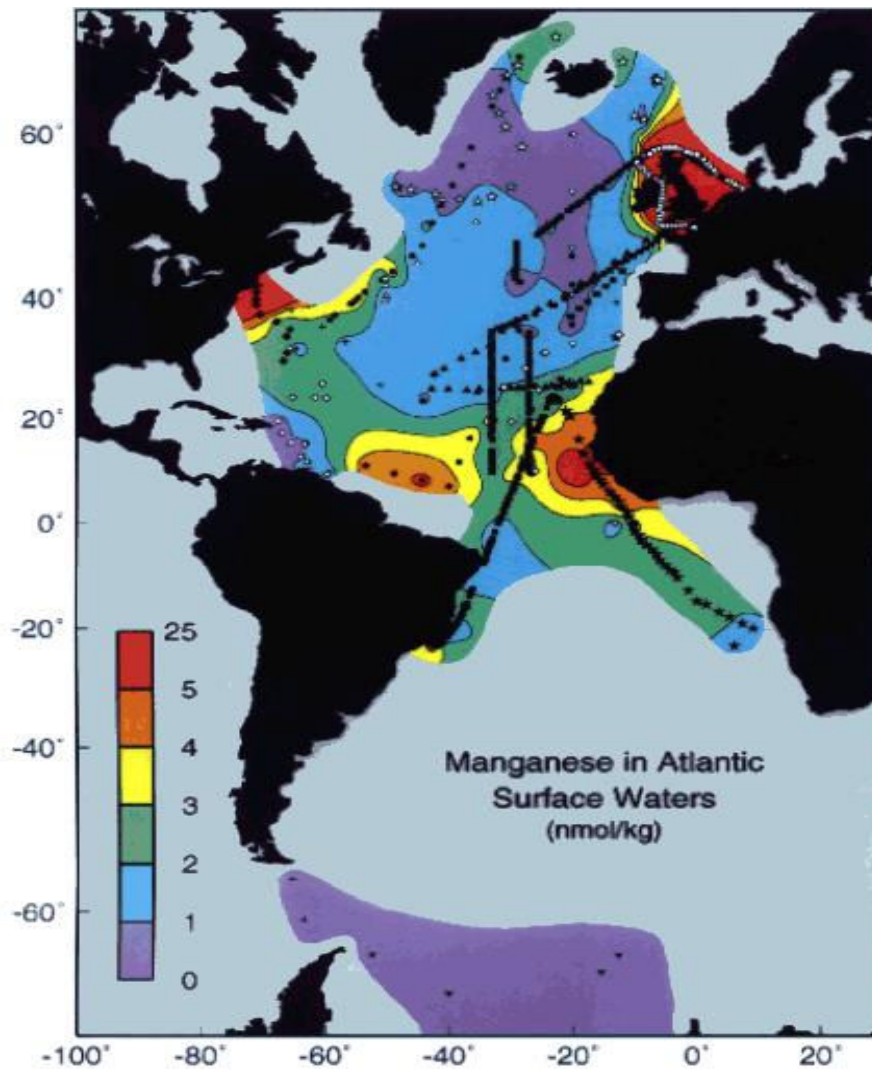
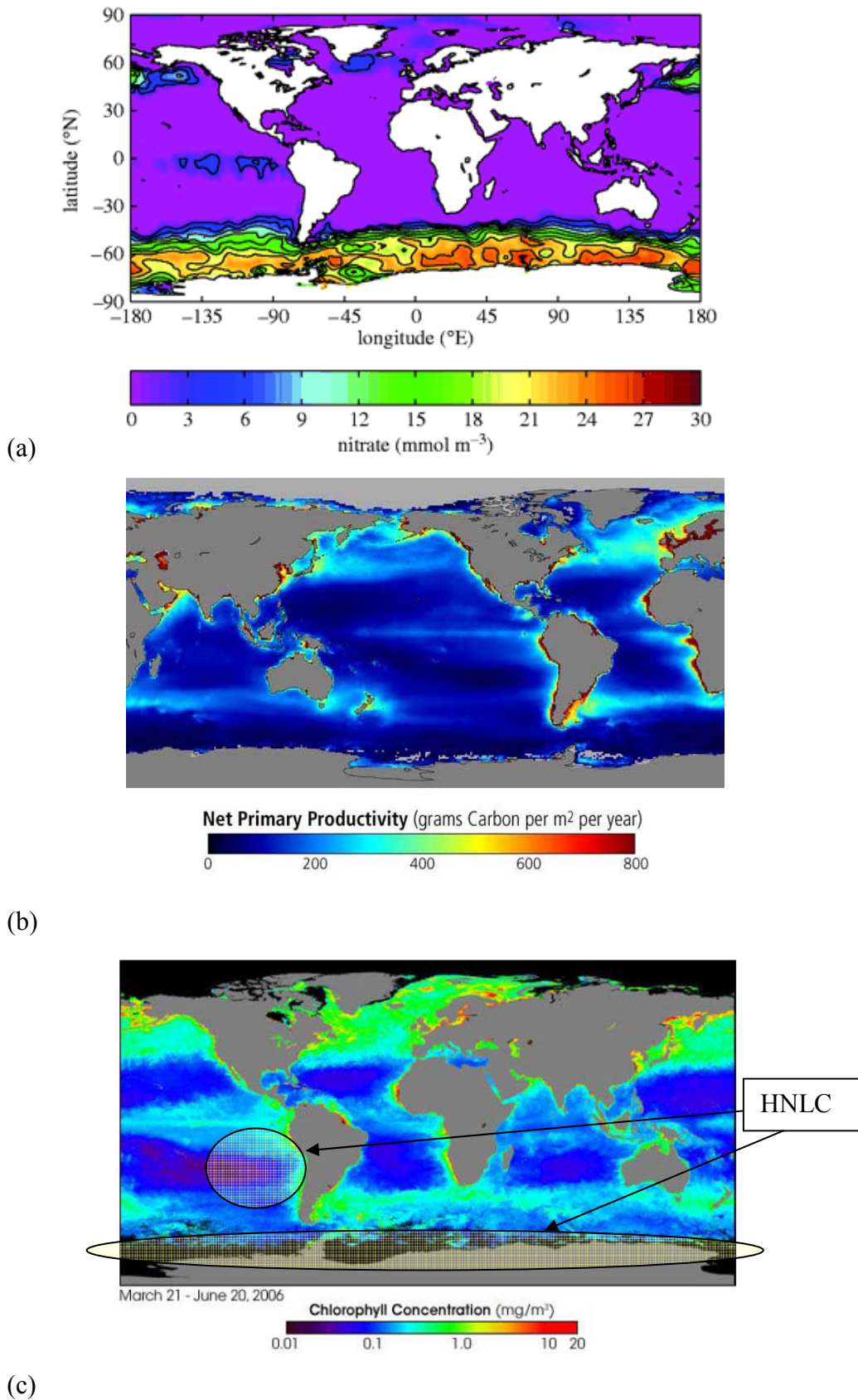


Figure 1.3 Typical profile of dissolved manganese in Atlantic surface (Shiller, 1997)

Low-nutrient low-chlorophyll (LNLC) waters can be found in the subtropical gyre systems of the oceans (Figure 1.4). These oligotrophic regions comprise approximately 40 per cent of the ocean surface and are characterized by wind-driven downwelling and a strong thermocline (both of which impede the nutrient supply from deeper water by vertical mixing) and hence exhibit very low surface water nutrient concentrations (Lampitt et al., 2008). To overcome the deficiency of nitrogen, diazotrophy ultimately prevents the ocean from losing the nitrogen required for photosynthesis (Falkowski, 1997; Tyrrell, 1999). For phosphorus, there is, however, no alternative supply route and it can therefore be considered as the ultimate limiting macronutrient (Tyrrell, 1999). The only sources available to fuel primary production are the stocks in deep water or those supplied from rivers or on airborne dust and unless

such sources exist, productivity will cease once local production exhausts the upper ocean pool.

The seawater molecular ratios (Redfield ratios) of carbon, nitrogen and phosphorus in phytoplankton on average are quite constant with stoichiometric ratio is C:N:P = 106:16:1 (This expresses the fact that one atom of phosphorus and 16 of nitrogen are required to "fix" 106 carbon atoms or 106 molecules of CO<sub>2</sub>) that has been initially measured by Redfield (1923) and he found that globally the elemental composition of marine organic matter (dead and living) was remarkably constant and remained the same from coastal to open ocean regions when nutrients are not limiting ocean productivity. Thus the amount of inorganic carbon taken up and transformed into organic forms is set up by the availability of the accompanying nitrate and phosphate in the subtropical gyres. Many other factors, other than the absence of these nutrients, may limit net and gross primary production. By contrast the High Nutrient Low Chlorophyll - HNLC areas present a paradox that needs an explanation since N and P are present what is missing to be causing such low primary production?



**Figure 1.4** (a) Global annual minimum distribution of surface concentrations of nitrate  $\text{mmol m}^{-3}$ , one of the principal macronutrients limiting primary production (Levitus world ocean atlas 1994), (b) net primary productivity of grams  $\text{C m}^{-2} \text{ year}^{-1}$  and (c) chlorophyll a  $\text{mg m}^{-2}$  (<http://earthobservatory.nasa.gov/Newsroom/view.php?id=23717>).

The HNLC condition has been observed in the equatorial and subarctic Pacific Ocean, the Southern Ocean, and in some strong upwelling regimes, such as off central and northern California and off Peru.

Dissolved Fe concentrations in open-ocean seawater are extremely low. It exists in seawater in two valence states +2 and +3. The Fe in the +2 state is thermodynamically unstable and oxidizes to the more stable +3. Fe (III) is believed to dominate in oxygenated seawater and has very low solubility (Morel et al., 1993). Above this solubility limit the Fe(III) solubility is controlled by organic complexation Fe (Barbeau et al., 2001; Buck et al., 2007; Rue et al., 1995; Van den Berg, 1995). These ligands, produced by bacteria and phytoplankton, keep Fe in solution and available for biological uptake (Barbeau, 2006; Kraemer, 2004). However, most of the dissolved iron (>99%) present in seawater is complexed by organic ligands (Gledhill et al., 1995; Millero, 1998; Rue et al., 1995).

The discovery that iron concentrations in surface waters is so low and shows a nutrient like profile, led some to speculate that iron availability limits plant growth in the oceans. This notion has been tested in bottle enrichment experiments throughout the major HNLC regions of the world's oceans and is now accepted that iron in HNLC waters can be the limiting or co-limiting nutrient (Maldonado et al., 1996; Martin et al., 1989; Mills et al., 2005). It has not yet been established which form of iron (organically complexed Fe(III), inorganic Fe(III), or Fe(II)) is bioavailable (Timmermans et al., 2001a). The various chemical forms of iron may, on the other hand, the bioavailability varies for various organism. It is possible, for example, that prokaryotic and eukaryotic species have different abilities to obtain iron bound to organic chelators (Hutchins et al., 1999).

Early bottle incubations studies carried out *in vitro* in the Gulf of Alaska confirmed that Fe limitation does control ocean productivity within HNLC regions (Boyd et al., 2007; Martin et al., 1988). These experiments have demonstrated dramatic phytoplankton growth and nutrient uptake upon the addition of iron relative to control experiments where no iron was added. However such small scale, enclosed experiments may not accurately reflect the response of the HNLC system. Later studies found some HNLC regions to be permanently Fe limited over time such as the Southern Ocean (Boyd, 2000) and Equatorial Pacific (Martin, 1994), and others to be seasonally limited such as the Gulf of Alaska and the Northern California Coast (Johnson et al., 2001).

The process of atmospheric Fe input to the ocean controlling the global carbon budget and temperature over glacial–interglacial timescales is known as the Iron Hypothesis (Martin, 1990). Several mesoscale Fe addition experiments including IronEx I and II (equatorial Pacific) and SOIREE and SOFeX (Southern Ocean), have been conducted to investigate the Iron Hypothesis and the impact on the carbon cycle. Each experiment found increased phytoplankton growth, especially diatoms, followed by an increased grazer population (Boyd, 2007). The later experiments found that surface ocean carbon dioxide levels decreased during the course of the fertilization. Fitzwater (1998) and Martin et al. (1994) have shown that biological productivity in some oceans regions is limited by iron and there are suggestions that other metals including manganese, copper and zinc may also be limiting, perhaps synergistically (Bruland et al., 1991; De Baar, 1990; Morel, 1994). However no mesoscale experiment to date has found an increase in organic carbon flux to the deep ocean or the permanent burial of carbon (Boyd, 2007) thus perhaps the addition of Fe may not be significant for the removal of CO<sub>2</sub> from the atmosphere.

The marine biogeochemical cycle of iron is presented in Figure 1.5. The sources of Fe can be rivers, coastal/shelf sediments, airborne dust blown from the deserts that are deposited either dry or wet and sediments. However, especially in the open seas the main source of trace elements of continental origin to oceanic areas is the atmosphere. Atmospheric inputs may therefore stimulate the development of marine ecosystems, with implications for biological uptake of atmospheric carbon (Boyd et al., 2007; Martin et al., 1988).

Once dust reaches the seawater most dissolved iron in situ is bound to organic ligands which strongly influence particle reactivity and scavenging loss rates. Dissolved iron is removed by two key processes: a) biological uptake b) adsorption/ scavenging onto particles, 90% of scavenged iron is lost to sediments and 10% to sinking particulates.

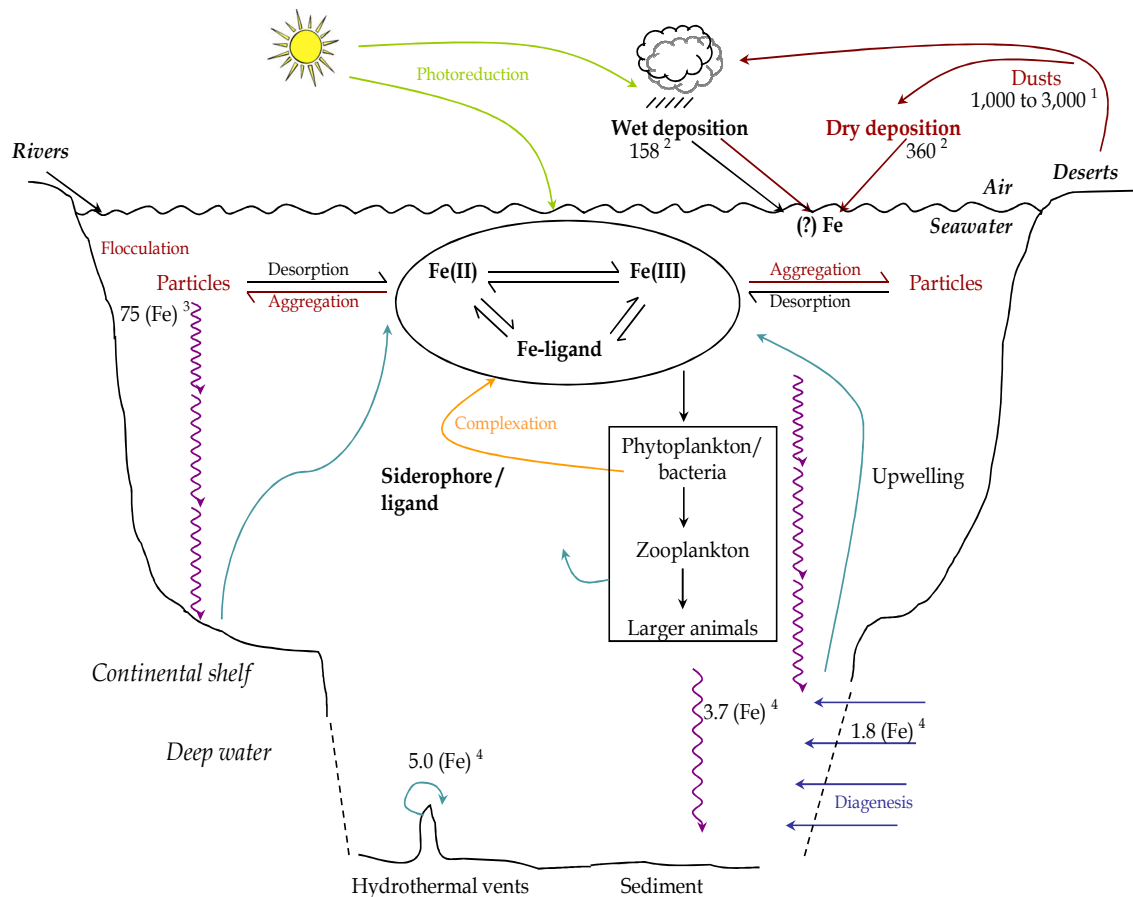


**Figure 1.5** The marine biogeochemical cycle of iron. Blue arrows: resuspension, Purple arrows: sedimentation: Black compartment: dissolved iron. Brown compartment: particulate iron. Units:  $10^{12} \text{ g yr}^{-1}$ . 1 Goudie (2008), 2 Jickells and Spokes (2001), 3 Chester (2000), 4 de Baar and de Jong (2001) (Seguret, 2009)

There is still much debate however as to what is the definition of true solubility of Fe. The separation between the soluble and particulate fraction is defined by physical separation rather than biological measures. In earlier years, solubility was defined as the fraction of iron that passes through a  $0.4\mu\text{m}$  pore diameter filter and recently the recommended pore size has been decreased to  $0.2\mu\text{m}$ . In Figure 1.6 are given dissolved and soluble species of iron with the equivalent sizes.

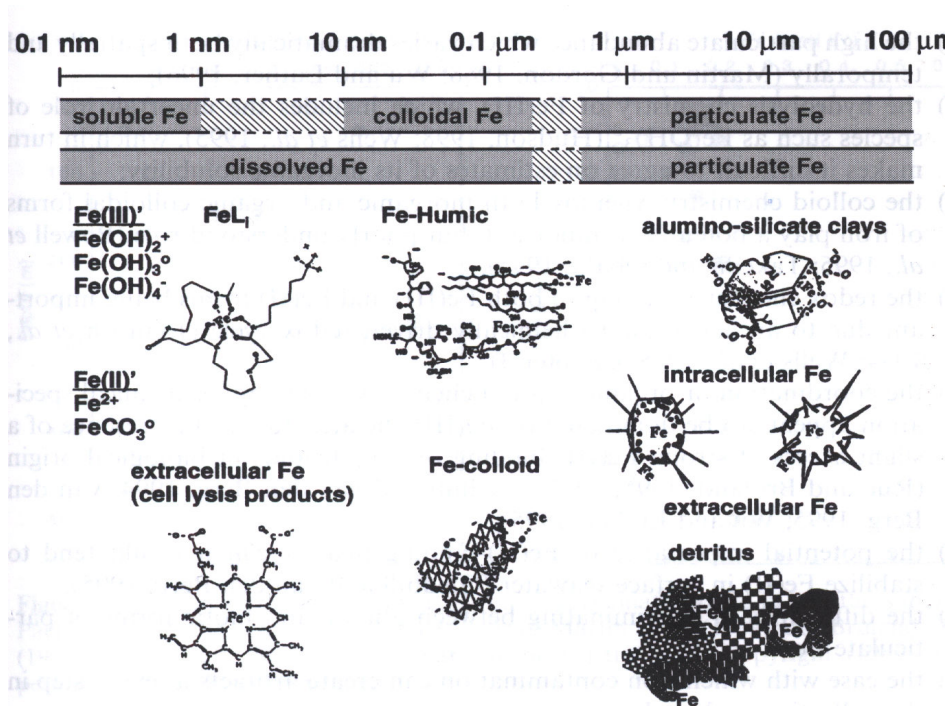


Figure 1.6 Various chemical forms and species of iron which can exist in dissolved and particulate phase (Bruland K. W., 2001).

The most important iron compounds present in atmospheric aerosol particles are hematite, goethite, magnetite and Fe (II), Fe (III) bound to silicates. For both Fe and Mn their hydrated ions and Mn (II) and Fe (II) complexes are water soluble whereas Fe(III) and Mn (IV) complexes occur largely in either the particulate or colloidal phase (Figure 1.6) Iron (hydr)oxides once formed chemically age toward more crystalline particulate phases.

However, not all iron in atmospheric particles is bioavailable in the ocean. Most researchers focus on soluble iron, which is usually considered to be Fe(II), although other forms of iron may also be bioavailable (e.g. Barbeau et al., 2001), and so the term bioavailable needs to be used with caution as we are still unclear about exactly which forms may be available to organisms and over what timescales. Soluble iron in soils is reported to represent about 0.5% of total iron (Fung et al., 2000; Hand et al., 2004). However measurements of iron dissolved from aerosols suggest a much higher solubility (e.g., Zhuang et al., 1992), implying substantial atmospheric processing. Reported solubilities are highly heterogeneous in space and time (Bonnet et al., 2004; Mendez, 2008) and a summary of studies investigating the solubility of aerosol iron is given in Table 1.1. The table also includes the practical approach adopted, parameters considered, dissolution medium with the filter / membrane used and the analytical

techniques used. A range of approaches have been adopted which can be broadly categorised by, (i) semi-continuous flow through reaction chamber (Wu et al., 2007), (ii) incubation (Bonnet et al., 2004) and (iii) instantaneous solubility (Buck et al., 2006a; Buck et al., 2008; Sedwick et al., 2007). Time scales considered in such studies range from instantaneous dissolution (Buck et al. 2006; Sedwick et al. 2007) to intermediate (hours to several days; Milne 2007; Bonnet and Guieu 2004) and long term kinetic dissolution studies (weeks, Mendez et al. 2008). Leach solutions used include ammonium acetate (Baker et al., 2006) Milli-Q water (Buck et al., 2006a; Sedwick et al., 2007) and seawater (Bonnet et al., 2004; Mendez, 2008; Wu et al., 2007).

**Table 1.1** A summary of studies investigating the solubility of aerosol iron including the matrix and filters used, parameters considered and the adopted analytical technique. CRM: certified reference material, PC: polycarbonate membrane, PP: polypropylene filter, What.: Whatman fibrous cellulose acetate filter (Seguret, 2009)

Matrix / Filter	Parameters	Technique	Solubility range (%)	Origin, conditions	References
seawater/What. 40	incubation for 3 h	FAAS	< 1 %	mixed, Mexican	Hodge et al. (1978)
seawater/ coal fly ash	incubation for 1 and 24 h, continuously stirred, temperature and pH controls	gamma counted on Ge(Li) diode	7.5 ± 0.5 %	marine, N. American, 1 h incubation	Crecelius (1980)
seawater/What. 41 and CRM	neutron activation of particulate and incubation for 1h, light/dark, continuously stirred	liquid scintillation counter	3.5 ± 0.5 %	marine, N. American, 24 h incubation	Hardy and Crecelius (1981)
seawater/What. 41	incubation for 1 h	FAAS	6 %	urban N. American	Hardy and Crecelius (1981)
Milli-Q water/What. 41	shaken for 1 h	GFAAS	1 %	NIST 1648	Chester et al. (1993)
seawater/ dust and CRM	particle concentration effect, incubation 24 h to 7 days	FI-CL	< 1 %	West Africa, crustal	Guernozi et al. (1999a)
seawater/ PP	instantaneous solubility	ICP-MS	< 1 %	mixed, west. Med. And Cape Verde	Bonnet and Guieu (2004)
Milli-Q water/ PP	release in upwelled waters	ICP-OES and GFAAS	6 % (1 to 18 %)	urban-rich from UK	Baker et al. (2006a)
ammonium acetate leach, pH 4.7/What. 41	release in upwelled waters	ICP-OES and GFAAS	2 % (1 to 2 %)	west. Mediterranean	Baker et al. (2006b)
			1 % (0.1 to 13 %)	west. Mediterranean	
			0.04 - 1.6 %	Saharan, 7 days, 10 - 0.01 mg L <sup>-1</sup>	
			0.45 - 2.2 %	NIST, 7 days, 10 - 0.01 mg L <sup>-1</sup>	
			6 ± 5 % (0.26 to 26.3 %)	Asian	Buck et al. (2006)
			9 ± 8 % (0.20 to 52.3 %)	Asian	Buck et al. (2006)
			1.2 % (0.5 - 4.1 %)	Saharan	Baker et al. (2006a)
			2.7 % (1.9 to 54 %)	S. Atlantic	Baker et al. (2006b)

Matrix / Filter	Parameters	Technique	Range solubility	References
Milli-Q water/ PC seawater/ PC	30 min sonication	ICP-OES	5 % (0.5 to 19 %) 0.7 % (0.003 to 2 %)	Saharan/Arabian Pen. Saharan/Arabian Pen. Chen <i>et al.</i> (2006)
Milli-Q water/ PC	instantaneous solubility, particle concentration effect	FI-CL	0.44 % to 19 % (~ 0.5 to ~ 5 nmol m <sup>-3</sup> )	Saharan and N. Am., ~ 0.5 to ~ 5 nmol m <sup>-3</sup> Sedwick <i>et al.</i> (2007)
seawater/ dust and CRM	incubation 24 h to 8 days, particle effect concentration	FI-CL	0.001 to 0.04 %	6 Saharan-type, 10 to 0.1 mg L <sup>-1</sup> Milne (2007)
seawater/ PC	semi-continuous flow- through reaction chamber	ID-ICPMS	0.05 to 2.4 % 1.9 to 5.9 % 2.4 to 9.5 %	Trop. Atlantic N. Atlantic N. Pacific Wu <i>et al.</i> (2007)
seawater/ dust	incubation from 1 to 35 days	ICP-MS	0.03 to 15 % (Saharan) 0.2 to 30 %	Saharan American Mendez <i>et al.</i> (2008)
Milli-Q water/ PC seawater/ PC UV-seawater/ PC	semi-continuous flow- through reaction chamber	ID-ICPMS	1.3 % to 19.6 % 1.3 to 1.4 %, to 13.1 % 1.6 %	Gulf of Alaska and N. Pacific N. American urban and N. Pacific N. American urban Aguilar-Islas <i>et al.</i> (2008)
seawater/ PP Milli-Q water/ PP	instantaneous solubility	ICP-MS	9 ± 5 % 15 ± 8 % (3 to 47 %)	N. Atlantic N. Atlantic Buck <i>et al.</i> (2008)
Milli-Q water /What.41	shaken 0.5 h/rest 0.5 h	ICP-MS	7.7 ± 4.5 %	Asian Hsu <i>et al.</i> (2008)

Mineral aerosols are soil particles that have been mobilized by strong winds and are entrained into the atmosphere. These particles are eroded soils, and their chemical composition and mineralogy may be similar to that of parent crustal rock. Dusts originating from the Saharan desert have brown, yellow and red hues due to the high content of hematite-Fe<sub>2</sub>O<sub>3</sub> and goethite-FeOOH. The most abundant minerals in the dust from the North Saharan are illite, carbonates, chlorite and palygorskite, whereas dust from the South Saharan contains more kaolinite and hematite (Usher et al., 2003). The nature of the mineral, e.g. clay, feldspar or iron oxide, impacts on the potential release of iron in seawater and rainwater. Journet et al. (2008) investigated in rainwater the dissolution of various minerals and observed a gradient in solubility inversely proportional to the concentration of iron present.

Satellite data (e.g., Prospero et al., 2002) suggests that the largest and most intense dust sources lay in the Northern Hemisphere. Figure 1.7 presents the iron dust flux, showing the biggest flux of iron to come off mainly from the Saharan region and the Gobi desert in Asia. Prospero et al., (2002) identifies the Bodele as one of the most persistently active dust sources in the world. The main source area lies within a region identified as playa (dry lakes). Furthermore, the plumes tend to start at the eastern (windward) edge of the playa. Winds or infrequent rainstorms constantly move sand into the Bodele playa system. This sand blasts the surface of the playas releasing a large and steady flow of dust to the atmosphere (Mahowald, 1999). In this project only Saharan soils were used.

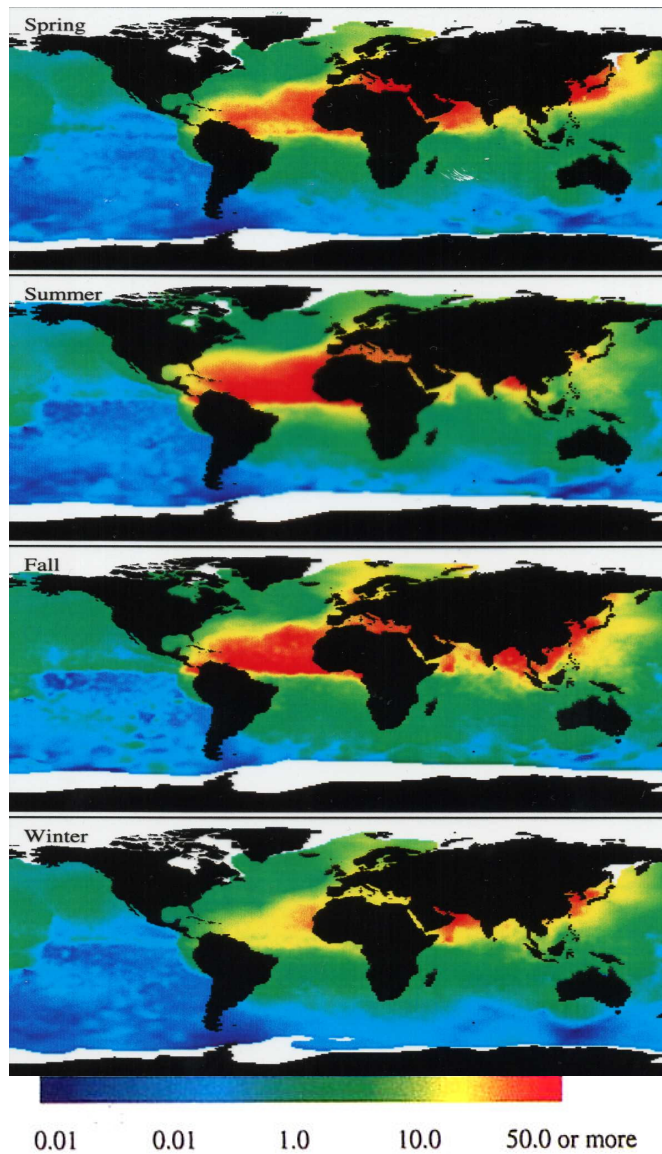


Figure 1.7 Atmospheric Iron flux mg/m<sup>2</sup>/month (Gao et al., 2001)

There are two ways that Saharan dust can be deposited to the sea surface, either by dry or wet deposition. Dry deposition takes place after dust has traveled for a long time in the marine boundary layer (Jickells, 2001) and then the coarser particles,  $d > 100 \mu\text{m}$ , are lost by gravitational settling and the finer ones,  $d < 6 \mu\text{m}$ , can be transported great distances. Wet deposition occurs via rainfall where the particles are scavenged below cloud and are entrained within raindrops in the atmosphere, prior to transport to the sea surface. The delivery of dust in the atmosphere is influenced by season, vegetation, soil aridity in the source area, natural climate variability and human land disturbance (Mahowald, 1999). However, in a biogeochemical context, the key flux to the surface oceans is not dust, but the soluble or bioavailable iron fraction associated with the dust deposition (Jickells et al., 2005).

Bioavailability of atmospherically delivered iron, as stated above, is dependent on its aerosol solubility in seawater, which is potentially controlled by a number of different factors. These may be divided into three broad categories: physical, chemical and biological.

During transport in the atmosphere the aerosols typically undergo around 10 condensation/ evaporation cycles (Pruppacher et al., 1995). The interaction of dust with clouds is not well understood, partly because, in general, aerosol-cloud interactions are not well understood, and particularly because there is a shortage in cloud microphysical measurements in dust dominated regions. This lack of a well-known relationship makes different researchers make very different assumptions about cloud-dust interactions (Desboeufs et al., 2005) because the dissolution rates are different and independent to the total metals content, thus the dissolution process is not a simple release function of total metals content. The difference of dissolution behaviour could be due to other parameters, like metals occurrence in surface, local pH, photoreduction.

Mineralogical evidence suggests that dust particles readily attract water (Koretsky et al., 1997), and thus is assumed that mineral aerosols are readily incorporated into clouds and can act as cloud condensation nuclei (CCN) (Rosenfeld et al., 2001).

During transport from the cloud to the ground, a process which takes minutes, acidic raindrops are partially neutralized through entrainment of water and species including ammonia and crustal dust. The final pH of precipitation generally ranges between 4 and 7 and does not necessarily reflect the pH conditions that an aerosol particle was exposed to in the atmosphere. Figure 1.8 reflects a schematic of the pathway of iron from the soil to the ocean. Due to in-cloud processes the aerosols resulting from evaporation of cloud droplets may be quite different from those that entered the cloud.

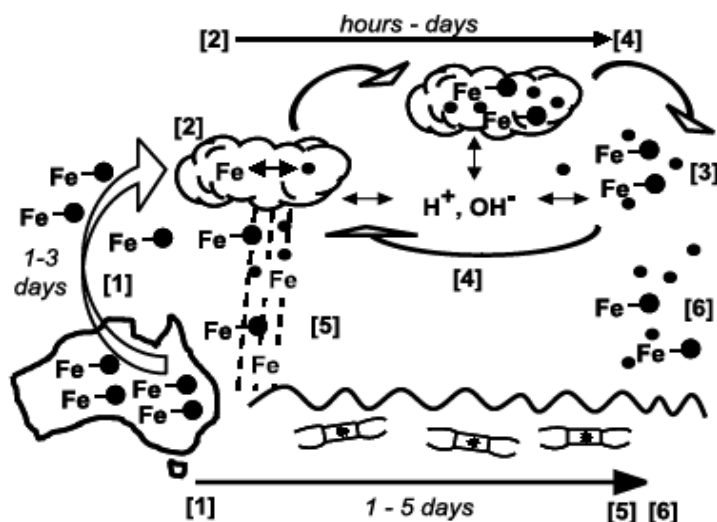


Figure 1.8 Schematic showing the iron pathway when it is uplifted from the soil [1] to the atmosphere, where it can form clouds [2] and be wet [5] or dry [6] precipitated to the oceans or continue the cycling in clouds [4] (Mackie et al., 2005).

So when a cloud condensation nucleus grows into a cloud droplet, particles may be exposed to acids such as  $H_2SO_4$  and  $HNO_3$  which are emitted mostly from anthropogenic sources or in the case of  $H_2SO_4$  it may evolve from biogenically-derived DMS. Its soluble material dissolves into the condensed water, determining the initial composition of the droplet itself. Part of the dissolved fraction from the leached mineral will be deposited back on the particle surface during the evaporation step. Consequently, a large fraction of the resulting aerosol is a blend of aerosols with varying chemical histories. Incorporation of acids and seasalt to form internally mixed aerosols (Andreae et al., 1986) during this cloud cycling, results in individual aerosol particles with hydration layers which are acidic and their pH could be as low as 0-1 (Lindberg and Harris, 1983; Zhu et al., 1993). These hydration layers are not only acidic but can also have a very high ionic strength (Clegg et al., 1990).

Thus, particles in the atmosphere that experience great pH and ionic strength variations and wetting and drying cycles during cloud formation and evaporation could contribute to weathering of the particle, modifying their chemical and physical properties (Desboeufs et al., 2005), thus governing the amount of metal that can be released from aerosols upon mixing into seawater (Jickells et al., 2001; Spokes et al., 1994; Zhu et al., 1992; Zhuang et al., 1992). Particles may therefore be influenced by the aerosol solid phase association (i.e. its solid state speciation) and have significantly larger water-soluble fractions than those initially activated. Zhuang et al. (1992) have reported that the solubility of iron in remote marine aerosols collected at four Pacific

island stations was 5-17 times higher than that of iron aerosols collected from an urban area near the Chinese loess plateau, at the same pH value. This means that iron has undergone transformations in aerosols during their transport in the atmosphere resulting in amorphous and thus more soluble forms. For example, urban aerosol material exhibits generally higher iron solubilities compared with crustal dominated aerosols, Chester et al. (1993, 1994) and Koçak et al. (2007) attributed this enhanced dissolution to the nature of the trace metal solid phase association in the aerosol material. Bonnet and Guieu (2004) used iron-rich Saharan mineral soil and anthropogenic particles (4.5 and 3.9% of iron respectively) in their studies. They attributed the greater solubility of iron (and other metals) in urban aerosols to the higher association of iron with the exchangeable and oxide solid phases located on the surface of urban particles, whereas for crustal material, iron is predominantly found chemically bound with the refractory aluminosilicate solid phase.

Moreover reactions of ferric iron with organic species such as oxalic acid in the atmosphere could play a significant role in producing soluble iron (Pehkonen et al., 1993; Zhu et al., 1993; Zuo et al., 1994; Zuo et al., 1992). Oxalic acid has anthropogenic sources such as incomplete combustion, ozonolysis and photooxidation of hydrocarbons and is common in cloud water (Warneck, 1999). Saydam and Senyuva (2002) found increases in soluble iron during in-cloud photochemical reductions with oxalate and suggested that soil fungi were a natural source of oxalate. Inorganic aerosol solutions can also be important if mineral aerosols are coated with hygroscopic species such as sulfates and nitrates (e.g. Zhuang et al., 1992; Zhu et al. 1992).

Iron solubility (defined as the fraction of Fe present as Fe(II)) was correlated with non-seasalt (nss)  $\text{SO}_4^{2-}$  concentrations in aerosol particles with diameters  $< 2.5 \mu\text{m}$  and did not observe any significant relationship between these parameters, thus the data did not support a clear relationship between either oxalic acids or sulfuric acids and iron solubility (Baker et al., 2006; Chen et al., 2004; Hand et al., 2004; Mahowald et al., 2005). While photochemical reduction in dust aerosols over the Atlantic can yield significant concentrations of Fe(II) in situ, Fe(II) comprises only a very small fraction  $< 0.1\%$  of the total soluble iron and the total soluble iron does not seem to be related to Fe(II) concentrations (Zhu et al., 1997).

Clearly, more studies on the atmospheric processes that convert insoluble iron to soluble iron are needed. All studies that have been made to define the dissolution of dust in seawater (Bonnet et al., 2004; Buck et al., 2006b) have focused on the dissolved

phase of the metals and their concentrations when they enter in the seawater. Few if any investigations have been conducted to examine the particle phase (transformation and characteristics of the particles) during cloud processing and subsequent to entering the ocean.

The interest shown in differentiating the crystalline iron (hydr)oxides and the amorphous iron species is because the latter are more chemically reactive due to their larger surface as demonstrated in the study by Anschutz (2005), by comparing the rates of reductive dissolution of goethite and ferrihydrite. Moreover field and laboratory studies have shown that the type of Fe (III) in terms of crystallinity determines to a large extent how efficiently photoreductive dissolution occurs (Sulzberger et al., 1995).

A further important chemical factors affecting metal solubility in seawater is particle concentration. Bonnet and Guieu (2004) carried out seawater dissolution experiments using various dust concentrations and they concluded that the highest iron solubilities in seawater of 1.6% and 2.2% for Saharan and urban particles respectively were found when the particle concentration was at its lowest ( $0.01 \text{ mg L}^{-1}$ ), compared to the lowest iron solubilities in seawater, 0.04% and 0.45%, for Saharan and urban aerosols respectively, were observed at the highest particle concentration ( $10 \text{ mg L}^{-1}$ ). Spokes and Jickells (1996) also indicated a decrease in the solubility of iron with increased dust particle concentrations using de-ionized water. With aerosol concentrations less than  $0.5 \text{ mg L}^{-1}$ , the solubility of iron present in the aerosol material was 7% and decreased to  $\sim 1.4\%$  at an aerosol particle concentration  $> 0.12 \text{ g L}^{-1}$ . Recently Milne (2007) carried out in situ incubation studies of a range of Saharan dusts in seawater. The solubilities varied from 0.02% at  $0.1 \text{ mg dust L}^{-1}$  seawater to 0.001% at  $10 \text{ mg dust L}^{-1}$  seawater. The effect of particle concentrations was clear within this range of dust concentrations. Therefore, when carrying out iron seawater dissolution studies, it is crucial to take into account the dust concentration used for the experiments as the lowest possible seems to be the ideal, because when the dust concentration is high particle surface is larger and adsorption onto particle surfaces higher.

In addition another important factor is the organic matter complexation with trace metals. Iron has shown enhanced solubilities up to 50% in the surface seawater containing relatively high concentrations of organic material. As mentioned earlier in the presence of organic matter, in aerosols and seawater, has the potential to increase the rate of Fe (III) photoreduction and hence enhance its solubility but also, through Fe(II) complexation, diminish its rate of re-oxidation. Rue and Bruland (1997) pointed out that

an enhancement of the phytoplankton activity leads to a greater degree of complexation of iron by two broad groups of organic ligands: (i) stronger ligands  $L_1$  having conditional complexation stability constants of the order of  $K' = 5 \times 10^{12} \text{ M}^{-1}$  and (ii) weaker ligands  $L_2$ ,  $K' = 6 \times 10^{11} \text{ M}^{-1}$ . Other studies including those initial studies of Haygood et al. (1993) and Gledhill and van den Berg (1994) have concluded the complexation of iron by organic ligands. For example Maldonado and Price (1999) and Barbeau et al. (2001) have shown that it is likely that siderophores contribute to the complexing capacity of iron in seawater; these complexing ligands are characterized by strong conditional stability constants. Furthermore, Kraemer (2004) confirmed that the presence of natural siderophores enhanced the solubility of iron oxide surfaces, via organic complexation. Aguilar-Islas et al. (2008) investigated the effect of the iron complexing ligand Desferal (Desferrioxamine B) on the dissolution rate of iron from urban material collected in north America and found a twofold increase compared to the control without addition of Desferal.

Except for the chemical factors affecting the solubility of iron in seawater there are also some physical factors that are as important. Biscombe (2004) investigated the effect of seawater temperature and stirring rates on the dissolution of aerosol associated metals, not including iron, in seawater and found that the solubilities of Pb and Zn increase with temperature and decreased with higher mixing rates. Therefore it is probable that the solubility of iron in seawater could be increasing as well with temperature and low stirring rate.

Light may also affect iron dissolution by photoreduction. A number of studies have investigated this effect on dissolved iron in seawater (Hong et al., 1986; Johnson et al., 1994; O'Sullivan et al., 1991) and using mineral particulates in the atmosphere (Zhu et al., 1997). Indeed, the photochemical process (or photoreduction), taking place in mineral particles suspended in the atmosphere, may reduce Fe(III) to Fe(II) and increase its solubility in seawater and hence its bioavailability for phytoplankton (Hong et al., 1986; Moffett, 2001). This process can occur at low pH ( $\sim 3.5$ ) through the hydrated forms of  $\text{Fe}^{3+}$  and  $\text{FeOH}^{2+}$ . The reaction provides an important source of  $\text{Fe}^{2+}$  but also OH radicals (Graedel et al., 1985). Under certain conditions, Fe (II) complexation by organics can retard the rate of its reoxidation to Fe (III) and so prolong iron availability in aqueous environment and so seawater.

Spokes and Jickells (1996) used natural sunlight and a solar simulator during their photoreduction solubility experiments in Milli-Q water using Saharan and urban

dusts. They simulated light and dark conditions and found an enhancement of Fe (II) production in the light compared with the dark but this also depended on the origin of dust. Indeed, soluble Fe (II) comprised 0.9% in the light and 0.25% of the total of the iron in the aerosol in the dark for the Saharan dust whilst in urban originated dusts, soluble Fe (II) was present at 8.4% in the light and 2.1% of the total of the iron in the aerosol in the dark. Subsequently, Zhu et al. (1997) evaluated the effects of light on soluble ferrous iron (FeIIs) and total soluble iron (FeTs) concentrations from aerosol filter samples collected at Barbados, using acidified sodium chloride solution, during day/night cycles. They found higher (FeIIs / FeTs) ratios during the daytime compared with the night samples. The mean FeIIs concentration in daytime ( $3.67 \text{ ng m}^{-3}$ ) was more than twice as high as that observed for the night samples ( $1.45 \text{ ng m}^{-3}$ ). However when placed in the dark, Fe (II) was rapidly re-oxidized.

As expected the biological factors need to be taken into account. The presence and absence of bacteria is very important and Biscombe (2004) carried out seawater solubility experiments for lead, copper and zinc that their solubilities increased with higher bacteria concentrations indicating uptake of dissolved trace metal onto bacteria surface. Iron solubility although not tested could act in a similar way. Moreover siderophores are produced by bacteria and they enhance aerosol iron solubility in seawater (Waite, 2001).

In conclusion measuring iron is a difficult task and all these factors need to be taken into account. The dust concentrations used should be as low as possible in order to mimic natural conditions, the type of the dust is important as the mineral iron associations influence its solubility and incubation times and addition of ligands need to be considered since iron seem to be released in minutes but also intermediate (hours) and long term (days) release have also been reported and bind to ligands. Lastly the analytical technique in order to measure iron must be sensitive enough to measure iron at pM/ nM concentrations.

## 1.2 **Aims and Objectives**

The aim of this project is to assess whether cloud processes during the passage of dust particles into the atmosphere can trigger the formation of nanosize Fe particles and an increase in Fe and Mn reactivity in the dust. Thus, a double approach was used by examining the particulate phase of the dust particles as well as the release of iron and manganese into seawater.

1) The first objective is to examine the mineral transformation of iron species present in Saharan soils (goethite, hematite) after low pH cycling and acid treatment towards more amorphous species. This objective will be examined using a combination of Field Emission Gun Scanning and Transmission Electron Microscopy (FEGSEM, FEGTEM) techniques in order to be able to examine the particles for neo-formation of amorphous iron nanoparticles and chemical leaches used to determine specific mineral iron species such as iron (hydr)oxides, iron oxides, iron species associated with silicate. In this study it is important to quantify, before and after the artificial weathering of Saharan soil particles, the amount of amorphous iron species such as ferrihydrite by using the hydroxylamine hydrochloride leach and to quantify crystalline species such as goethite and hematite which are the dominant species in Saharan soil by using citric buffered dithionite leach.

2) The second objective is to determine whether the solubility of iron and manganese has been altered by cloud processing. It is hypothesized that the solubility of both iron and manganese increases if the dust particles have been subjected to atmospheric cycling. This hypothesis will be examined by simulating the cloud processing of Saharan soil particles and then measure the iron and manganese released during seawater dissolution experiments in the laboratory and during the SOLAS D326 Cruise. The techniques used for the dissolved iron measurements were the Flow Injection with DPD, FI-CL for the experiments carried out at sea

3) Lastly, a series of bioassays experiments were carried out at sea in order to assess the impact of particle processing in the biota present in the seawater.

This thesis consists of 6 chapters. This first Chapter contains a background to the subject area and gives objectives through which this project will try to take existing ideas and hypothesis a step further. In the second Chapter, the methods used during this project are described. Chapters 3, 4, 5 are results chapters, where Chapter 3 investigates how the particulate phase of the Saharan soils are changed after cloud cycling

---

simulations, while Chapter 4 focuses on dust added incubation experiments carried out in the laboratory and during the cruise to assess the impact on the solubility of iron and manganese of cloud processed particles before their addition to seawater. Chapter 5 addresses how the atmospherically processed iron particles may influence the phytoplankton community. Lastly Chapter 6 reviews the conclusions of the individual results chapters and proposes future work.

## Chapter 2

### Methods

#### **2.0 Introduction**

This chapter will describe the way in which samples were prepared and treated for analysis and the adopted analytical methods. The analytical figures of merit will be presented for each adopted analytical technique.

#### **2.1 Sample Preparation**

In this project two contrasting Saharan soils were used. The first originated from the region of Niger (Kouré; Latitude: 13° 18' 51 N, longitude: 2° 34' 18 E) and it was used for lab experiments only (Figure 2.1). The other soil originated from Mali (Timbadior: Latitude: 15° 19' 60N, Longitude: 1° 31' 60W) area shown in Figure 2.1 and was used for both laboratory and in situ experiments.

The Mali soil was provided by Dr Geoffrey Lloyd who collected it during the Trobit project in Africa and the Niger soil was provided by Dr. Matt Box. The sampling was simple, handpicked surface soil scooped into a plastic bag.

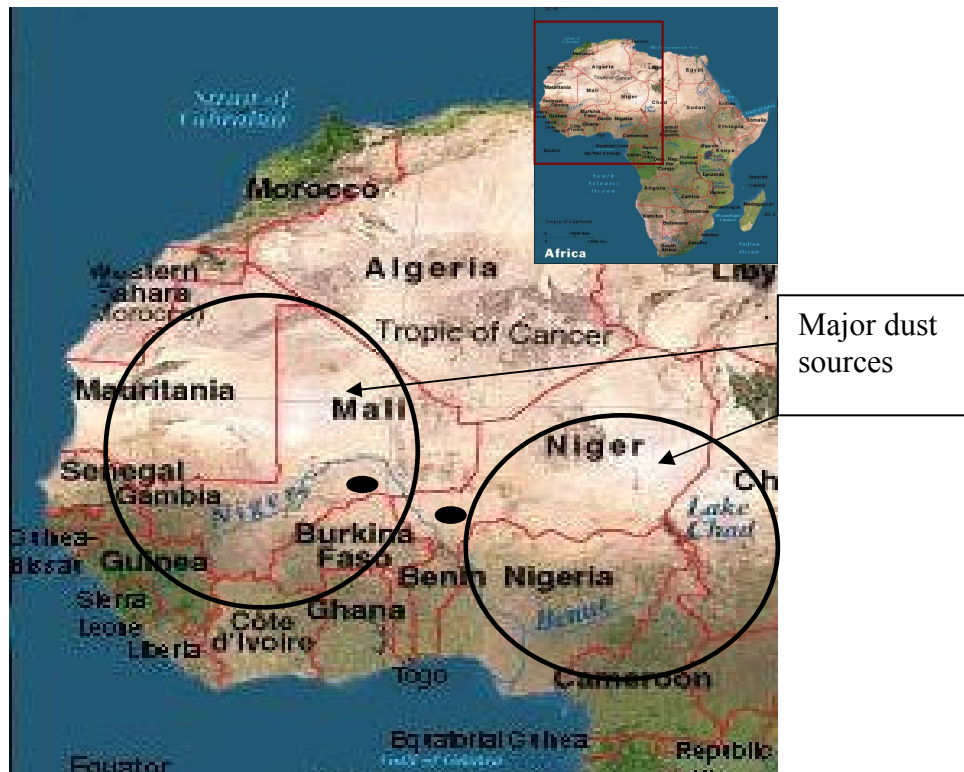


Figure 2.1 Location of the two sampling sites in Mali and Niger that were used for this project and in circles the major dust sources (Stuut et al., 2009).

Both soils were sieved through a 20 $\mu$ m diameter nylon mesh, as that size mesh was the smallest that could be used in order to dry sieve the soils. This size fraction represents the 65-80% of the dust that reaches the ocean and no publications exist to our knowledge that used a smaller sized mesh for dry sieving. There was an attempt to dry sieve soil through a 7  $\mu$ m size mesh but it proved to be impossible.

The Mali and Niger locations were partly chosen because they were provided to us and more importantly the specific locations are considered major areas of dust sources to the ocean.

## 2.2 Atmospheric Processing Simulation

The simulation of atmospheric processing was conducted using two different approaches; the first was according to an experiment published by Spokes et al. (1994) and the other followed the observation of particles in the atmosphere encounter sulphate.

### 2.2.1 The Spokes and Jickells Approach

In this approach in order to determine the effects of varying pH cycles on aerosol metal solubility the adopted method was based on the Spokes and Jickells (1994) approach. Around 10 mg of sieved soil ( $< 20\mu\text{m}$ ) from both regions, Mali and Niger was added to an acid washed beaker containing 500ml MQ water, where stirring was provided magnetically, under a Class 100 laminar clean flow bench. After approximately 24h the system was acidified to  $\text{pH} \sim 2$ , a value comparable to that which aerosols may encounter in clouds. Since Saharan aerosol dissolution rates are essentially independent of acid type,  $\sim 6\text{M}$  sub boiled distilled nitric acid Q- $\text{HNO}_3$  was used for lowering the pH. The system was allowed to react for a further 24hours and then restored to  $\text{pH}$  5-6 using sub boiled  $\text{NH}_4\text{OH}$ . After a further 24 h the pH was lowered once more and the cycle was repeated. Part of the solution was retrieved, just before the end of the last cycling, with a syringe and filtered through a  $0.2\mu\text{m}$  cellulose filter in an acid clean tube. When the cycling had finished the solution was filtered through a  $0.2\mu\text{m}$  polycarbonate filter and this filter was stored in a tube inside the freezer at  $-8^\circ\text{C}$ . The 24h intervals were used in order to comply with the times used during Spokes and Jickells experiment where they were probably used for convenience.

All the glassware, plastics used for this experiment had been washed initially with detergent, then rinsed and washed with 50% HCl and 50%  $\text{HNO}_3$  (analytical grade). The filters used for the last step were previously acid cleaned with  $\sim 10\%$  Q-HCl. The reaction beakers were illuminated continuously throughout with normal fluorescent light so that effects solely from photochemical processes would be eliminated. The sub boiled  $\text{HNO}_3$  and  $\text{NH}_4\text{OH}$  were prepared in a class 100 clean laboratory at the NOC (National Oceanography Centre), Southampton before the experiments. About 24 replicates for each soil, Mali and Niger were processed using this technique. Some of them were analysed by chemical leaching. Others were stored in the freezer for subsequent dissolution experiments with seawater.

The experimental system does not allow the wetting and subsequent drying of the samples, but rather aims to reproduce the pH ranges likely to be encountered by aerosols at the atmosphere and assess whether metal solubility at a particular pH is affected by prior exposure to low pH. The dust was cycled twice, since multiple cycles of pH adjustment did not affect the final degree of remobilization (Mackie et al., 2005; Spokes et al., 1996).

The samples that followed this procedure will be termed from now on as MSJ for the Mali soil and NSJ for the Niger soil.

### 2.2.2 Acid Treatment

A different way to simulate the pH cycling was used for a further set of samples, where the dust was treated with concentrated acid and then allowed to dry, mimicking the wet/dry cycle for particles in the clouds. These modified soils were to be used to investigate the impact on the Fe and Mn seawater solubility and they were also examined under electron microscopic techniques to investigate the iron mineralogy.

In detail around 10 mg of Mali and Niger sieved samples were weighed into acid washed tubes and then placed in a Class 100 laminar flow clean bench. A small amount of Primar grade 0.05M HCl (around 80 $\mu$ l) for the laboratory experiments and 19 $\mu$ l 0.025M H<sub>2</sub>SO<sub>4</sub> for the cruise experiments was used to wet the dust and then it was left to dry under the laminar hood and under normal fluorescent light. It was visually possible to see that the whole soil sample had been wet. Studies have shown that Saharan aerosol dissolution rates were essentially independent of acid type (Spokes, Jickells et al. 1994) so our choice of using HCl was made because we did not want to introduce into the seawater dissolution experiments anything other than H<sup>+</sup> and Cl<sup>-</sup> which are already abundant in the seawater. For the cruise experiments the H<sub>2</sub>SO<sub>4</sub> was used to simulate the encounter of dust particles and SO<sub>2</sub> in the clouds.

The samples after this treatment will be referred to as MB for Mali samples and NB for Niger ones where B stands for Baker (Alex) who proposed this idea of cloud simulation.

## **2.3 Seawater Dissolution Experiments**

### **2.3.0 Cleaning Bottles Procedures**

All the Polycarbonate bottles used for the dissolution in seawater experiments were acid cleaned according to the Fitzwater et al. (1982) protocol for cleaning this type of bottles. In short the cleaning procedure was as follows: initially the bottles were filled with 2% micron detergent for three days, afterwards rinsed with MQ water three times and left with MQ water overnight. After the MQ was discarded the bottles were soaked in an acid bath of 3% HCl Primar grade for 5 days until they were ready for use.

The Low Density Polyethylene (LDPE) 125ml Nalgene bottles that contained the sub samples for manganese and iron analysis, soaked initially for a week in 2% decon detergent bath, rinsed four times with MQ water and placed in an acid bath of 50% HCl for a week and after being rinsed 4 times with MQ water left in 50% HNO<sub>3</sub> acid bath for one more week. Finally the bottles were rinsed four times with MQ water and were placed inside polyethylene bags for the laboratory incubations. The bottles for the shipboard incubations were filled with MQ water and spiked with Q- HCl 1µl/ml.

All other materials used for the experiments such as syringes were cleaned initially with 2% decon detergent and after being rinsed with MQ water were acid cleaned with 50% HCl acid. All the filters used for sub sampling and retaining the particles were acid cleaned with 10% HCl and rinsed with MQ water.

In this work, HCl and HNO<sub>3</sub> are purified using a quartz sub-boiling distillation unit based upon vaporising a liquid heating element, a 'cold finger' for condensation of acid vapors and 1L Teflon bottles where the acids are collected. The sub-boiled acids when prepared at the clean room laboratory of the National Oceanography Centre, and has been tested to provide very satisfactory results for almost all trace metals at low ppb levels.

### **2.3.1 Seawater Dissolution Experiments in the Laboratory**

Seawater dissolution experiments were designed for laboratory and in situ locations in order to define the release of metals from Saharan soil into seawater. Polycarbonate Nalgene bottles of 1 L were used for the incubations. After the cleaning

procedure the bottles were rinsed with low nutrient seawater and then filled with the same seawater. The seawater, acquired from the Canary Basin during the Poseidon 332 cruise, it was filtered twice through 0.2 $\mu$ m polycarbonate filter, once while filling up the tank and the second time before filling up the polycarbonate bottles. It was kept at low temperature in a dark cold room (4<sup>0</sup>C) at the National Oceanography Centre, Southampton. The dissolved iron concentration of the seawater was measured to be 0.26  $\pm$  0.02 nM.

The bottles with the seawater were left to equilibrate overnight in order to eliminate iron adsorption on the container wall and the next day roughly 10mg Saharan soil processed and not processed was added. The laboratory temperature was steady at 20<sup>o</sup>C. This amount of Saharan soil was more convenient to handle through the treatment of soil in order to artificially weather the particles and it represents the amount of dust during a heavy dust event (Bonnet et al., 2004; Glaccum et al., 1980).

The caps of the bottles were pierced and Teflon tubes were pushed into solution to allow sample collection. A length of silicon tubing helped connect the Teflon tube to a syringe that was used for sub sampling at the times: 3min, 30min (for laboratory incubations only), 6h, 24h, 48h (for laboratory incubations only) and 5 days. The bottle was stirred before sampling in order to be homogenised and the precise times of sub sampling for each bottle were noted. The number of replicas for all experiments was 3. The solution acquired from the bottle in the syringe was filtered through a 0.2 $\mu$ m filter into acid clean LDPE bottles and then it was acidified with 6M sub boiled quartz distilled HNO<sub>3</sub> at 1 $\mu$ L/mL of solution. The blanks for these experiments were seawater filled polycarbonate bottles without any dust added.

### **2.3.2 Seawater Dissolution Experiments on Aboard Ship**

The seawater dissolution experiments were conducted during the D326 SOLAS Cruise on board of the RSS Discovery during the period 5 January 2008- 5 February 2008. The procedure was similar to the one used for the seawater dissolution experiments in the laboratory. Twelve polycarbonate bottles were used for each seawater incubation (of Saharan soil) carrying the same principle of Teflon tubing through the cap of the bottles used for the sub sampling during the course of the experiment which was performed in a clean manner inside a clean laboratory and in a

laminar flow hood Class 100. Teflon bottles were too expensive and also according to a study by Fischer et al., (2007) polycarbonate bottles are the best choice to use for less iron adsorbed onto the container walls.

The seawater for the first experiment was collected on the 11/01/08 from the morning (~ 7-8 am) Titanium CTD cast at station 16394B with coordinates 25 40.2N 28 48.3W. The depth of the seawater was 30m and it was used without being filtered on the same day. For the other two experiments the seawater was collected at the station 16419B with coordinates 16 09.6N 30 38.1W on the morning Titanium CTD cast on the 25/01/08 and it was filtered through a 0.2 $\mu$ m filter directly into the polycarbonate bottles for the Light experiment and in a carbuoy for the Dark experiment. The carbuoy was double bagged using black bags to prevent the sunlight and it was stored in the fridge for another two days before being used for the experiment. The average value of the background seawater dissolved iron concentration was  $0.13 \pm 0.02$ nM.

The addition of dust and the sub sampling took place in a clean laboratory under a laminar flow hood. After each sampling the polycarbonate bottles were sealed with parafilm, double bagged and placed in incubators on the deck of the ship under direct sunlight and constant temperature as surface seawater was constantly flowing through the incubators (Figure 2.2). The bottles from the dark experiment were treated similarly with the only difference being that before they were put in the incubator, they were first put in double black plastic bags. The sub samples were acidified on the same day with 1 $\mu$ L/mL of solution 6M HCl Romil SpA.



**Figure 2.2 Incubators on board of the RRS Discovery during the SOLAS D326 Cruise.**

At the end of each experiment the polycarbonate bottles were rinsed with 20ml Q- HCl 10% in order to take up any iron that had adsorbed on the walls of the bottles. Unfortunately we were unable to perform the analysis before the end of the thesis.

A simple schematic of the course of the experiments using Mali soil particles is given in the following Figure 2.3 for our better comprehension.

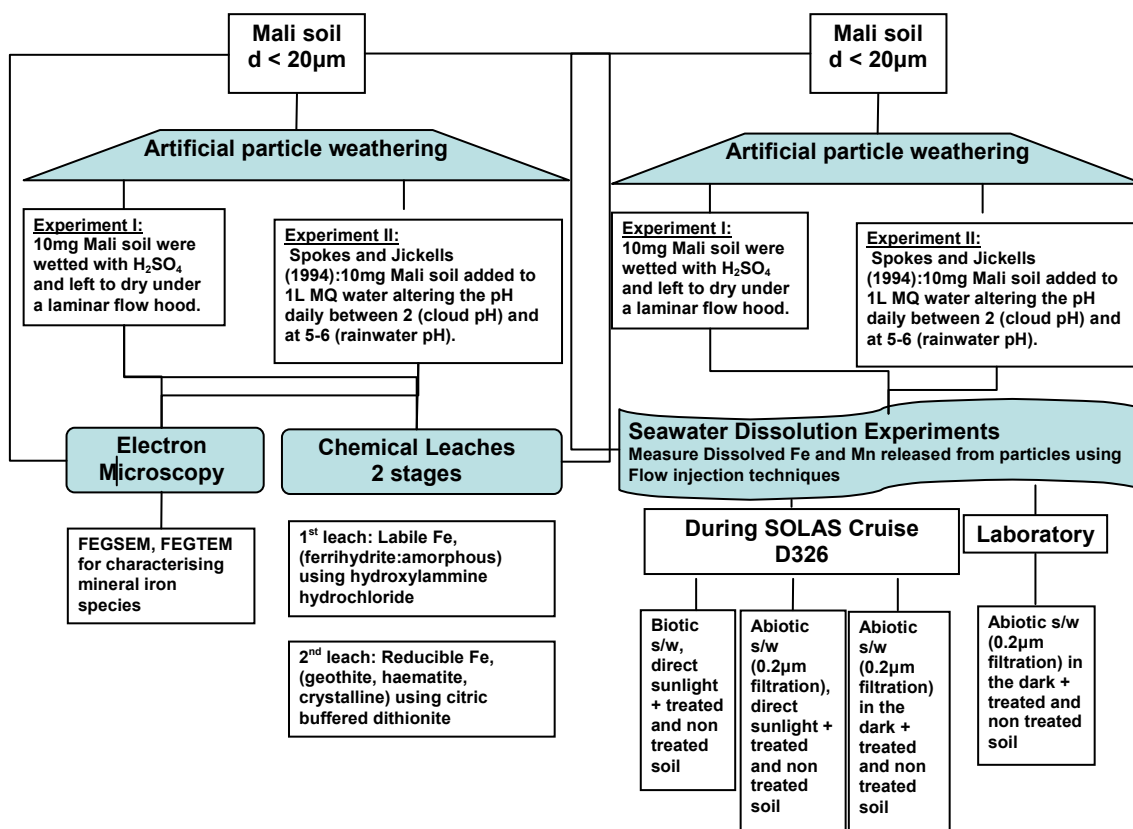


Figure 2.3 Schematic of the sequence of the experiments.

## 2.4 Iron Analysis

Trace metals analysis and in particular iron is a difficult task due to both the low concentration and the seawater matrix. Thus the analytical method used needs to be able to separate the analyte from the bulk of the seawater matrix and to have increased sensitivity in order to measure concentrations as low as 50pmol. During the years for the determination of dissolved iron various methods have been used such as chelation/solvent extraction methods, co-precipitation methods, chelation/solid phase partitioning, voltammetric techniques and chelating ion exchange resins.

Flow Injection (FI) methods are the most recent methods used for the determination of trace metals such as iron and manganese and FI methods were used for this study. This was due to the fact that these techniques exhibit extremely low detection limits, low reagent and sample consumption, the sample handling is simple, the system is automated, the risk of contamination is low as it is an enclosed system and the

preconcentration step takes place in line the system. Lastly the FI system has relatively low cost and is suitable for both shipboard and in situ determination.

### 2.4.1 Laboratory Incubations

Acidified (pH 1.7) seawater samples, sampled at 3min, 24h, 48h, 5days were measured using flow injection analysis with in line preconcentration step and spectrophotometric detection (Lohan et al., 2006; Lohan et al., 2005; Measures et al., 1995). This method is based on the in line preconcentration of Fe (III) on a nitriloacetic acid (NTA) resin, placed in a Global FIA 2-cm mini-column and on the ability of eluted Fe (III) to catalyze the oxidation of N,N-dimethyl-p-phenylenediamine dichloride (DPD, Sigma-Aldrich). All Fe (II) is oxidized to Fe (III) by the addition of H<sub>2</sub>O<sub>2</sub> (Trace metal Grade, Fisher Scientific) to a final concentration of 10μM in the sample prior the DPD oxidation step. The DPD was weighed in a tube and then dissolved with the appropriate amount of deionized MQ. The manifold was checked regularly for contamination by not passing through sample and examining the peak that appeared after the mixing of H<sub>2</sub>O<sub>2</sub>, buffer, DPD and HCl. The analysis was performed with the analytical system manufactured by Dr. H. Planquette and it is described in the paper by Planquette et al. (2007). The detection limit of this method was 0.02nmol/L. The scheme of the manifold is shown at Figure 2.4 and the analyser is shown in Figure 2.5 and it is consisted of an 8-channel peristaltic pump (Gilson) with PharMeds tubes (Cole Palmer) of various internal diameters to obtain the appropriate flow rates for the reagents to pass through to a 6-port valve (VICI, Valco instruments) that was used in two different positions: loading/rinsing and eluting.

Acetate buffer was prepared with ammonium acetate crystals obtained by bubbling filtered high purity gaseous ammonia (BOC) through sub-boiling distilled acetic acid. Hydrochloric acid was purified by sub-boiling distillation. To minimize contamination, sample and reagent bottles were positioned within a class-100 flow laminar bench. Prior to analysis, the entire manifold was rinsed for 2 hours with 1.5N Q-HCl diluted from 6N Q-HCl, however, 2.1 cm Global-FIA mini-columns packed with NTA Superflow resin were used in line for the buffer/DPD and the rinsing solutions to decrease the risk of contamination. The H<sub>2</sub>O<sub>2</sub> solution (5%) and DPD solution (0.05M) were prepared daily.

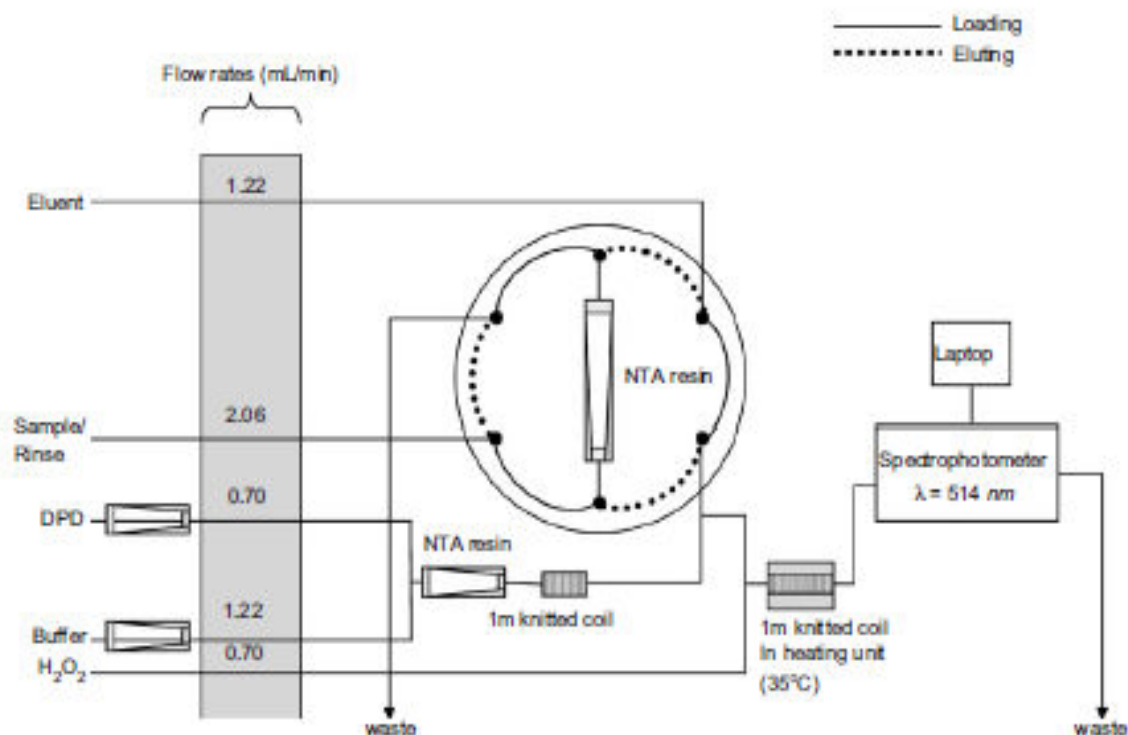


**Figure 2.4** Manifold configuration for rinse, preconcentration and determination of total dissolved iron in seawater (Planquette et al., 2007).

Before the loading step the NTA resin column was rinsed for 30sec followed by the loading step where the sub-samples from the dissolution experiments, buffered at pH 1.7, were pre-concentrated on the NTA resin containing column for 1-2 minutes depending on the expected concentration of DFe. Each sample was repeated thrice. Then the iron bound on the resin was eluted with HCl (1.5M) and it was mixed with DPD and H<sub>2</sub>O<sub>2</sub> forming a pink coloured solution. The pH of the solution stream was maintained at 5.6 using the ammonium acetate buffer. The absorbance was measured at 514nm wavelength using a UNICAM 7825 spectrophotometer fitted with 1-cm flow through cell. The system was controlled by using a programme on software LABVIEW 7.2 (National Instruments) including signal acquisition and data processing. The time for one analytical cycle was approximately 15 min and a minimum of two replicate analyses per sample were made. The range of standards varied according to the soil type and whether they had previously been processed or not. Our experiments produced samples with quite high concentrations and some of them had to be diluted in order to be within detection range.

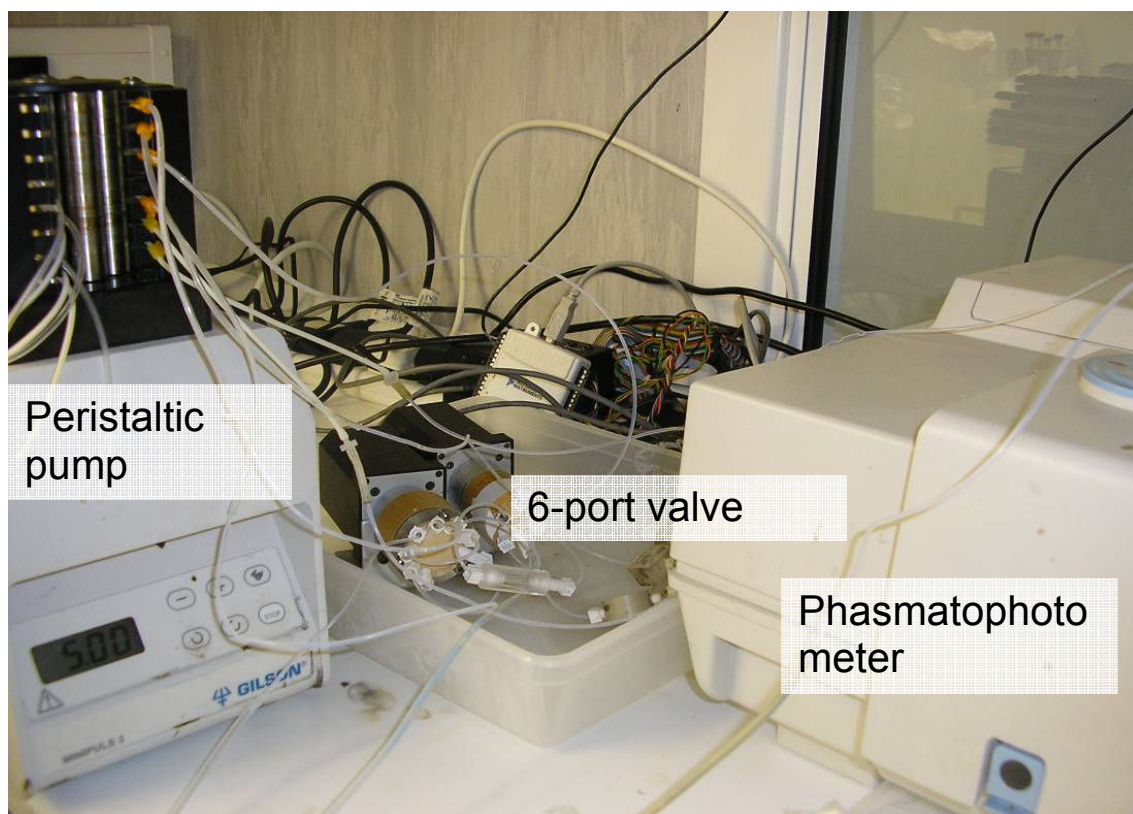


**Figure 2.5** Photograph of the iron analyzer that was used for the laboratory analysis.

The detection limit of this method is 0.072 nM defined as 3\* standard deviation of the blank and the NASS-5 ( $3.71 \pm 0.63$  nM) gave a value of  $3.67 \pm 0.18$  nM.

It is important while using this technique to be certain at all times that the system has the correct pH 5.6 by checking the waste line. Moreover before each analysis the flow rates should be checked by timing 1 ml of each solution gathered in a graded tube. The column did not show signs of malfunction.

## 2.4.2 Shipboard Incubations

An iron flow-injection analysis system has been optimized for the analysis of iron in low concentrations. This method is based on a luminol-based

chemiluminescence detection for total reduced dissolved Fe following preconcentration on a column of 8-hydroxyquinoline (8-HQ) immobilized on Toyopearl gel (Bowie et al., 1998 and Landing et al., 1986). Two thirds of the samples (two out of three replicates) were measured by Micha Rijkenberg during the cruise and I measured the rest of them in the clean laboratory facilities using the same analyzer at the NOC Southampton. The data from the cruise matched the land laboratory data.

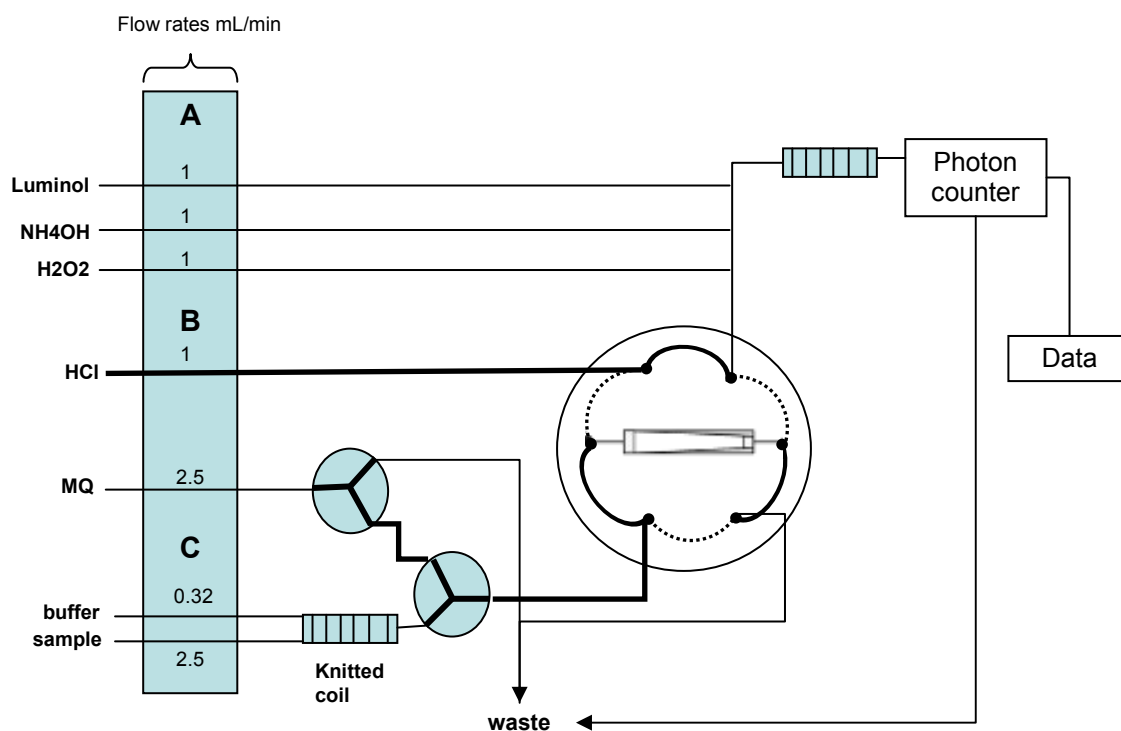


Figure 2.6 Design of the flow injection analysis system for the measurement of total Fe(II).

All solutions were prepared using 18.2 M $\Omega$  cm<sup>-1</sup> MQ-water (Millipore). A 0.02 M Fe(II) stock solution was prepared by dissolving 1.9607 g of ferrous ammonium sulphate hexahydrate (Fe<sup>II</sup>(NH<sub>4</sub>)<sub>2</sub>(SO<sub>4</sub>)<sub>2</sub>·6H<sub>2</sub>O) in 250 ml of 0.1 M HCl (Romil SpA) and 1  $\mu$ M cleaned sodium sulfite (Sigma–Aldrich) was added to this stock to prevent oxidation of the Fe(II). This stock solution was used during the cruise (made up monthly). Other standards were prepared daily in 0.01 M HCl (Romil SpA) by serial dilution.

A 0.01 M luminol (5-amino-2,3-dihydro-1,4-phthalazinedione, Sigma–Aldrich, used as received) stock solution was prepared in 0.1 M Na<sub>2</sub>CO<sub>3</sub> (Sigma–Ultra, minimum 90%, Sigma–Aldrich). A 10  $\mu$ M luminol reagent working solution was prepared in 0.1 M Na<sub>2</sub>CO<sub>3</sub> (Sigma–Ultra, minimum 90%, Sigma–Aldrich), 0.01 M

NaOH (99.99% semiconductor grade, Sigma–Aldrich) and 10  $\mu$ M dimethyl glyoxime (Sigma–Aldrich). A 2 M ammonium acetate stock solution was prepared using acetic acid of SpA grade (Romil) and ammonia of UHP grade (Romil). The pH of the 0.4 M ammonium-acetate buffer was 6.5. The buffer was cleaned in-line using an 8-HQ column.

The FIA consisted of three peristaltic pumps A, B and C as depicted in Figure 2.6. Peristaltic pump A was used to pump Luminol,  $\text{NH}_4\text{OH}$  and  $\text{H}_2\text{O}_2$  at rate 1ml/min, the peristaltic pump B pumped HCl and MQ and pump C the buffer and the sample in such rates that the final pH of buffer mixed with sample is 4.0. A photograph of the iron analyzer is given in Figure 2.7.

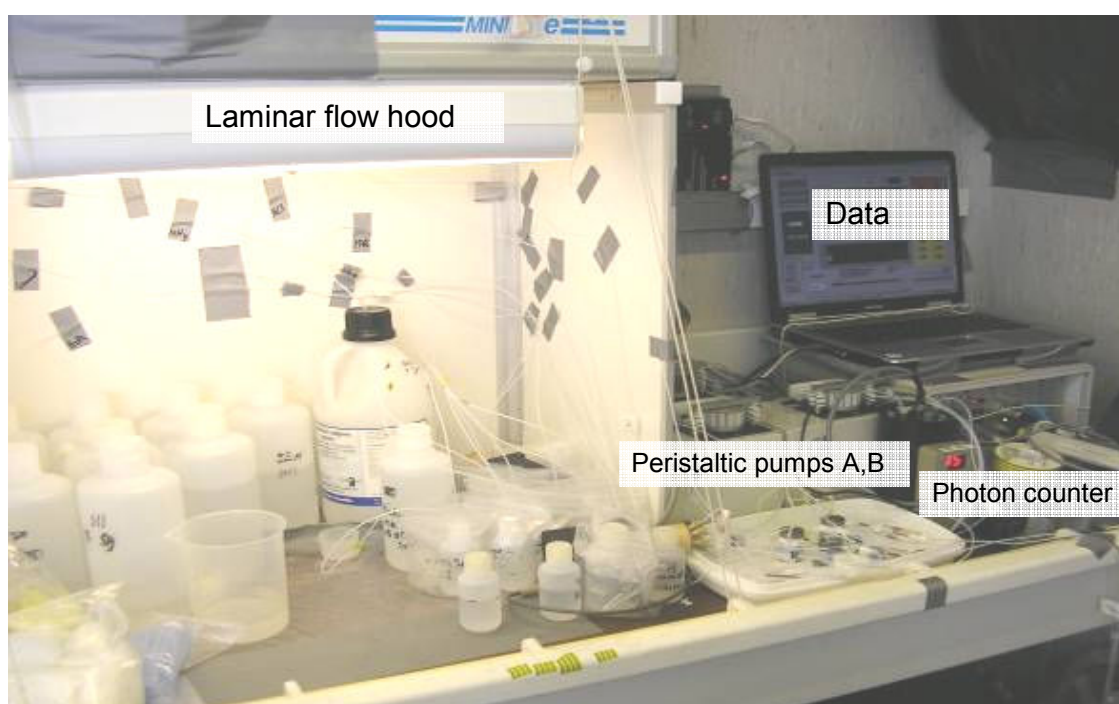


Figure 2.7 Picture of the Iron FI-Cl Analyzer system used during the cruise(Lohan et al., 2006).

During a loading time of 4min the sample passes over the column. The four-port selection valve then switches and the column is rinsed with DI water for 1 min to remove sea salts. The iron later is eluted with 0.3M HCl in reverse flow direction. The eluent mixes and reacts with 100 mM luminol, 0.8M ammonia and 0.5M  $\text{H}_2\text{O}_2$  having a pH of 9.3 before introduction in the detector.

The instrument was calibrated by the method of standard additions using peak height measurement. Iron solution was added in acidified low iron seawater collected at the sampling stations. The analytical blank was on average  $0.015 \pm 0.003$  nM DFe ( $n = 8$ ). The detection limit,  $3 \times$  the standard deviation of the lowest standard addition, was on average  $0.05 \pm 0.03$  nM Fe. An average concentration of  $0.56 \pm 0.05$  nM DFe

( $n = 8$ ) was obtained for an Fe reference material from the Ironages inter-comparison exercise (bottle 93), while the reported inter-comparison value was  $0.59 \pm 0.21$  nM DFe (Bowie et al., 2006).

## **2.5 Manganese Analysis**

Manganese was also analyzed using a flow injection analysis technique. The samples were buffered to pH 8.5 using Q- NH<sub>4</sub>OH due to their acidification after sub-sampling seawater from the dissolution experiments. The manganese was preconcentrated on a packed column containing a metal binding resin (Toyoparl 650M). The column was prepared by closing one end of the column and slowly pipetting inside the resin with. During the packing process the liquid was sucked out the column using a syringe attached at the closed end in order the resin to settle inside homogeneously without leaving gaps. This resin binds and concentrates transition metals while allowing alkali and earth alkali ions pass through. The sample was eluted with an acidic carrier and in this case 0.9 M HCl was used. On the way to the detector, the carrier was mixed with a borate buffered reagent containing tiron (1,3-Benzenedisulfonic acid) and 2,2-dipyridyl. The oxidation of tiron by hydrogen peroxide formed a coloured semiquinone that was detected at 440nm (Figure 2.8). Under alkaline conditions Mn catalyses the reaction. Dipyridyl is added as an activator and limits interference. The method is based on the method of Mallini and Shiller, 1993.

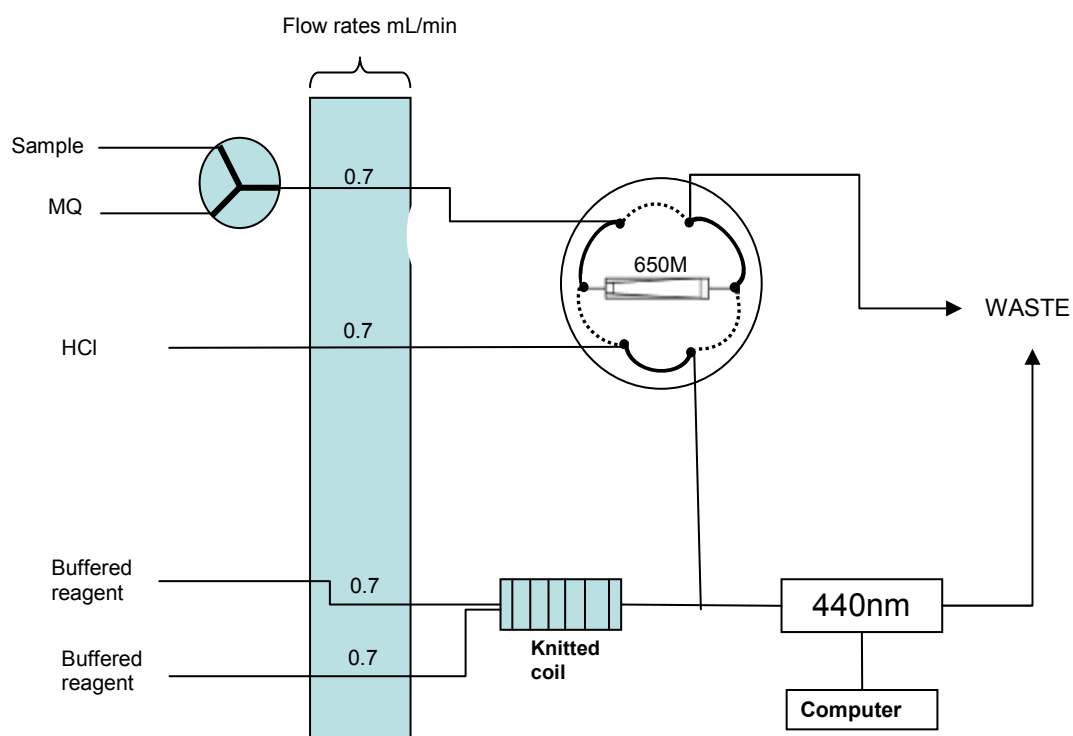


**Figure 2.8** Schematic diagram of the FIA colorimetric Mn system based on that Mallini and Schiller (1993).

The accuracy of the analytical technique was tested with NASS-5 ( $[\text{Mn}] = 16.72 \pm 1.04 \text{ nM}$ ) certified seawater. The measured values were  $14.95 \pm 0.32 \text{ nM}$  and CASS 4 for higher values ( $50.61 \pm 3.45 \text{ nM}$ ) with our value being  $49.64 \pm 3.07 \text{ nM}$ . The detection limit,  $3 \times$  the standard deviation of the lowest standard addition, was  $0.05 \pm 0.03 \text{ nM}$

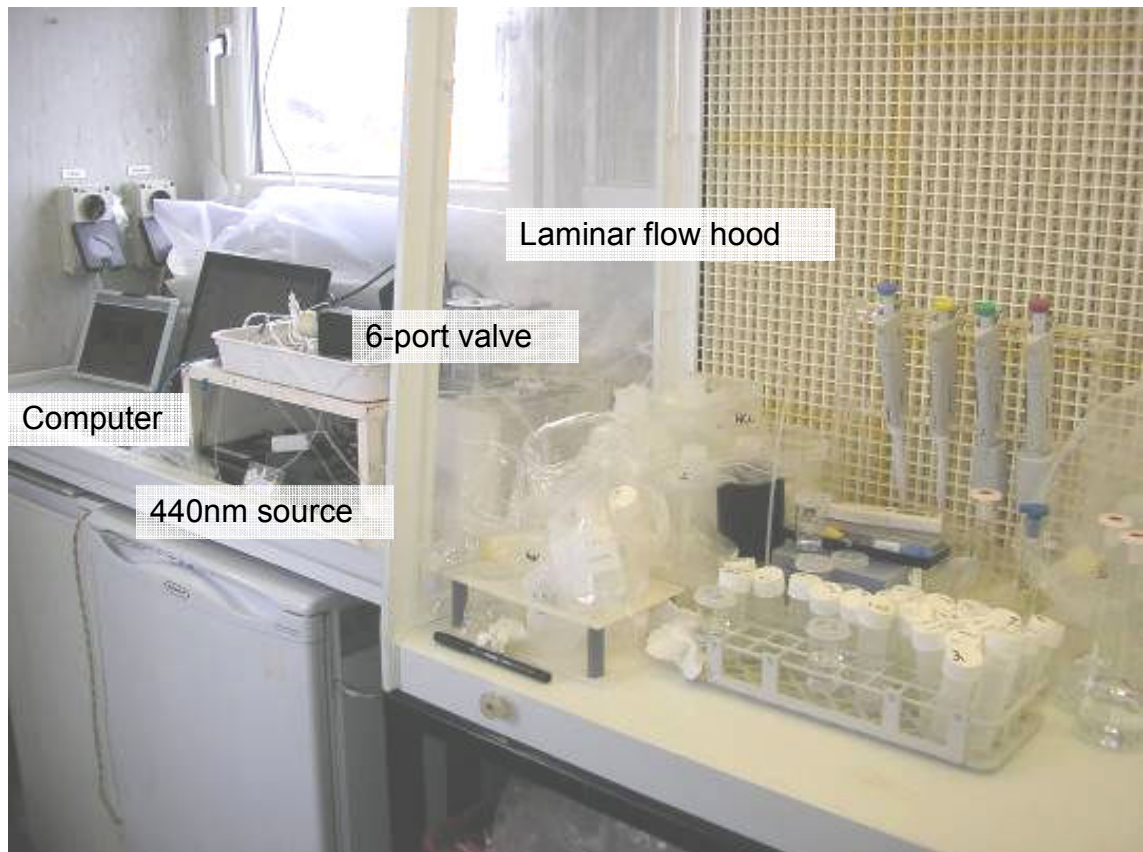


Figure 2.9 Photograph of the manganese analyser used during the cruise

## 2.6 Iron and Manganese Extractions

Soils contain various iron compounds that differ in solubility, reducibility and extractability. Sequential extractions were conducted in order to define the amount of the amorphous iron species and the amount of manganese bound to carbonate and oxide phases. Poulton and Canfield (2005) developed a sequential extraction procedure for iron in sediments. In this project only two stages of the sequential extraction scheme were used because those iron mineral phases deriving from these stages were of interest.

Stage one of the leach, employed 1M hydroxylamine hydrochloride with constant shaking for 24 hours to release the loosely bound fraction of iron species (easily reducible) or else called the ‘free iron’ fraction, that includes ferrihydrite and lepidocrocite.

The second and final stage using buffered sodium dithionite, releases the iron mineralogical species that are less easily reducible, including goethite and hematite (Poulton et al., 2005; Sulzberger et al., 1995). Since the extraction with citric buffered

dithionite has not been performed for manganese, it is not yet known what forms of manganese were extracted during this leach.

Specifically, around 10mg of dust or dust on filter was placed in 13ml centrifuge tubes and 5ml of 1M hydroxylamine-HCl solution in 25%v/v acetic acid was added (Chester, 1990). After 24 hours of extraction with constant agitation the samples were centrifuged then the supernatant was carefully removed, the soil was washed with 5ml MQ water centrifuged again and the water was discarded. Subsequently in the same centrifuge tube 5 ml of sodium dithionite solution was added. The sodium dithionite solution was buffered to pH 4.8 with 0.35M acetic acid/ 0.2 M sodium citrate (Mehra, 1960). After 2 hours the extraction was completed and the supernatant was kept for analysis by the flame atomic absorption spectrophotometer (Varian SpectrAA 10).

The standards were prepared in the same matrix as the digestions, and analyzed by standard addition for Fe (III) solution. For the precision of the citric buffered dithionite method two internal standards were used with a value of  $0.28 \pm 0.01\%$  Fe and  $0.33 \pm 0.02\%$  Fe and our values were  $0.26 \pm 0.01\%$  Fe and  $0.32 \pm 0.02\%$  Fe respectively. The blanks were prepared by the using the reagents without the addition of soil and then measured as a sample. The results were below the detection limit.

Total Fe and Mn were measured by Matt Pattey PhD student at the NOC using the HF digestion method.

## **2.7 Field Emission Gun Scanning Electron Microscopy FEGSEM**

FEGSEM (Field Emission Gun Scanning Electron Microscope) shows very detailed 3-dimensional images at much higher magnifications than are possible with a light microscope.

Quantities of 10-20 mg of dust were dispersed in ethanol and placed in an ultrasonic bath so the agglomerates could be disaggregated. An aliquot of the dust suspension was placed on a stub and the ethanol was evaporated. The dust on the stub was coated with a fine layer (3nm) of platinum and the specimen was placed inside the microscope's vacuum column through an air-tight door. After the air was pumped out of the column, an electron gun [at the top] emitted a beam of high energy electrons. This beam travels downward through a series of magnetic lenses designed to focus the

electrons to a very fine spot. As the electron beam hit each spot on the sample, secondary electrons were knocked loose from its surface. A detector counted these electrons and sent the signal to an amplifier. The final image has been built up from the number of electrons emitted from each spot on the sample.

A model soil mimicking the Saharan soil was prepared, which contained 60% quartz, 35% kaolin and 5% synthetic goethite. The quartz material was acid washed with HNO<sub>3</sub> at high temperature to dispose of any amount of iron oxides and the kaolin soil was washed and dried before mixing took place. An aliquot of this soil was wetted with acid and was left to dry under an infrared lamp. The images provided by this soil helped understand the more elaborate images taken from real soil.

Energy Dispersive X-ray Spectroscopy was used in order to find the elements present in areas of interest of the samples such as iron, silicon, oxygen and manganese.

## **2.8 Field Emission Gun Transmission Electron Microscopy FEGTEM**

FEGTEM is a microscopy technique whereby a beam of electrons is transmitted through an ultra thin specimen, interacting with the specimen as it passes through it. An image is formed from the electrons transmitted through the specimen, magnified and focused by an objective lens and appears on an imaging screen, a fluorescent screen in most TEMs, plus a monitor, or on a layer of photographic film, or to be detected by a sensor such as a CCD camera.

The FEGTEM sample was prepared by depositing a few drops of the acetone and soil mixture onto a holey carbon coated copper TEM grid and evaporating to dryness. The sample was then immediately inserted into the high vacuum chamber of the TEM. When an area of interest was encountered Energy Dispersive X-ray Spectroscopy as well as Electron Energy Loss Spectroscopy (EELS) was used to characterize the particles present.

Electron Energy Loss Spectroscopy is complementary to X-ray spectroscopy, and it can be utilized for qualitative and quantitative element analysis as well. EELS is based on transmission electron microscopy is the only way to characterize the electronic structure of identified nano-scale materials (<http://www.scienceofspectroscopy.info>).

## **2.9 X-ray Diffraction Analysis (XRD)**

X-ray diffraction (XRD) is a versatile, non-destructive technique that reveals detailed information about the chemical composition and crystallographic structure of natural and manufactured materials.

A crystal lattice is a regular three-dimensional distribution (cubic, rhombic, etc.) of atoms in space. These are arranged so that they form a series of parallel planes separated from one another by a distance  $d$ , which varies according to the nature of the material. For any crystal, planes exist in a number of different orientations - each with its own specific  $d$ -spacing.

Some milligrams of soil were ground with a pestle and mortar and pressed into a back-loaded aluminium specimen holder with a 27mm internal aperture and scans were taken using a Philips PW1050 X-ray diffractometer (CuK $\alpha$  radiation), with a post sample monochromator at a standard power setting of 40kV and 30mA.

## Chapter 3

### Particulate Iron and Manganese

#### 3.1 Introduction

Saharan Dust has been reported to have reached areas all around the world such as South America, Northern Europe (Jickells, 2001; Mahowald et al., 2005; Wu et al., 2007). Mineral particles are found in the atmosphere when strong wind currents over hot desertic areas mobilise soil particles that can reach very high altitudes; from there it can be transported worldwide by winds, covering distances of thousands of kilometers. The Bodélé Depression of northern Chad is the world's greatest source region of mineral dust into the atmosphere. Observations indicate that dust emission events are triggered when near-surface wind speeds exceed 10 m/s, associated with synoptic-scale variability in the large-scale atmospheric circulation (Mahowald, 1999; Mahowald et al., 2005).

These mineral particles are transported because of a combination of various factors such as wind velocity, physical properties of the soil (e.g. particle size distribution) and surface conditions of the terrain (e.g. surface roughness) can cause particle aerolization. These mechanisms are accountable for moving the particles by wind and are shown in Figure 3.1: (1) suspension for particles  $<70\mu\text{m}$ , (2) saltation for particles  $70\text{-}500\mu\text{m}$ , which are the dominant processes, (3) creep for particles  $>500\mu\text{m}$  and (4) sandblasting for particles  $0.1\text{-}10\mu\text{m}$  (Usher et al., 2003).

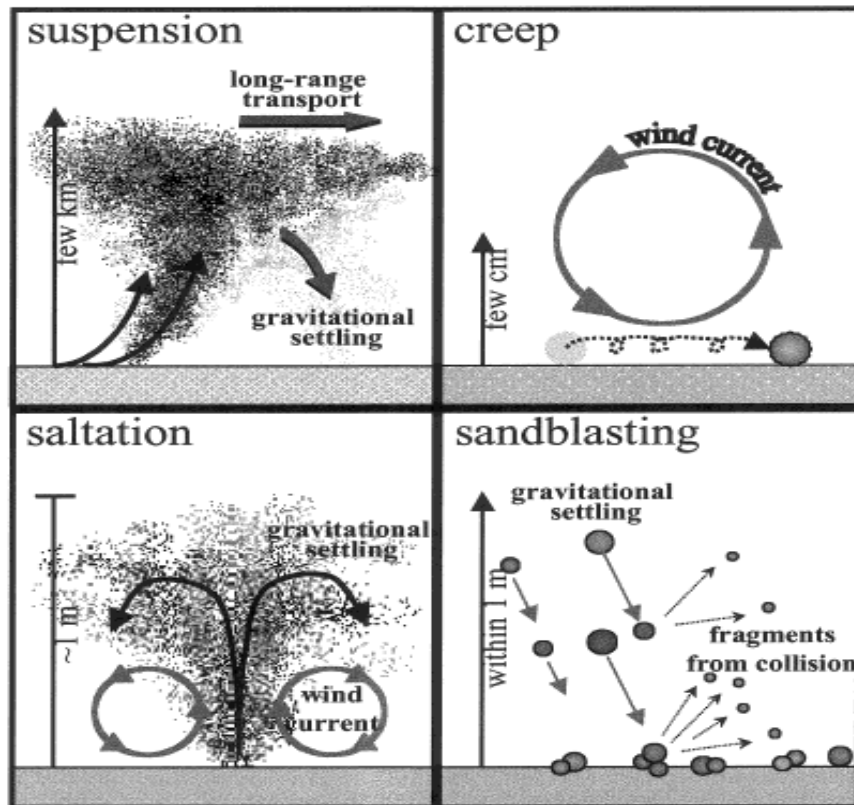


Figure 3.1 Schematic representation of the possible wind induced entrainment processes to move, emit, and transport mineral dust particles from the source into the troposphere (Usher et al., 2003).

The mineral dust is eroded soils so their chemical composition is similar if not identical to that of crustal rock (Usher et al., 2003). The larger coarser particles are typically composed of quartz, feldspars and carbonates and the smaller finer particles are often clays or micas but their relative contents are variable according to the collected area. Dusts from African regions have more brown, yellow and red colour which is due to the higher iron content (hematite). Investigations report that the southern Sahara and Sahel regions contain more kaolinite and hematite than other Saharan areas (Usher et al., 2003).

Usher et al (2003) report that the major chemical forms of iron initially present in aeolian mineral dust are likely to be crystalline Fe (III) oxides and (hydr)oxides e.g hematite,  $\text{Fe}_2\text{O}_3$  and goethite,  $\text{FeOOH}$  which dominate in Saharan, whereas more amorphous iron such as ferrihydrite exists only in small quantities since the aging of the dust transforms it to more crystalline forms such as goethite. Although ferrihydrite with time will convert to more stable iron oxides the transformation can be retarded by adsorption of various species both organic and inorganic (Jambor et al., 1998).

Crystalline hydroxides such as hematite, goethite, magnetite are much less soluble than amorphous iron hydroxides such as ferrihydrite and clay minerals (Journet et al., 2008). For example Zhu et al. (1993) found that the solubility of iron derived from ferric hydroxide can be  $10^5$  higher than when coming from hematite in the same conditions.

So far there have been no measurements to determine the chemical forms of iron in such a complex medium as the atmospheric liquid phase (Deguillaume et al., 2005). In the study of Deguillaume et al (2005), they mainly focus on the amorphous fraction of iron (ferrihydrite) which until recently few geochemists or mineralogists seemed to be aware that the 'amorphous  $\text{Fe}(\text{OH})_3$ ' phase widely used in geochemical calculations is an inaccurate representation of ferrihydrite (Jambor et al., 1998).

Two of the most significant roles of Ferrihydrite in the geochemical cycle are as an adsorbent of various trace elements and as a control on the concentration of iron in surface waters. Our interest in this project lies with the role of ferrihydrite to control the concentration of iron in seawater since amorphous iron species and more specifically ferrihydrite has a solubility of  $\sim 0.08\text{nM}$  (Liu et al., 1999; Wu et al., 2001) in seawater while more crystalline oxides such as goethite and hematite have too low solubility to be detected in laboratory experiments (Wu et al., 2001)

The amount of amorphous iron in Saharan soil is very small to make an important impact when dust is deposited in the seawater. However, if more crystalline iron forms such as goethite, which are the dominant iron species in Saharan soil as already reported, transform during the dust transport into more amorphous species it is suggested that would make a difference in the seawater solubility of iron.

This project tested the hypothesis that cloud processing transforms the mineralogy of iron species towards the formation of more amorphous species. It also alters the mineralogy of other minerals in the Saharan soils including those containing Mn.

### 3.2 Atmospheric Processes

There are several factors influencing the solubility of Fe and Mn from aerosols such as the pH of the aqueous phase, the mineralogical composition of the particles, (eg. Spokes et al., 1994, Desboeufs et al., 1999) as well as the interaction with acidic gases and organic compounds and photochemical reactions during the transport of dust particles to the seawater (Figure 3.2). In this study we decided to focus our atmospheric simulation on the first two factors.

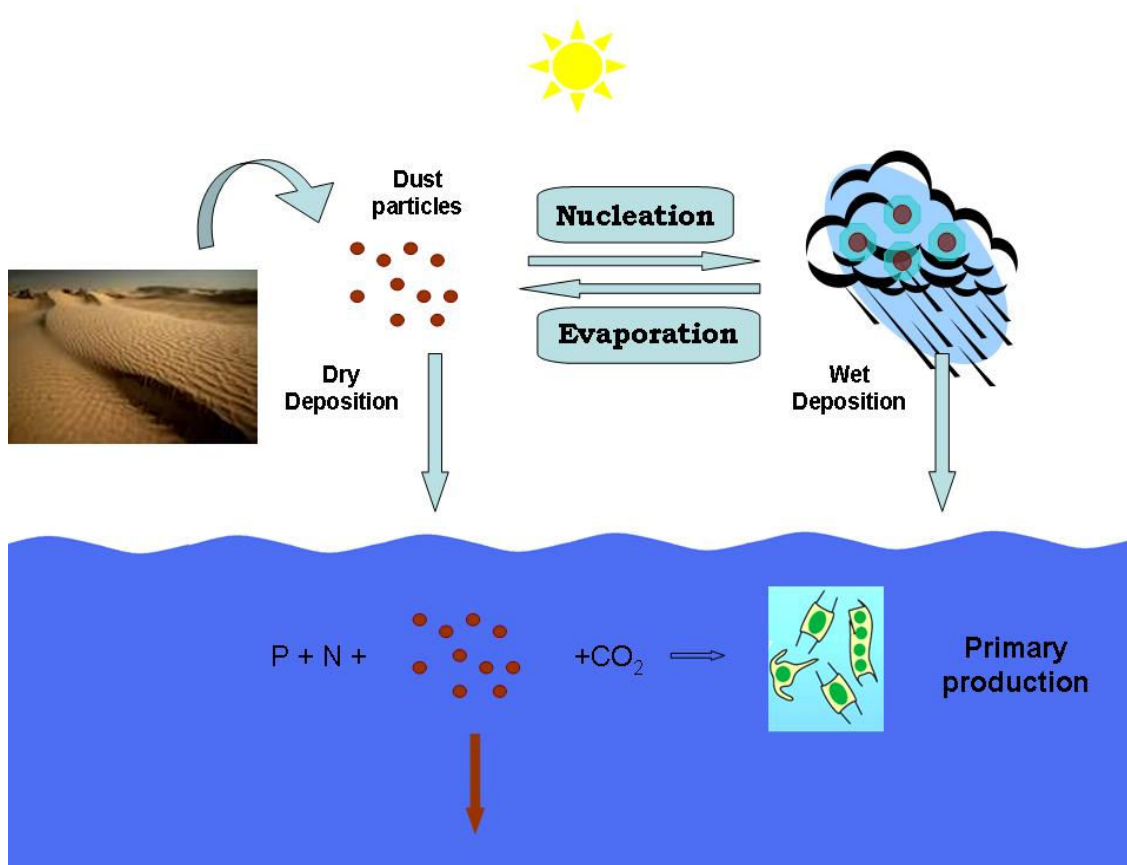
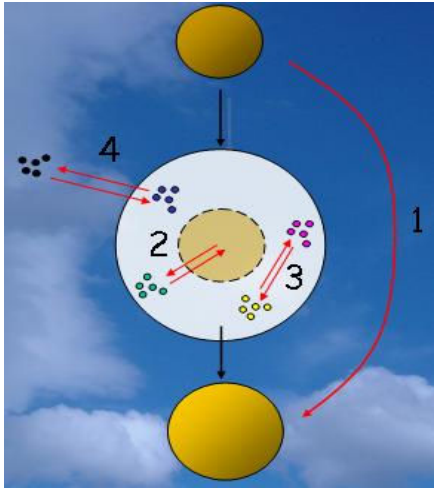


Figure 3.2 Schematic of the journey of mineral particle in the atmosphere and deposition in the seawater.

It has been postulated by Zhuang et al. (1993) that the mechanism by which the lability of aerosol metals is increased in the atmosphere, thus influencing the amount of metal that can be released on mixing into seawater, is low pH cloud cycling. During the cloud cycling the mixing of mineral dust with sulphate/sulphuric acid produce acidic hygroscopic aerosols as a result of coalescence processes within clouds. This possible mechanism might increase the solubility of atmospheric iron in cloud water or

rainwater. Due to cloud processes the aerosol resulting from evaporation of cloud droplets may be quite different from that which entered the cloud.

The four main processes that aerosol particles take part in during the nucleation and formation of clouds are shown in Figure 3.3. These are: (1) the CCN composition and size can change after the droplet has evaporated, (2) dissolution of soluble content of the particle, (3) and aqueous reactions inside the water droplet and (4) transfers between atmospheric gases and liquid phase.



**Figure 3.3 Possible main processes impacting aerosol particles within the cloud droplet**

Atmospheric trace gases such as  $\text{HNO}_3$ ,  $\text{SO}_2$  and  $\text{NH}_3$  (Deguillaume et al., 2005) are taken up within the cloud droplets and affect the amount of water soluble material by modifying the pH. Part of the dissolved fraction from the leached mineral will be deposited back on the particle surface during the evaporation step.

Studies such as Loye- Pilot et al. (1986), Desboeufs et al. (1999), Mendez et al. (2008), both from rainwater studies and laboratory experiments, have shown that dissolved – particulate speciation of trace metals in rainwater is pH dependent. Solubility values increase as the pH of the mineral dust decreases (Desboeufs et al., 2005; Spokes et al., 1996; Spokes et al., 1994).

### **3.2.1 Assessment of processes**

Two different experiments were designed and carried out in order to simulate cloud processing. This section explains what is taking place during cloud processing and in what way the mineralogy of the soil particles might be affected. A simplistic

schematic picture of what is proposed to be taken place at the iron oxides mineralogy is shown in Figure 3.4

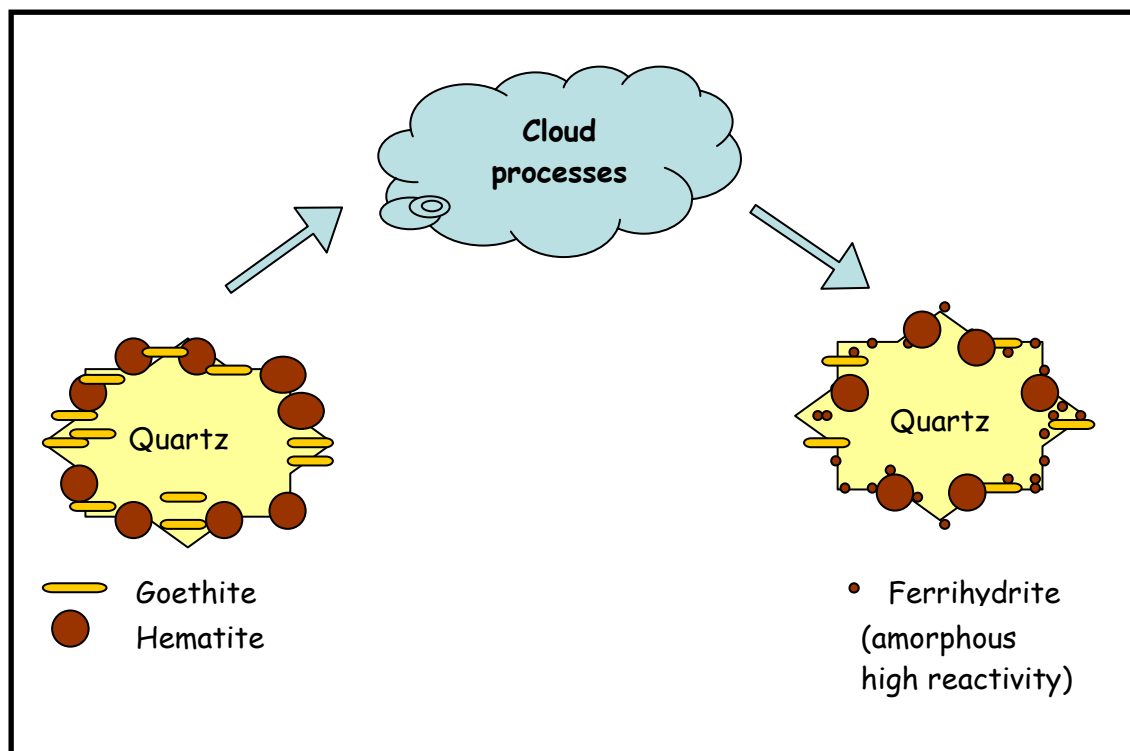


Figure 3.4 Schematic picture presenting the hypothesis of the alteration in the mineralogy of iron oxides that have been cloud processed.

The first experiment was carried out according to the Spokes, Jickells et al. (1994, 1996) experiments, where around 26 mg of soil were added in 1L MQ water and the pH of the solution was cycled twice between 2 and 5-6 with one day interval. The only difference in our experiment was the amount of soil used (10mg) and the origin of the soil was from another Saharan region.

The aim of this experiment was to reproduce the pH ranges likely to be encountered by aerosols in the atmosphere. Due to the way this experiment was set up, it did not allow the particles to dry out between the cycles.

### 3.2.1.1 Dissolution of Hematite/Goethite

During the dissolution by the acid, protons are adsorbed to the surface of the oxide and facilitate the detachment of iron (III) from the lattice. A detachment process of a surface metal species can occur subsequent to the polarization and weakening of the critical metal-oxygen bonds at the hydrous oxide surface (Zinder et al., 1986). The

electron after it has been transferred to the oxide surface is free to move in the surface layer until it has been consumed by the metal ion that becomes the center of the detachable group (Zinder et al., 1986). That metal ion is reduced and the surface protonation of the nearest-neighboroured oxide or hydroxide, takes place (Suter et al., 1991). The surface protonation is fast and after reduction of the central metal ion, the existing coordination sphere of the metal center will be labilised.

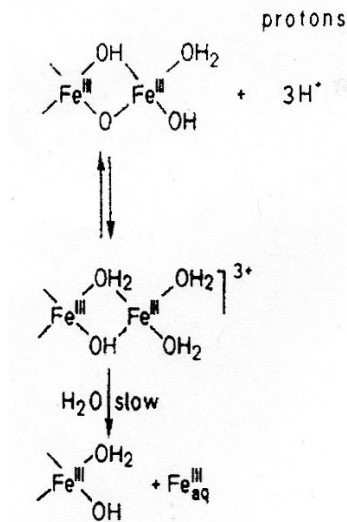


Figure 3.5 Representation of the reaction mode for the dissolution of Fe(III) (hydr)oxides by protons. Surface coordination controls the dissolution process (Sulzberger et al., 1995; Sulzberger et al., 1989; Sunda et al., 2003)).

The above theory derived from studies on goethite but it is also applicable to other reducible oxides (Sulzberger et al., 1989; Suter et al., 1991). The principle of the rate limiting detachment after ligand coordination, protonation and reduction steps may be valid for the dissolution kinetics of any type of oxide. In nature reduction may occur by different pathways such as by bintate complex formers that form chelates, by reductants such as ascorbate, by light.

During low pH (Spokes et al., 1994) there is fast binding of H<sup>+</sup> on the iron oxides that results in the weakening of the bonds in the proximity of a surface Fe (III) centre; this is followed by a slow detachment of the surface Fe (III) species into solution.

As the pH is increased iron is precipitated. Figure 3.6 shows the geochemical bench graphs of the influence of pH on the speciation of goethite and hematite, the most abundant ferric oxide phases in Saharan desert. Spokes et al (1994) obtained results

showing that iron solubility for Saharan dusts increased by a factor of 5 when the pH goes from 6 to 2. At pH 6 Fe(III) is precipitated as an amorphous iron (hydr)oxide species such as ferrihydrite (Hove et al., 2008). In addition, some of the dissolved Fe(III) may be adsorbed on the surface of iron oxides. Iron (II) also adsorbs strongly above pH 5 on hematite (Suter et al., 1991).

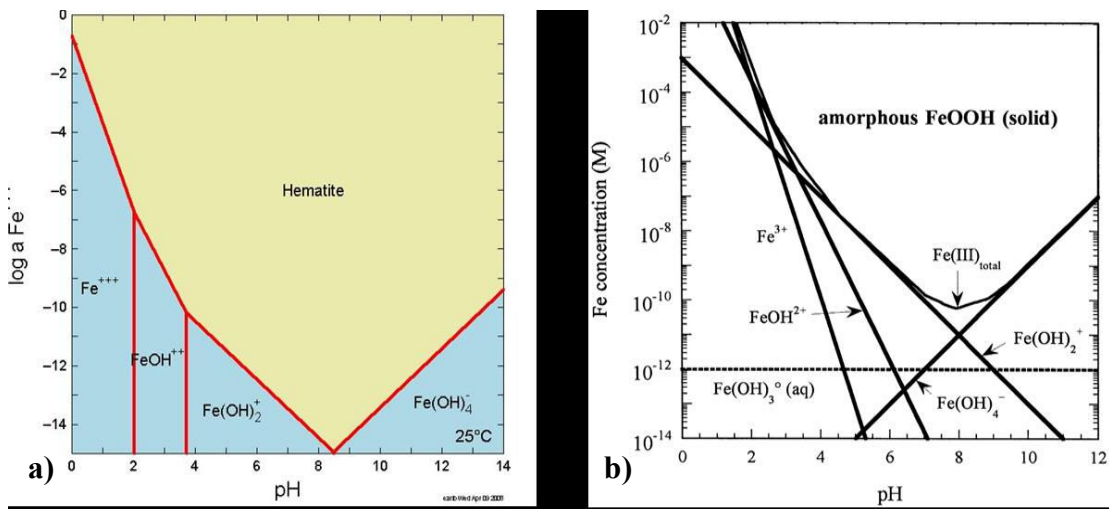


**Figure 3.6** Minteq geochemical bench graphs of iron concentration versus pH for a) hematite and b) goethite(Stumm et al., 1981) minerals.

Thus, it is believed that after artificially processing the Saharan soil more labile and soluble species of iron were produced such as amorphous iron nanoparticles colloids quite possibly ferrihydrite. These particles were subsequently used for the seawater dissolution experiments.

The second experiment was set up to simulate cloud processing by wetting of soil particles with H<sub>2</sub>SO<sub>4</sub> and letting them dry. It was set this way to represent the encounter of dust particles with gases such SO<sub>2</sub> or DMS in the atmosphere and because the processed soil particles were easy to recover. The encounter of dust particles with oceanic dimethylsulfide (DMS) is very important because it is the major natural source of sulfur to the atmosphere and contributes both to the tropospheric sulfur burden and to particle formation and growth in the atmosphere. The atmospheric sulfate aerosol particles that evolve from biogenically-derived DMS emissions play a role in the global radiation balance directly through the upward scatter of solar radiation and indirectly as cloud condensation nuclei (CCN) (Bates et al., 1998; Bates et al., 2000).

The Saharan soils contain roughly 3% iron. Most of that iron is present as hematite and goethite, which are crystalline iron oxides. Addition of sulphate quickly

caused the adsorption of sulphate onto the surface of the mineral particles that changed the pH of the surrounding area. So, sulphate became rather advantageous as it could easily from this position exchange electrons with a Fe(III) surface centre. Fe(III) would reduce to Fe(II) which has a weaker O-bond than Fe(III) O-bond, that can be easily broken. Thus the surface Fe(II) was released into solution (Sulzberger et al., 1989). Almost all of the dissolved fraction from the leached mineral will be deposited back on the particle surface during evaporation step. The particles were probably coated with soluble materials such as FeSO<sub>4</sub>, since iron in solution under its III oxidation state forms FeSO<sub>4</sub> complex with sulphate ions, and amorphous iron species such as ferrihydrite (Hove et al., 2007) that had been formed and precipitated and where adsorbed silicate material.

Whether the observed Fe(II) arises from active Fe(III) reduction, which may be photochemically mediated, or simply reflects the speciation of the metal within the aerosol itself cannot be determined from these experiments. Enhancement of solubility as a result of low pH cycling and possible organic complexation could, however, increase the availability of these metals once deposited to seawater. Zhu et al. (1993) suggest that the Fe which precipitates after pH cycling has a “loose” structure, which is rapidly dispersed, perhaps as colloids, on input to seawater. Even if the element is not properly dissolved, Zhu et al. (1993) suggest that it may exist in form which is chemically more available to organisms.

### **3.2.1.2 Manganese Dissolution**

It is hypothesized that after artificially processing the Saharan soil particles not only the iron mineral species but also the manganese mineral species would change and in order to see if there was any change in the mineralogy, sequential extraction leach was performed.

Within aqueous environment, Mn has two dominant oxidation states, insoluble Mn(IV) and Mn(II) which is soluble in water. According to Spokes et al., (1994) Mn is less soluble before acidification. Their results show that low pH enables reduction to occur, releasing soluble Mn(II) into solution which, as a result of its slow chemical reoxidation kinetics (Kessick et al., 1975) remains in solution. Also the dissolution process of Mn, in the Spokes et al (1994) study, appeared to be irreversible and this

suggested that no simple relationship could exist between pH and solubility in rainwater. Rather, the solution phase Mn concentration may depend strongly on whether the aerosol has been subjected to low pH leaching (Spokes et al., 1994).

### 3.3 Iron Sequential Leaches

Initially leaching experiments were performed on non-treated Mali (MS) which contained 3.7% Fe (w/w) and Niger (NS) soil which contained 4.7% Fe (w/w) as defined by the total digestion performed by Matt Patey. Then the same sequential extraction was conducted on the filters with the retrieved dust (MSJ, NSJ) from the experiments as described in section 2.2.1 Spokes and Jickells (1994) low pH cycled soil and 2.2.2 Acid cycled (MB, NB) soil.

The initial leach was performed with hydrochloride-acetic acid see section 2.6 which released the metals held within carbonate and (hydr)oxide phases mainly ferrihydrite and lepidocrocite. This phase is called the ‘easily reducible phase’ and the letter used as abbreviation to describe it will be H. The second leach was performed with citric buffered dithionite that extracted mainly crystalline oxides such as goethite and hematite. This phase is termed the ‘reducible phase’ a D will be used to refer to it. The results from the leaches are shown in Table 3.1.

**Table 3.1 The percentage of Fe (% w/w) in total Fe content in soil, in Niger and Mali soil samples processed and non- processed (n=3).**

NIGER		SOIL(non treated)	SJc	MB(HCl)a	MB(H <sub>2</sub> SO <sub>4</sub> )b	Spokes et al. 1996	
Easily reducible iron species	FeH	1.0±0.1	1.6±0.3	3.5±0.2		0.02	%loosely bound
Reducible iron species	FeD	35.2±2.3	37.9±2.7	29.6±2.4		2.4	%as oxide or carbonate
MALI						97.6	%Residual
Easily reducible iron species	FeH	1.2±0.05	1.8±0.2	3.6±0.3	4.6±0.4		
Reducible iron species	FeD	31.1±2.4	50.1±3.6	37.4±0.4	28.6±1.9		

*a Acid treated soils with HCl used for laboratory dissolution experiments*

*b Acid treated soils with H<sub>2</sub>SO<sub>4</sub> used on cruise dissolution experiments*

*c Low pH treated soils according to Spokes and Jickells (1994)*

Both the non treated Mali and Niger soils appeared to contain roughly the same amount of the easily reducible oxides 1% and the amount of citric buffered dithionite extracted iron species around 30-35%. In the same Table 3.1 are presented the results

from the sequential extraction used for Saharan dust from the study of Spokes et al. (1994). For their first extraction they used acetate and they claim to have extracted the loosely held iron species and hydroxylamine hydrochloride used for the second extraction to extract the oxides and carbonate associated iron species. The first leach provided 0.02% Fe and the second leach 2.6% Fe of the total iron present. In our study hydroxylamine hydrochloride was used for the first leach and it provided a smaller number for the soil used in this study which is logical since in Spokes et al., (1994) they used aerosol dust particles  $< 2 \mu\text{m}$  diameter. It is expected aerosol dust particles to contain more reactive iron since the processes in the atmosphere take place that can alter iron reactivity and the increase in the % Fe of the hydroxylamine hydrochloride leach for the treated soils re-enforce that notion. The second leach of this project with citric buffered dithionite was not performed from Spokes et al., (1994) thus it can not be compared.

The single most striking observation to emerge from the data comparison was an increase in the amount of hydroxylamine hydrochloride-acetic acid leachable fraction in the both Niger and Mali soil samples that have been processed either with the Spokes and Jickells experiments, or the acid treating experiment, as shown in Figures 3.7 (a), (b) and Figures 3.8 (a), (b).

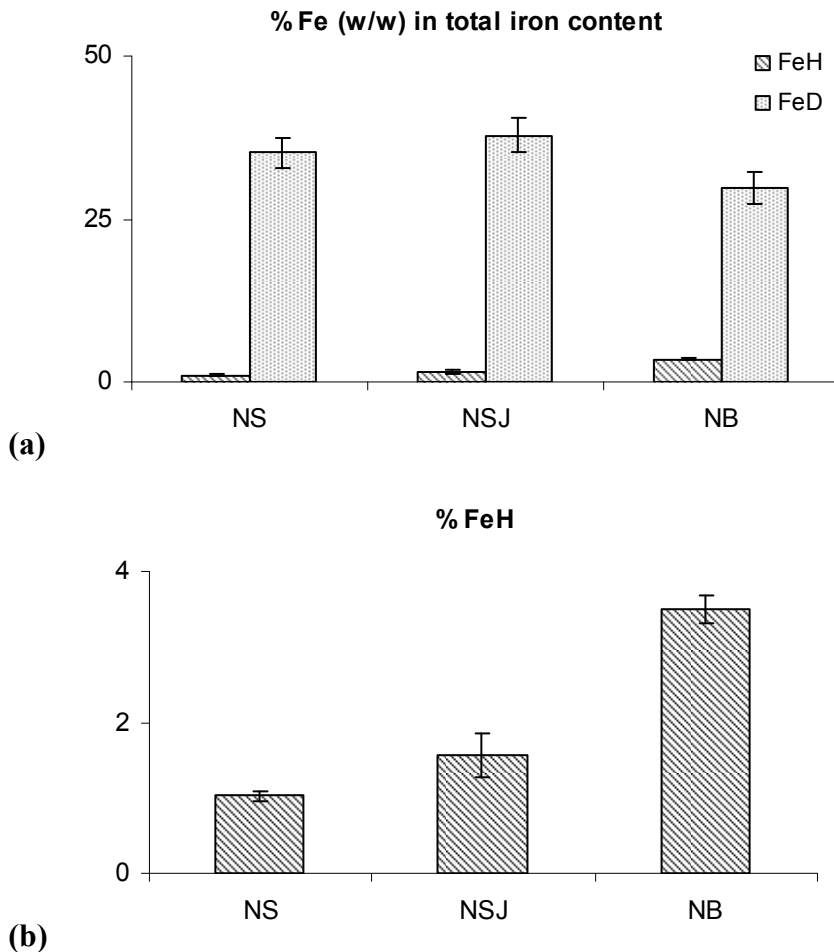


**Figure 3.7 a) Percentages of Fe (w/w) in total iron content of Niger soil: easily reducible iron species, FeH, amorphous iron oxides (ferrihydrite, lepidocrocite) and reducible iron species, FeD, crystalline iron oxides (goethite, hematite) (n=4; NS = not treated dust, NB= acid treated dust, NSJ = low pH acid cycled in MQ water), b) zoomed in the percentages of FeH.**

In detail the non treated Niger soil contained 1% FeH, easily reducible iron species, and around 35% FeD, reducible iron species such as hematite and goethite. However, after the simulated cloud processing, the amount of FeH increased to 1.6% for the NSJ samples and to 38% for the NB.

The same picture occurred for the Mali soil, 1.2%FeH was contained in the non treated soil while 1.8% FeH was contained in the low pH cycled soil (MSJ), 3.6% FeH contained in the HCl acid treated soil (MB) and 4.6% FeH was present in the H<sub>2</sub>SO<sub>4</sub> acid treated soil that was used for the dissolution experiments during the cruise.

The confidence level for the FeH among the three different soil types (NS, NSJ, NB) was more than 99.9% and the same was for FeD value for NS-NB and 95% for NS-NSJ.

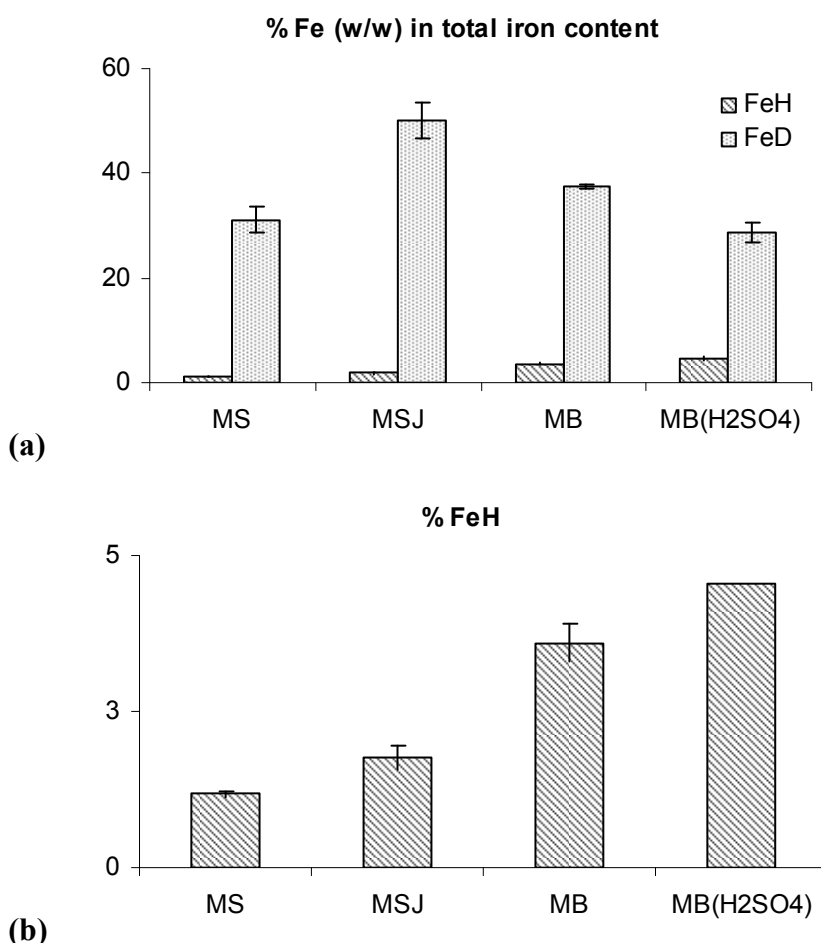


**Figure 3.8 a) Percentages of leached Fe (w/w) in total iron content of Mali soil: easily reducible iron species, FeH; amorphous iron oxides (ferrihydrite, lepidocrocite) and reducible iron species, FeD; crystalline iron oxides (goethite, hematite) (n=3; MS = not treated dust, MB= acid treated soil, MSJ = low pH acid cycled soil, b) zoomed in the percentages of FeH.**

The important finding in this study is the increase in the FeH leached fraction after the soil samples had been treated. It did not matter what the origin of the soil was as no major difference in the amount of the amorphous iron oxides between Niger and Mali samples was found. Probably the processes altered the mineralogy of the iron species contained in the soils as suggested in the previous section. Thus, iron-containing crystalline species have transformed into more amorphous iron oxides and soluble iron salts that were extracted in the initial step of the sequential extraction. Although these two soils contain different amounts of total iron (3.7% Fe<sub>tot</sub> Mali and 4.7% Fe<sub>tot</sub> Niger soil), the amount of the reducible iron are similar and similar amounts of iron was transformed into easily reducible phases.

However it is rather interesting that the amount of easily reducible iron species, FeH of the acid treated (MB, NB) samples increased more than the samples that were low pH cycled (MSJ, NSJ). Maybe due to the different processes used for the processing of the soils and most significantly the pH effect, they could influence the mineralogy of the soils differently, however, without any further experiments we can not be absolutely certain as to what really took place and to what extent.

Another important finding was that the type of the acid used for the treatment did matter since the FeH fraction increased to 4.6% when the Mali soil was treated with H<sub>2</sub>SO<sub>4</sub> from 3.6% FeH amount contained in Mali soil that had been treated with HCl.

The test for significance of difference was calculated for all possible pairs (MS, MSJ, MB) for the values FeD and FeH and was found to be more than 99.9% in all cases.

### **3.4 Manganese Sequential Leaches**

Leach data on the dust samples defined the two fractions of Mn species. The first fraction, MnH, hydroxylamine hydrochloride leach, probably contained all the manganese present as loosely associated and surface hydroxide phases (MnO<sub>2</sub>) in the soil. The second fraction the manganese, MnD, citric buffered dithionite, associated with oxide phases. The results from the leaches are given in Figures 3.9 and 3.10. The total amount of Mn was 0.06% for the Niger soil and 0.07% for the Mali soil in total amount of soil.

The initial leachable fraction of manganese, MnH, was 22.2% for the Niger soil and 31% for the Mali soil which is comparable to leachable Mn amount from the hydroxylamine hydrochloride extraction at the Spokes et al., (1994) study, and the citric buffered dithionite leachable fraction, MnD was 10.3% and 8.5% respectively. The amount of manganese extracted MnH for the acid treated Niger and Mali soil were 21.2% and 34.7% and the amount of manganese extracted MnD were 8.7% and 8.5% respectively.

The value of the MnD for the MS and MB was not significantly different (confidence level 53%) and the confidence level for the MnH is 84% so there is a significant difference between the two MnH values for MB and MS. The Niger acid

treated and the non treated soil have significantly different MnH and MnD values because the confidence level is 95% and 83.1% respectively.

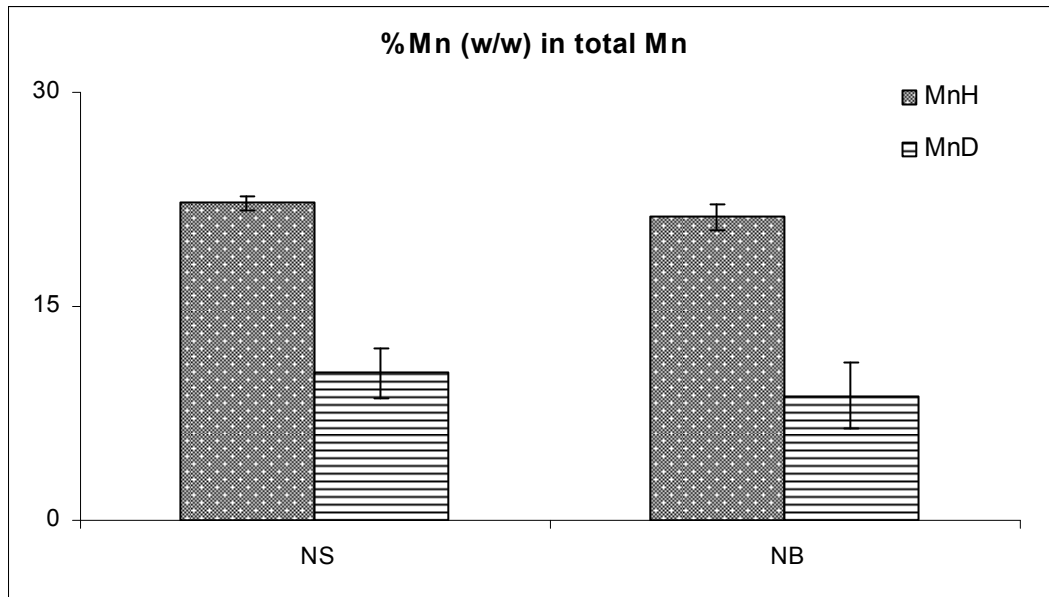


**Figure 3.9** The percentage of leached Mn (w/w) in total Mn content of soil from the two leaches in Niger samples (n=3; NS: not treated soil, NB: acid treated soil).

Interestingly, when the soils were acid treated (MB, NB), we got roughly the same values of leachable manganese during the two sequential leaches as shown in Figure 3.9 and 3.10. However, after the processing of the soils we did not notice a big change in the amount of leached manganese in the first or the second step. Maybe, because the manganese bounded in stronger residual associations was not affected by the acid treatment of the soil.

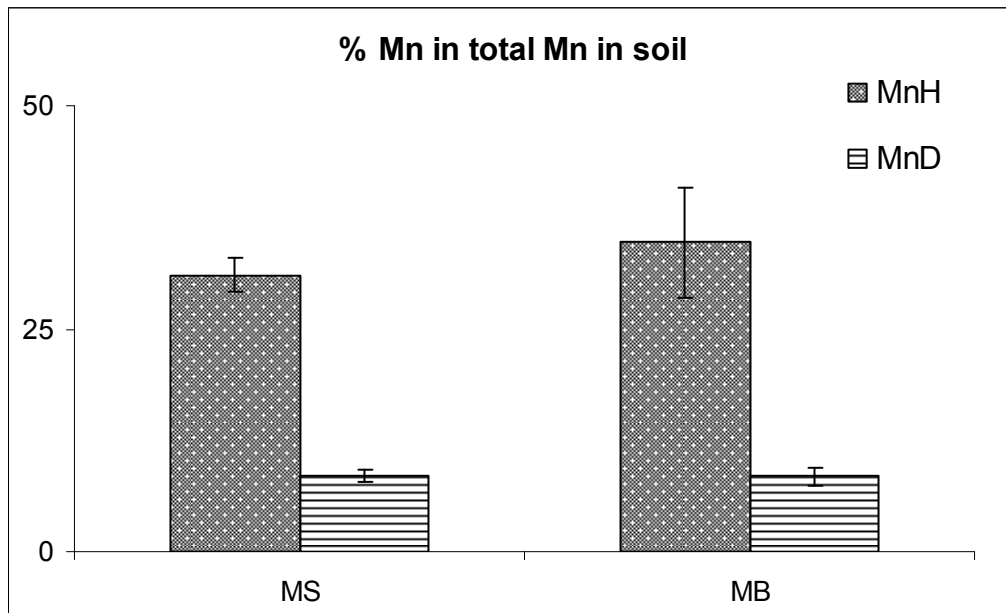


**Figure 3.10** The percentage of Mn (w/w) from the two leaches in Mali samples (n=3; MS = not treated dust, MB= acid treated dust).

The low pH cycled soils, MSJ and NSJ, had already released into the fresh water all the leachable manganese during the processing of the soil. Manganese remained in solution even after the pH was raised to 5 during the processing, due to the slow dissolution kinetics of the manganese and its high solubility under such conditions. Thus, the concentrations of the MSJ and NSJ soils were below the detection limit of the flame AAS (atomic absorption spectrometer) that was an expected outcome since according to the Spokes et al. (1994) study, 90% of the leachable manganese had passed into solution during the initial treatment of the samples and it did not re-precipitate after the change in the pH to higher values.

## **3.5 Microscopy**

### **3.5.1 XRD Data**

Niger and Mali samples were analysed using an X-Ray Diffraction method (XRD). The analysis could not be performed quantitatively due to the lack of the amount of sieved Niger and Mali soils needed for the analysis. X-ray diffraction patterns provided little information as to the iron-containing phases present in these source materials probably due to the small amount of iron-containing species. The results of the XRD patterns mostly support general publications eg. Usher et al., (2006) as to which minerals are present in Saharan soils. Both soils had similar mineralogy and comprised primarily of quartz, small amounts of feldspars, mica and kaolinite as shown in Figure 3.11. For the Niger soil a small hematite peak was present, whereas no iron oxide peak was evident for the Mali soil.

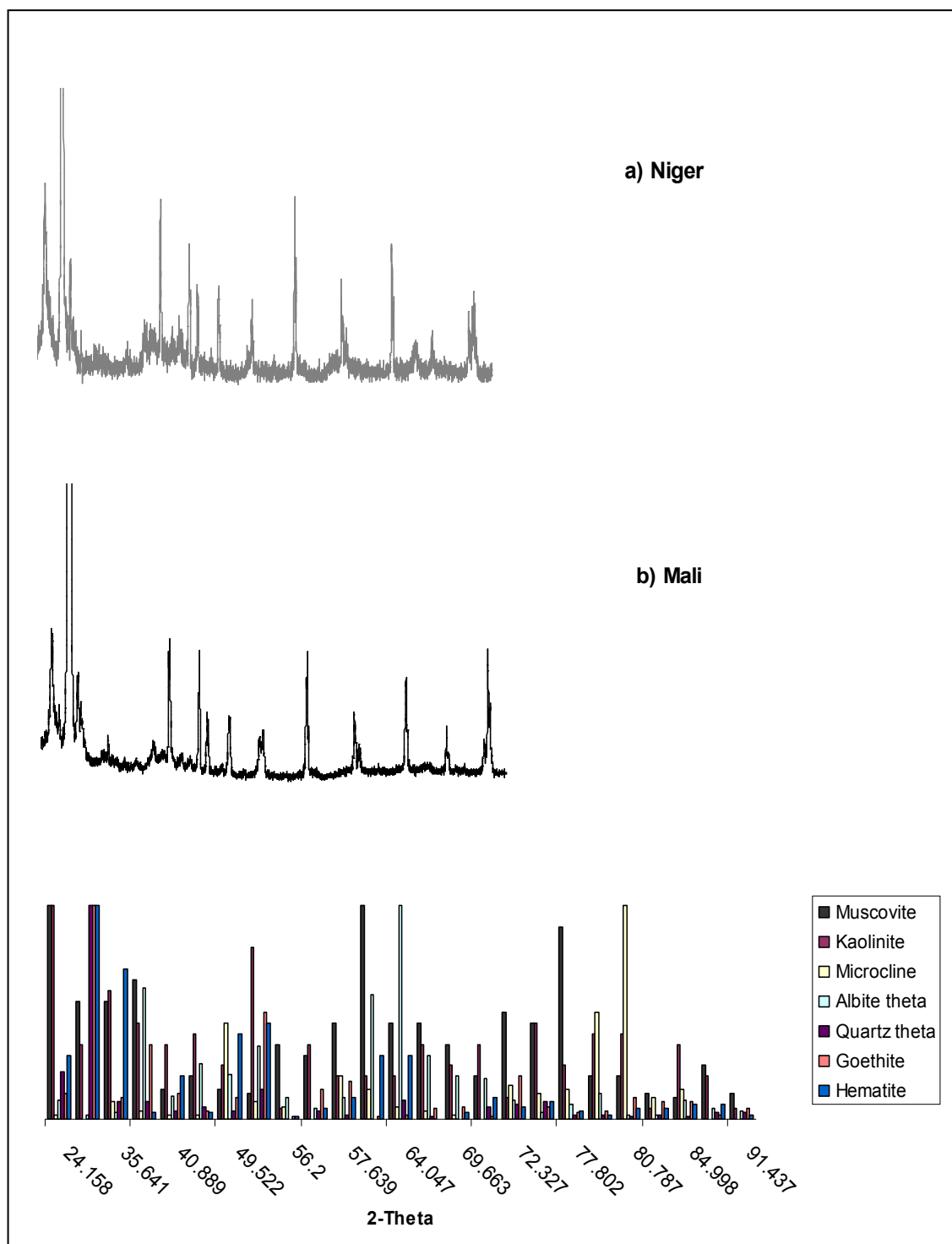
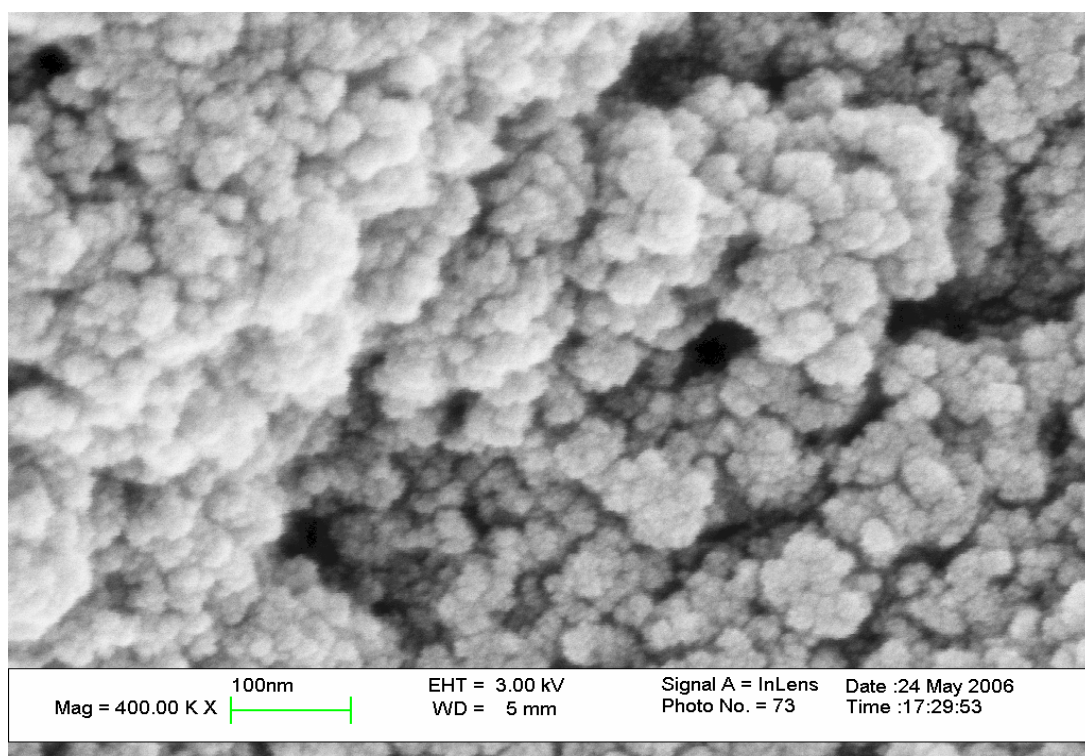


Figure 3.11 X-Ray Diffraction pattern for the a) Niger, b) Mali soil and c) the 2-Theta values for the various minerals.

### 3.5.2 Electron Microscopy

Niger and Mali soil samples were examined in detail to acquire representative images of the sample and Energy Dispersive X-ray Analysis (EDS) was performed on occasions. Magnification was performed in a stepwise fashion as the change of the aperture size and accelerating voltage, which the analysis requires, can cause a loss of the area of interest which was a significant reason why there are not XRD figures for every image with interesting areas acquired from the microscopy.

The total Fe present in the soils used for the experiments is around 4% and less than 1% of the total iron is present as iron oxides, thus, in the few mg that were placed on the stub would be very difficult to find interesting areas of iron nanoparticles that we assume are amorphous ferrihydrite and furthermore would be harder to quantify.



**Figure 3.12 FEGSEM image of synthetic ferrihydrite nanoparticles.**

In the above Figure 3.12 (courtesy Miss L. Brinza) is a picture of synthetic ferrihydrite nanoparticles taken from the FEGSEM microscope which provided a comparison between similar morphological images that were acquired in the soil samples Niger and Mali. The synthetic ferrihydrite was produced following the procedure described in Schwertmann and Cornell (1991) and the procedure used in order to be examined at the FEGSEM was similar to the procedure used for our

samples. It is important to notice the climax of this image which clearly suggests that the nanoparticles of ferrihydrite are within the range of 5-10nm.

A typical electron microscope picture is shown in Figure 3.13, where FEGSEM images of the a) Niger soil and c) Mali soil are shown and they are typical images of feldspar, quartz and smectite that seem to dominate. Iron oxides could not be identified in the pictures simply with visual contact. The XRD data supported the mineralogy of these images. The magnification scale at the bottom of each image was quite different because Niger soil was examined in an earlier time phase so a) Niger sample had a scale of 2 $\mu$ m and c) Mali sample 200nm and the particles are rather large. However we should keep in mind that the diameter of the beam that was used for the XRD analysis is 1 $\mu$ m. An important finding from the XRD analysis of both samples (Figure 3.13 (b), (d)), was the quite large peak of Si which dominated the soils and Cu peak due to the stub used, and the peak of Fe probably from iron-containing particles residing on the surface of the particles, because if it was trapped in aluminosilicate particles it would not give a signal as the beam hits the surface.

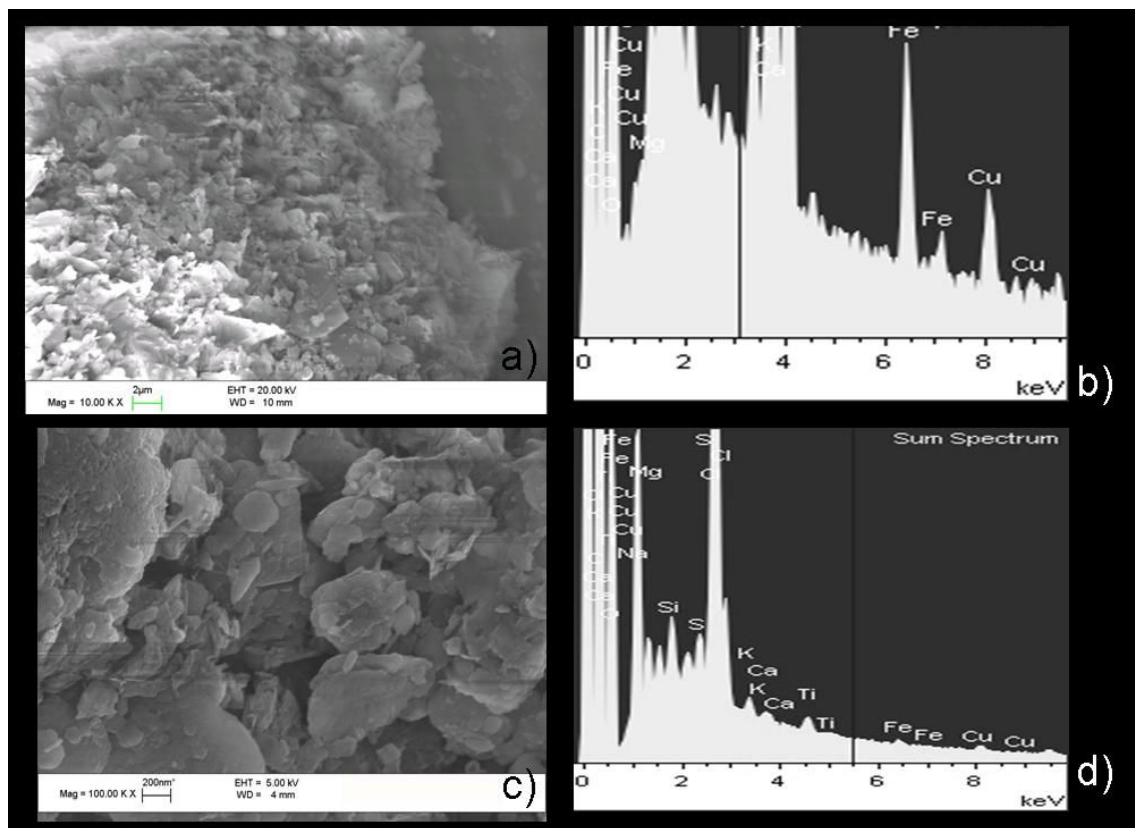
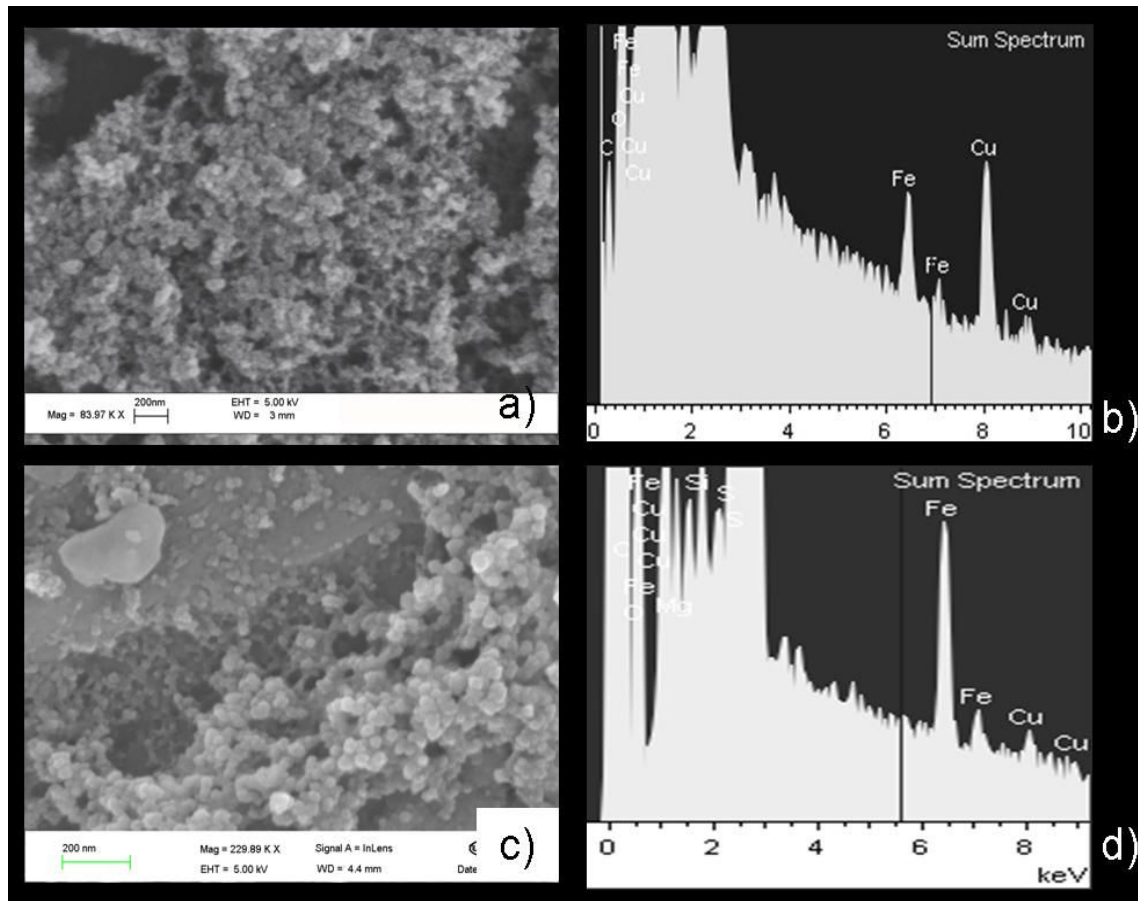


Figure 3.13 SEM images of the non treated a) Niger (NS) and c) Mali (MS) soil with corresponding XRD spectrums b) Niger and d) Mali soil respectively.

Changes in the mineralogy of the soils were examined after the acid treatment of Niger and Mali soil (NB, MB). The specimens on the stubs were examined thoroughly in order to find significant areas that resemble the morphology of amorphous iron oxides mainly ferrihydrite as shown in Figure 3.14. It is suggested by Mackie et al., (2007) that previous identifications of ‘amorphous iron’ are incorrect and ferrihydrite is a better descriptor of an admittedly poorly characterized iron oxide (Cornell, 2003).



**Figure 3.14** SEM images of the a) acid treated Niger soil (NB) with b) corresponding EDX spectrum showing an Fe peak and of the c) acid treated Mali soil (MB) with d) corresponding spectrum EDX showing an intense Fe peak.

In both images Figure 3.14 a) and c) the scale is at 200nm that means that the particles present are around 5 to 20 nm. The number of the images was not big due to time available. The morphology of the samples, nanoparticles network, resembled that of synthetic ferrihydrite (Figure 3.12) as well as the size of the particles. Representative XRD spectrums of these areas are shown in Figure 3.14 b), d) and Fe peak is present in both spectrums and does support the notion of ferrihydrite being formed after the treatment.

Low pH processed Niger and Mali soils (NSJ, MSJ) also provided interesting areas similar to the areas provided by the acid treated soils, although it was much more difficult for such areas to be found. These areas of interest are presented at Figure 3.15 a) with scale 100nm, c) with scale 200nm and it is obvious that the nanoparticles are more mixed with larger particles in these samples. This heterogeneity explains the larger number of elements present at the XRD spectrums in figure 3.15 b) and d).

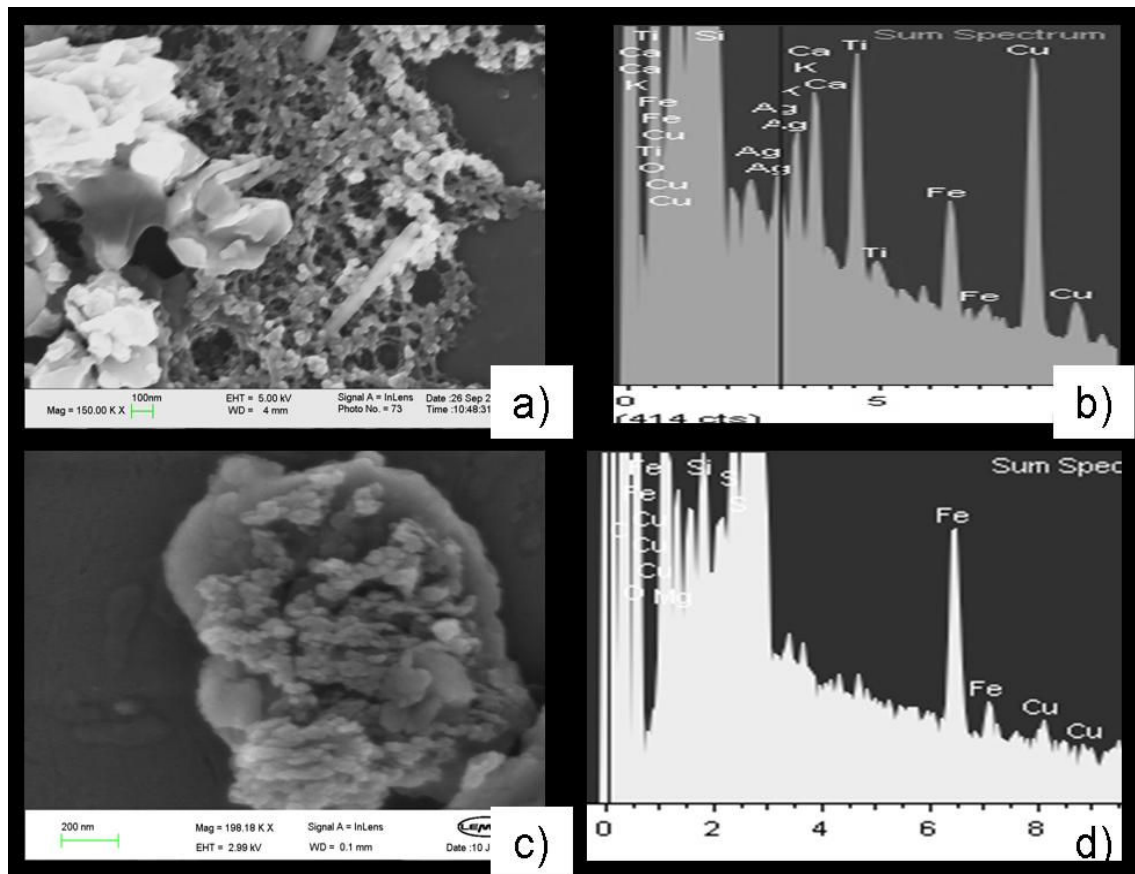


**Figure 3.15** SEM images of the a) low pH cycled Niger soil (NSJ) with b) corresponding EDX spectrum and of the c) low pH cycled Mali soil (MSJ) with d) corresponding XRD spectrum.

Thus, we did not come across with visible iron nanoparticles when the non processed soils were examined. Whereas, when the treated soils were examined we found areas with nanosized particles that presented an iron peak in the XRD spectrum and these nanosized particles had morphology that resembled synthetic ferrihydrite. However, it can not be argued with certainty that the areas found in the treated samples were areas of ferrihydrite. Thus, Field Emission Gun Transmission Electron Microscopy – FEGTEM was used as more information and higher resolution microscopy were required concerning the mineralogy of the nano-sized particles.

Field Emission Gun Transmission Electron Microscopy (FEGTEM) was used with the significant help of Mike Ward and provided more information about the nanoparticles present in our samples. In Figure 3.16 are given the results from the low pH cycled Mali soil (MSJ) where a) is an area of interest at 50nm scale and b), c) consecutively zoomed area. This area represents amorphous material. In Figure 3.16 d) is the Bright Field Image of the specific area. The bright spots on the image represent crystalline material present in that area and the bright circles represent the amorphous particles and the distance from the centre to the circles are characteristic for ferrihydrite ( $2.5\text{\AA}$ ,  $1.8\text{\AA}$ ).

Along with the FEGTEM this area was analysed with the Electron Energy Loss Spectroscopy, which is a common method used for iron (hydr)oxides, and the results are given in Figure 3.16 e) where the spectrum provided with two characteristic peaks, one of Fe at 710eV and O at 510eV.

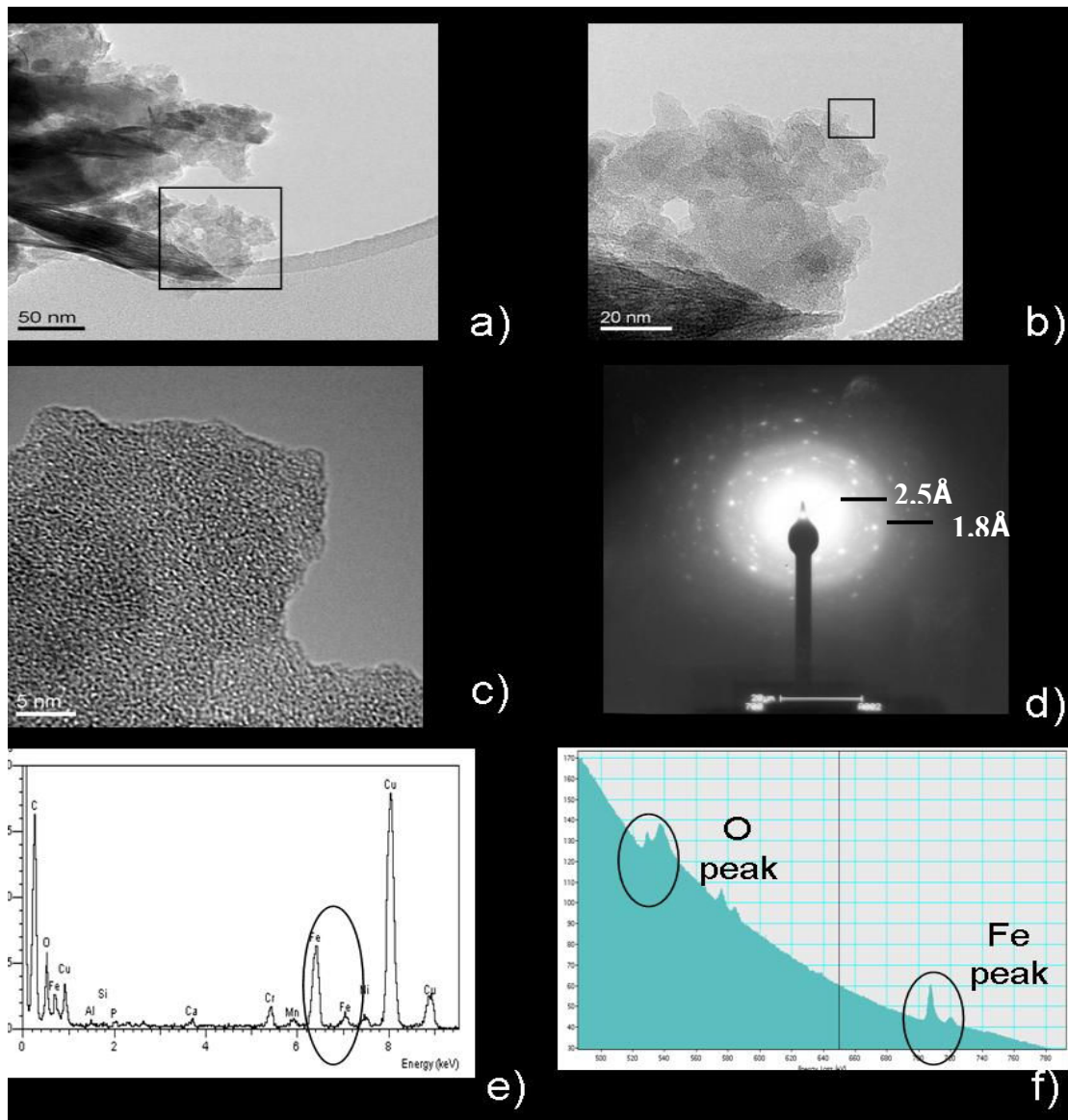


**Figure 3.16** FEGTEM image of low pH cycled Mali soil (MSJ) of the a) greater area of interest in 50nm scale, b) area in 20nm scale, c) zoom in the marked square given in image (b) in 5nm scale, showing details of lattice fringe geometries, d) SAED ion pattern of specific area, e) EDX spectrum showing the metals present in the area and f) EELS spectrum.

The FEGTEM results obtained from the acid treated Mali soil (MB) are given in Figure 3.17. The region depicted is much clearer an amorphous mineral than images showing areas from the low pH cycled Mali soil, MSJ. The XRD spectrum, figure 3.17 c) shows an iron peak, (Cu peak come from the material of the grid) and d) the nanodiffraction pattern of specific area identifies ferrihydrite material present.

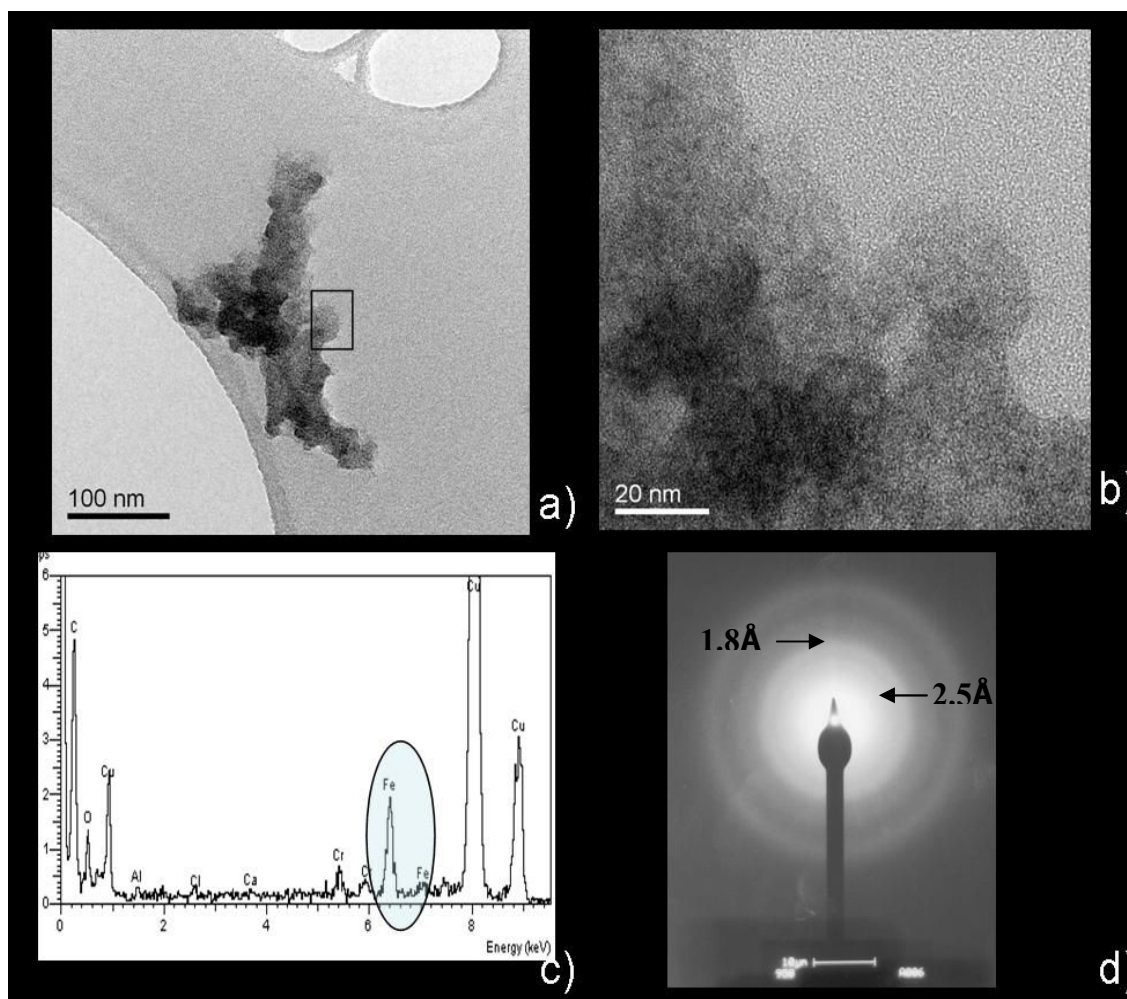


**Figure 3.17** FEGTEM image of acid treated Niger soil a) greater area of interest, b) zoom in 20nm showing details of lattice fringe geometries, c) corresponding XRD spectrum and d) SAED pattern of the aggregate with indexed Bragg distances corresponding to 2-line ferrihydrite.

The FEGTEM images indicated the presence of amorphous iron in the processed soil (MB, MSJ). These images supported by EDS, EDSA and EELS data concluded that this amorphous iron present was ferrihydrite. Thus, it is quite probable that the FESEM images from the processed soils were nanoparticles of amorphous ferrihydrite.

The present findings are consistent with our hypothesis that the mineralogy of iron changed after the simulation of cloud cycling, which caused the formation of amorphous iron nanoparticles and more specifically ferrihydrite and is coherent with the latest publication of Shi et al. (2009) that used the same methods to simulate cloud processing (Shi et al., 2009). In the chapter to follow, these artificially processed particles will be further examined in release of iron in seawater.

### **3.6 Conclusions**

The results of this research support the idea that the mineralogy of Saharan soil is altered when it is subjected to artificial cloud processing. The sequential leach showed an increase in the hydroxylamine-HCl leachable fraction. This is important because it represents the easily reducible iron species that are most likely to be dissolved later upon impact with seawater.

The evidence from the microscopy justifies the suggestion of more amorphous iron species being formed in the processed soils and that amorphous species was ferrihydrite. On the other hand microscopy on non treated soils did not show any areas with amorphous iron species.

The results on manganese indicate that during the low pH cycling all the manganese was released in the soluble fraction and it did not reprecipitate and thus it could not be measured after the extraction experiments. This finding could imply that manganese could dissolve in cloud water, remain dissolved and be readily available for the phytoplankton upon reaching the seawater. The leachable manganese from the non treated soil in the first and second step of the extraction was roughly the same as the acid treated one.

The findings of these experiments have an important implication regarding the cloud cycling of Fe/Mn associated with dust. The metal mineralogy in the dust probably changes when the dust particles encounter gases that alter the pH within the cloud. Our results suggest that nanoparticles of ferrihydrite and soluble compounds are formed; these later could dissolve into seawater, releasing metals that could be available to organisms. That is important in the open seas where aeolian dust is a major source of new nutrients. It also suggests that wet deposition could offer immediate dissolved metals rather than dry deposition where metals would be released from the particle phase more slowly.

In the following chapter the release of iron and manganese into seawater from treated and non treated Saharan soils will be the subject of examination in order to get a quantitative measure of the impact of these processed soils.

## Chapter 4

### Dissolution Experiments with Saharan soil

#### 4.1 Introduction

A series of dissolution experiments were conducted in order to understand how Saharan dust inputs can change the concentration of dissolved iron and manganese in surface seawater. In this study we address the question of how much iron and manganese dissolves from untreated Saharan soils and whether there is a change in the amount of Fe and Mn released into seawater if the dust has undergone “cloud processing” before being deposited into seawater.

The soils used in the dissolution experiments originated from Mali and Niger. Samples from both locations were used for the laboratory experiments, whereas for the onboard incubations only Mali soil was used. These soils were treated in two different ways to simulate cloud cycling as described in sections 2.2.1 and 2.2.2 and together with the non treated soil where used for the dissolution experiments.

To our knowledge this is the first set of experiments that use Saharan soil processed in a way to simulate cloud cycling in dissolution experiments. We compared these results to non processed soil in order to examine the effect of cloud processing on the dissolution of iron. In addition biotic and abiotic seawater sampled during the cruise were used to compare the release of iron in the two media. These experiments were considered to be more realistic since the seawater has not been stored as well as including the impact of natural biotic communities. So our hypothesis is this: Does the atmospheric processing of natural soil particles lead to an enhanced release of iron into solution?

The methods used for the seawater dissolution experiments in the laboratory and during the SOLAS D326 cruise were fully described at Chapter 2. In brief, the procedure of the experiments was the addition of processed and non processed soil in

several bottles filled with seawater at  $23 \pm 2$  °C in direct sunlight or in the dark, which were later sub sampled at specific times in order to be analysed for dissolved Fe and Mn using flow injection analysis.

In order to measure dissolved iron sub-samples were taken from the bottles that contained processed and non treated Mali and Niger soil in 1L seawater. All the experiments were carried out in triplicates in a Class 100 laminar flow hood under normal fluorescent lights. The non treated replicate samples bear the acronyms MS1, 2, 3 and NS1, 2, 3, for Mali and Niger untreated Saharan soil respectively. The samples cycled at low pH in MQ water are named MSJ1, 2, 3 (Mali-Spokes Jickells) and NSJ1, 2, 3 and finally the samples treated with acid are named MB1, 2, 3 and NB1, 2, 3 (B stands for Baker as in Alex Baker as he proposed the initial idea of treatment). The dust loading was chosen to be 10 mg/L of seawater as it was low enough to allow the use of the treated soils and the comparison with similar published projects.

The sub sampling for the dissolution experiments in the laboratory was made at the times: 3min, 30min, 6h, 24h, 48h (for Mali soil) and 5days. These times were chosen due to the rapid release of iron into solution and also the rapid loss from solution and in order to be coherent with other studies such as Mendez et al., (2008), Bonnet and Guieu (2006). For experiments carried out on the ship the sub sampling was the same with the laboratory except for the 30min and 48h times that did not take place. The precise times of sub sampling for each bottle were noted. The solution taken into the clean syringe was filtered through a 0.2µm filter into acid clean tubes and then it was acidified with sub boiled quartz distilled HNO<sub>3</sub> at 1µL/ mL of solution.

## 4.2 Results

### 4.2.1 Iron

#### 4.2.1.1 Dissolution Experiments in the Laboratory

The results from the experiments on Mali and Niger soil carried out in the laboratory showing the change in dissolved iron, DFe, versus log time (hour) are given in Figure 4-1 (A) and (B) respectively. This figure and all other figures following in this chapter show the average values from the three (3) replicates of each type of soil along with the blanks where seawater without the addition of soil was used and treated as samples. The error bars are standard deviations among the three replicates. The DFe values from the blank experiments were low, not exceeding 0.6nM.

The concentration values for the dissolved iron are generally low especially for Mali soil. The dissolved Fe concentration for the non treated Mali and Niger soil increased within tens of minutes, from 1.1nM at time 3min to 1.3nM at 6 hours for Mali soil and from 0.9nM to 1.4nM for Niger soil. However, the dissolved iron decreased later on reaching the concentration after 48 hours of 0.7nM for Mali soil and 0.9nM for Niger (Figure 4.1 (A), (B)).

The processed Niger and Mali soil (Figure 4.1 (A) Mali soil, (B) Niger soil) showed higher initial iron release than the non-processed soils which decreased rather quickly over a few minutes. For the acid processed Mali and Niger soils (MB and NB) the initial release over the first 3 min was 2.2nM and 5.95nM which decreased after six hours to 1.8nM and 2.3nM respectively and by the end of the experiment the dissolved Fe concentrations reached similar levels of around 1nM for all samples. A similar trend was followed by the low pH processed Mali and Niger soil (MSJ & NSJ) that initially released 2.3nM and 3.6nM, and these concentrations quickly decreased to 1.3nM and 1.3nM within 6 hours and by the end of the experiment reached 0.7nM and 0.8nM respectively.

For Mali samples the initial value of MS was significantly different from the MSJ and MB samples with confidence levels 95.3% and 99.9% respectively, but the MSJ and MB values were not found to be significant different between them. Moreover comparing MS with blank values were found to be significantly different by 99.9% confidence levels which became 92.8% for the concentration at time 120h.

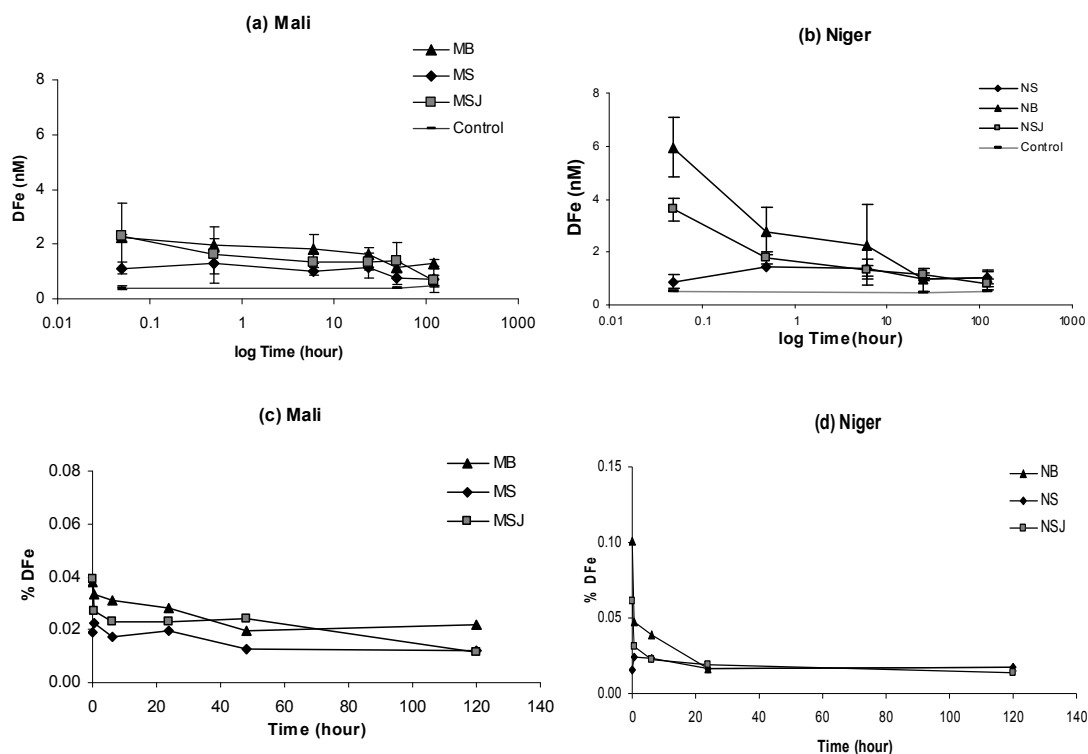


**Figure 4.1** Dissolved Fe (DFe) versus log time for (a) Mali soil, (b) Niger soil during the laboratory experiments and percentage of dissolved Fe for (c) Mali and (d) Niger soil respectively (particle concentration  $10\text{mg L}^{-1}$ ,  $20^{\circ}\text{C}$ ).

The end concentrations of MS-MSJ were not significantly different; however MS-MB presented significant difference with confidence levels 96.7%. Moreover all values were significantly different to the blank values.

For the Niger soil the initial values of NS-NSJ, NS-NB and NSJ-NB were all statistically different with confidence values over 99% as was NS compared to blank with confidence level 99.6%. The concentrations at the end of the experiment were not found to be significantly different thus in all samples the concentration dissolved Fe was at the same level.

#### 4.2.1.2 Dissolution Experiments Carried Out at Sea

The seawater dissolution experiments were conducted during the D326 SOLAS Cruise on board RSS Discovery during the period 5 January 2008- 5 February 2008. During the cruise, three dissolution experiments were conducted: a) abiotic seawater in the dark; b) abiotic seawater under direct sunlight and c) biotic seawater under direct sunlight. The aim of these experiments was to determine whether the solubility of iron

and manganese had been altered by simulation of cloud processing and how the different parameters of each experiment, light, dark, unfiltered seawater, might have affected the solubility of Fe and Mn. Moreover, the same Mali soil was used for both the dissolution experiments conducted in the laboratory and on the cruise and one of the objectives was to compare the results.

The results taken from the abiotic seawater experiment under dark conditions that was carried out during the cruise are presented in Figure 4.2. This experiment was conducted in the dark as with the laboratory experiment of Mali soil. It is noticeable that the dissolved iron concentrations are much lower in the laboratory experiment compared to the on board experiment using the same soil. The processed soils during the laboratory experiment did release more dissolved iron than the non processed soil. The differences between the experiments on board and in the laboratory are that the seawater used on board was fresh unlike the seawater used for the laboratory which had been stored for a long time and the MB soil in the laboratory experiment was acid treated with HCl whereas on board it was treated with H<sub>2</sub>SO<sub>4</sub>.

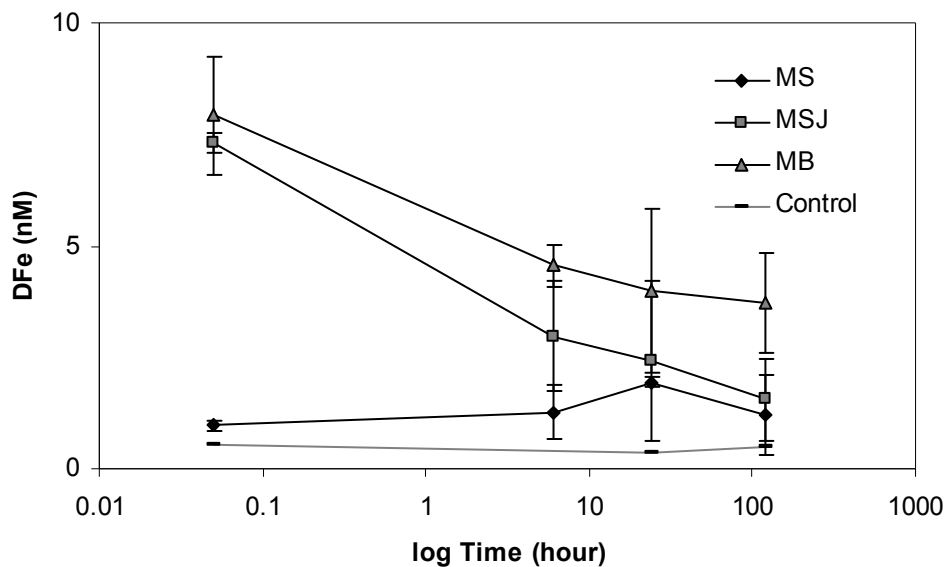


**Figure 4.2** Dissolved nM Fe (DFe) versus log time for Mali soil during the abiotic, dark experiment, conducted during SOLAS cruise D326.

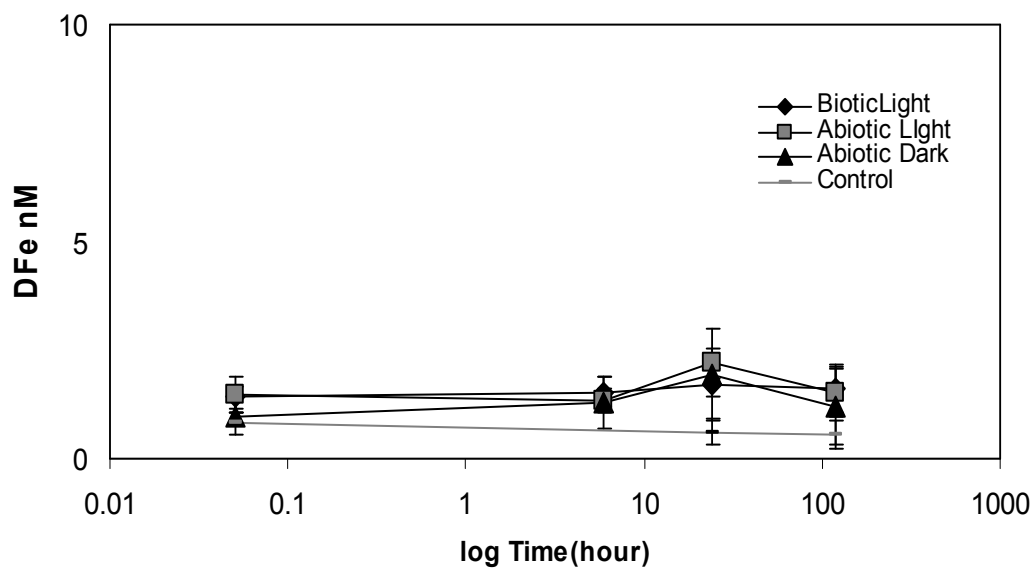
The initial values of processed soils are elevated compared to the laboratory experiments, around 7-8nM, whereas, the non-processed Mali soil gave concentrations around 1nM similar to the initial concentrations of both the Mali and Niger soil from the laboratory experiments.

In Figure 4.3 the results of DFe versus log time, obtained from the three seawater dissolution experiments carried out during the cruise for the different soils used, are given: graph (A) non treated soil (MS), graph (B) acid treated soil (MB) and graph (C) low pH cycled soil (MSJ).

The most striking result to emerge from this data is that the processed samples (MB), (MSJ) initially release more iron in the seawater than the non treated sample (MS) and this difference in the [DFe] reached values between 3.5–10nM in all three experiments.

In the biotic light dissolution experiment, the initial release of Fe in the processed samples was much smaller than in the other two experiments carried out in “abiotic” seawater, where [DFe] was around 5.0 nM for the MB and 6.8 for the MSJ sample.

### (A) MS



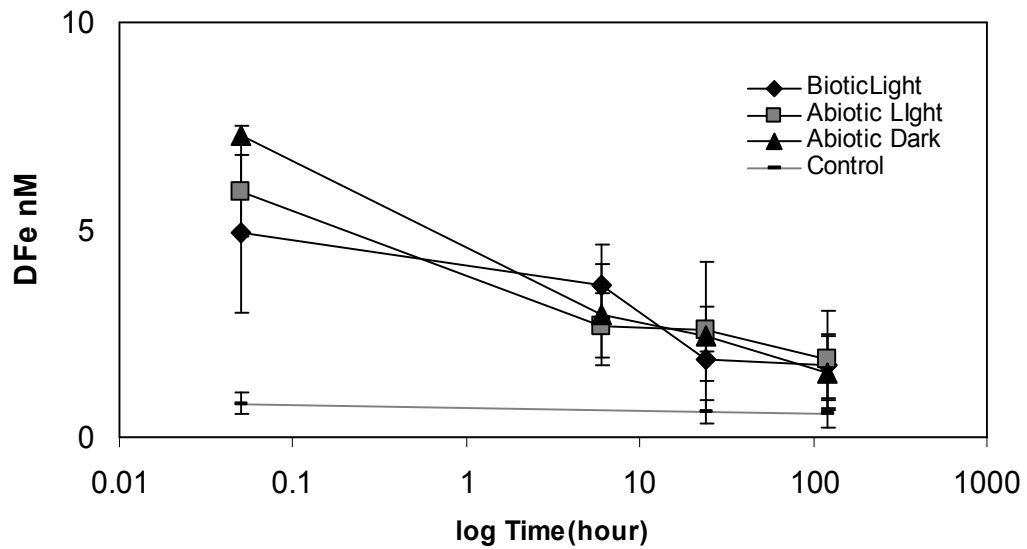
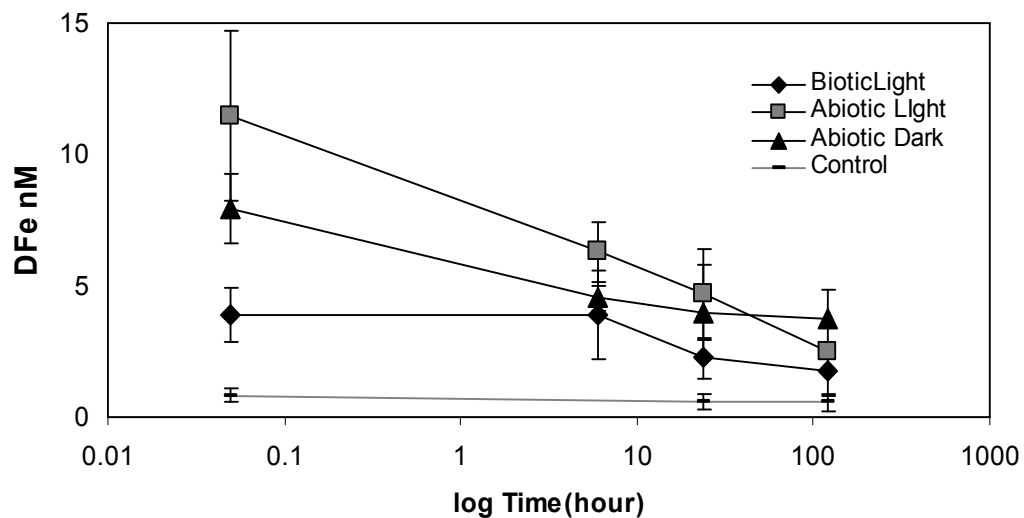
**(B) MSJ****(C) MB**

Figure 4.3 Dissolved iron DFe (nM) versus time (hour) for the three dissolution experiments for (A) Mali Soil MS, (B) Mali soil, low pH cycled MSJ and (C) Mali soil, acid treated (MB) during the on board experiments.

At the end of the experiments, after 5 days, the concentrations of dissolved iron seemed to decrease to a consistent concentration, 1-1.5nM for all the soils used in the experiments, both processed and non processed.

Statistics showed that the initial values of MSJ were significantly different however the confidence level between biotic light and biotic dark experiments was not very high 78.8 compared to the confidence level between abiotic light- dark experiments that was 98.2%.

The initial values of MB samples (figure 4.3 (c)) for the abiotic light and dark experiments were found to be significantly different with confidence value of 96.2% and significantly different as well from the biotic light values with 99.9% confidence level.

#### **4.2.2 Manganese**

Dissolved Mn was measured in the sub-samples acquired from the dissolution experiments by the soils without any treatment (MS1, 2, 3 and NS1, 2, 3 from Mali and Niger soil respectively), samples cycled at low pH in MQ water (MSJ1, 2, 3 and NSJ1, 2, 3) and finally samples weathered with acid (MB1, 2, 3 and NB1, 2, 3). The SJ (both Niger and Mali) samples were initially cycled at low pH with MQ water. As a result, almost all the soluble manganese was released into the water during that process compared to the iron that was recovered by the end of the process (Spokes et al., 1994). The dissolved manganese concentrations measured in experiments using NSJ and MSJ soils, were similar to dissolved manganese present in the seawater used for the experiments, at around 3-4nM. Although the dissolution trend seems to be the same for the MB and NB samples, with high initial release over the first minutes of the experiment and later staying at about the same levels, there is a significant difference in the concentrations of dissolved manganese. The initial [Mn] after the first three minutes was  $64 \pm 4$ nM and  $28 \pm 1$ nM for MB and NB respectively. In contrast the initial release of Mn for MS was  $14 \pm 1$ nM and for the NS was  $18.0 \pm 0.3$ nM. However by the end of the experiment the dissolved Mn had reached similar values  $23 \pm 1$ nM MS and  $19.0 \pm 0.2$ nM NS (Figure 4.4 (A) and (B)).

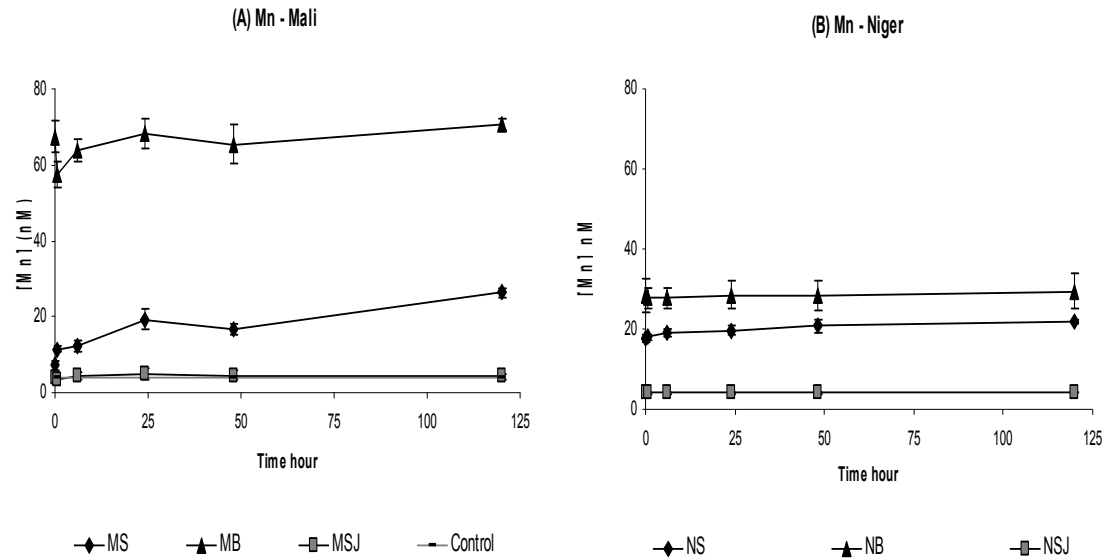


**Figure 4.4 (A), (B) Dissolved Mn for (A) Mali soil, (B) Niger soil respectively versus time, during the laboratory experiments.**

The blank values for the experiments presented in Figure 4.4 are not very visible since they are the same concentrations of the low pH cycled treated samples NSJ and MSJ. The percentage of soluble Mn at the start of the experiments was 15%Mn for NS, 23%Mn for NB and 5.9%Mn for MS, 55%Mn for MB. At the end of the experiments the % soluble Mn did not increase much for the acid treated soil as it was 24% for the NB and 58% for the MB however for the MS it increased to 22% and 18% for the NS.

Figure 4.5 demonstrate the results of Mn released during the three dissolution experiments (A) with abiotic (filtered through 0.2 $\mu$ m) seawater in the dark, (B) with abiotic (filtered through 0.2 $\mu$ m) seawater under direct sunlight and (C) with unfiltered biotic seawater under direct sunlight.

The data from all experiments show a rapid release of dissolved manganese into seawater which reached a maximum value after 6 hours for the treated MB samples but for the non treated MS sample although the dissolution rate decreased significantly, it still gradually released manganese until the end of the experiment. For the MB samples it is clear that the solution has either reached the saturation limit as that is suggested in the study of Guieu et al., (1994) or it could be that all available, soluble Mn has been lost from the particle.

The MB processed samples released the same amount of manganese into the seawater, around 60nM dissolved Mn, and the conditions under which the experiments took place seem to make little difference. For the non processed sample (MS) used for

the biotic light experiment however, the manganese released into solution is obviously smaller than the manganese released in the abiotic light experiment and is only a few nM lower than the abiotic dark experiment. It is also apparent that the dissolved manganese from the MS sample during the abiotic light experiment is higher than the dissolved manganese again from the MS sample from the abiotic dark experiment.

The percentage % of soluble manganese released for the non treated soil was 34.5%, 42.9%, 32.1% for the abiotic dark, abiotic light and biotic light respectively and for the acid treated MB soil was 52.5%, 51.1%, and 55.2% respectively. The release of manganese is obviously greater when the soil is treated and the light-dark, abiotic-biotic do not seem to be important for the treated soil.

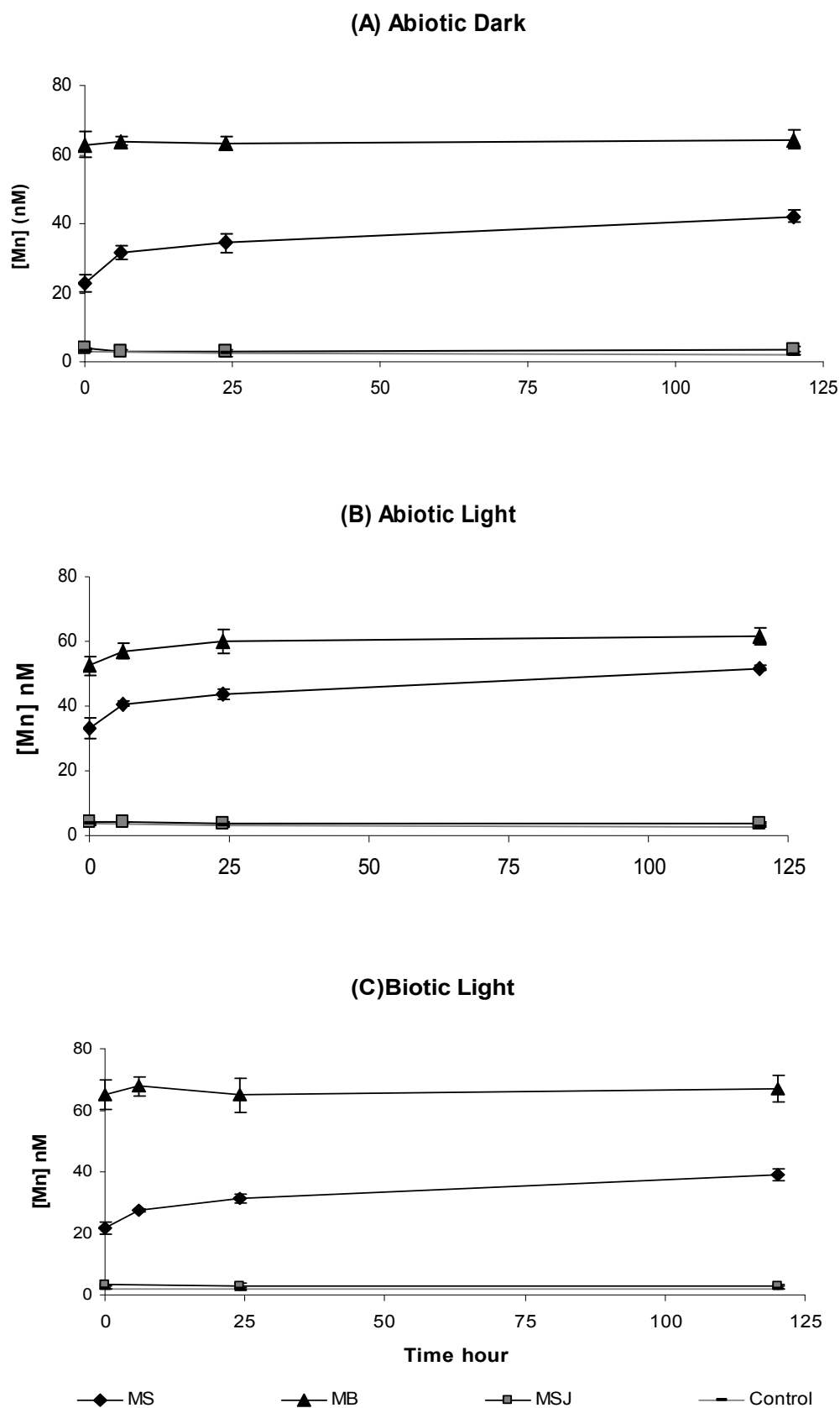


Figure 4.5 Dissolved Manganese [Mn] (nM) versus time (hours) (A) Abiotic Dark, (B) Abiotic Light and (C) Biotic Light experiments during on board incubations.

### 4.3 Discussion

#### Iron

The most obvious and interesting observation was that the processed soil in all experiments carried out, either in the laboratory or during the cruise and for both soils Niger and Mali soils, released initially much higher concentrations of dissolved Fe than the samples of non processed soil.

In order to explain this it would be helpful to consider what might be taking place during the artificial treatment of the soils. The acid processed (MB and NB) samples have been treated with HCl for the laboratory experiments and with H<sub>2</sub>SO<sub>4</sub> for the onboard experiments. The protons produced by the acids adsorb on the surface of the oxides and facilitate the detachment of Fe (III) from the lattice (Suter et al., 1990) by making the outer Fe (III) to exchange electrons with the surface centre and this electron transfer leads a surface Fe (II) ion. This surface Fe (II) ion can easily become detached from the surface due to its higher lability in the crystalline lattice surface of the Fe (II)-O bond compared to the Fe (III)-O bond (Stumm et al., 1992). The Fe (II) can later react with SO<sub>4</sub><sup>2-</sup> and Cl<sup>-</sup>, forming FeSO<sub>4</sub> and FeCl<sub>2</sub> at the surface of the particles, which are quite soluble. After evaporation dust particles coated with soluble materials are left behind as well as amorphous nano-sized iron species which precipitate on the surface of the soil particle as depicted schematically in Figure 4.6.

Spokes and Jickells (1994) showed that for samples which have been treated at a pH of around 2, almost half of the iron present in solution (MQ water) is reduced to Fe(II) detected using Ferrozine method. However at high pH values and in the presence of oxygen due to fast oxidation kinetics, Fe (II) is oxidized rapidly to Fe (III) which hydrolyzes to nanoparticles of amorphous Fe (III) oxides. It is hypothesized that nanoparticles of amorphous iron oxides (eg. ferrihydrite) are formed during the cloud processes, and these ferrihydrite phases are more soluble than the crystalline iron oxides, which are the most common mineralogical species of iron contained in Saharan soils. Solubility is due to their larger surface and their loose structure probably like sponge rust (Zhu et al., 1993) because they were possibly formed rather rapidly. The size of these amorphous particles can be very important since nano-size material can pass through a 0.2 µm filter that is used to separate dissolved Fe. Later by increasing the

pH the Fe (II) adsorb on the iron (hydr)oxides or oxidize to Fe (III) and precipitate as amorphous iron oxides (ferrihydrite).

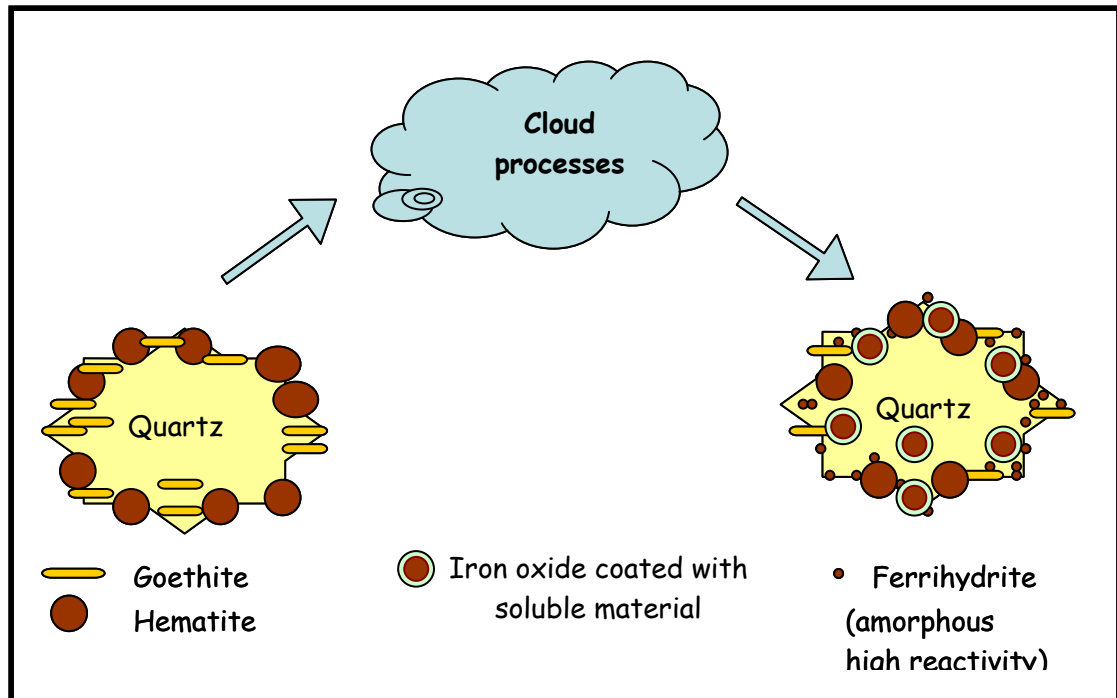


Figure 4.6 Schematic representation of what happens to the mineralogy of Saharan dust particles after cloud processing.

The acid cycled soils (NB and MB) are different to the low pH cycled soils since their treatment does not include an aqueous medium. It is a more harsh treatment since the soil particles are directly attacked with acid that easily form soluble salts and coat the surface of the particles, as well as detach surface Fe(III) which can either adsorb on the particles and/or precipitate as amorphous ferrihydrite upon evaporation or when entering into seawater. The content of Fe (II) in the Mali and Niger soil is very small if there is any, due to the quick Fe oxidation rates. There is however a small amount of easily reducible species present in the Saharan soils before entrained in the atmosphere. In this study the results of the easily reducible leach of iron were discussed in Chapter 3 and it is approximately 1% of the total iron.

The results of this study show a high initial release of dissolved iron into seawater when the soils have been previously cloud processed compared to the non processed ones. These weathered particles once they came into contact with seawater, being coated with soluble material, release firstly the Fe (II) almost instantaneously (Wu et al., 2007) together with Fe(III) that could have been adsorbed on the particles during the process. This accounts for the high initial dissolution that was observed during our dissolution experiments and is the same process as adding iron sulphate or chloride to

seawater. The pH of seawater is around 8, thus iron should oxidize fairly rapidly and as found by the study of Mendez et al. (2008), iron dissolution and adsorption occurs within seconds of dust addition. However, the pH in the neighbourhood area of the particles would possibly decrease due to the soluble material coating these particles. This way the iron dissolution may be enhanced (Bonnet et al., 2006) and keep iron dissolved for a longer period compared to non treated particles.

Another possible explanation for the iron dissolution pattern seen could be the presence of amorphous iron nanoparticles that were created after the processing. The amount of Fe released followed the order MB>MSJ>MS which is the same order found for the amount of easily reducible iron content and Fe(II) salts produced during the processes, given in Chapter 3, (MS<MSJ<MB: 1.2% (0.01mole/Kg)<1.8% (0.02mole/Kg) < ~4.6% (0.32mole/Kg) and NB>NSJ>NS: 3.5% (0.01mole/Kg) > 1.56% (0.03 mole/Kg) >1.02% (0.26mole/Kg)). An implication of this is that the iron mineralogy changed during the processing of our samples and produced iron mineral species that were more soluble in seawater.

The rate of change of the concentration of iron in seawater decreased with time and after the sampling and within 6 hours in the course of the experiments the dissolved iron concentrations of all soil types converged on around 1nM. This Fe removal can be explained by the quick oxidation kinetics of Fe at pH 8 to oxyhydroxides which with time crystallize to more crystalline forms (Schwertmann et al., 1999).

Among the replicates for each experiment highest variability was noticeable in the first sample datum. This was probably due to the rapid Fe uptake onto particulate and colloidal matter and iron oxidation which occurs within seconds (Mendez et al., 2008) and our sub-sampling times are not fast enough (average 3-4 minutes) to determine the initial dissolution concentration before most of the dissolved iron had been removed. It is therefore likely that our results are a minimum of how much iron could be dissolved if we consider the amount of all the easily reducible iron species being solubilized (given in Chapter 3) as an indication of the maximum release possible.

Desboeufs et al. (2005) suggested that the released of observed iron is not related to the total metal composition or the particle origin, but are directly associated with the type of mineral associations whereby the metals are bound in the solid matrix, and this is the direct result of the origin of the soil and of its weathering history.

These findings suggest that the metal solubility can be influenced by the time the mineral particles remained in the atmosphere and if has been cycled through clouds

during its transport (Baker et al., 2006; Bonnet et al., 2004). Many studies eg. Bonnet and Guieu (2004) and Hsu et al. (2005) have shown that urban rich aerosols show higher dissolution of metals than crust rich aerosols and that it is not a matter of which material contains the higher content of total iron but it is more of a question of what is the mineral form the iron is present as in each sample. Thus it is suggested that the key to understanding trace metal solubility characteristics lies in the solid state speciation of the metals in the parent aerosol (Jickells, 2001). Our findings here support this idea, since the processed soils which have an altered mineralogy compared to the original soils did release more iron into the seawater although the content of iron within the soil was the same.

Journet (2008) suggested that soluble iron is released from clays and feldspars rather than iron oxides and hydroxides and in fact the highest dissolved iron derives from amorphous impurities of iron. However they did not consider the presence of amorphous iron (hydr)oxides such as ferrihydrite to be important for the release of iron at pH 2. This is contradicted by the study of Schroth (2009) in which they used XAS spectra and showed that iron in African dust was entirely associated with the pedogenic minerals ferrihydrite, goethite and haematite. Moreover Jambor and Dutrizac (1998) suggested that in the past ferrihydrite particles were mistakenly addressed as iron impurities, and it is not clear whether the clays used in the study of Journet et al., (2008) study, were pre-treated in order to get rid of the iron (hydr)oxides that usually coat clays. In addition, the protocol used for the chemical leach in the same study does not realistically reproduce the conditions under which Fe is released from aerosol particles once they are deposited onto the surface of the ocean, because the pH of rainwater is not usually as low as 2 and the particulate loading is quite high (40mg/L).

### **4.3.1 Comparison of Mali and Niger Soil**

In this study on comparing the Niger and Mali soil samples that have not been treated it is observed that they released a similar amount of iron although they have different total iron content 3.6% Mali soil and 4.5% Niger soil. Thus it can be suggested that the amount of iron released into seawater is not related to the total amount of iron present in the soils but rather depends the mineralogy of the soil. The processed soils released more iron than the non processed ones for both soils, however the Niger

processed soils released much more iron than the Mali ones. Since it is concluded that the amount of iron in the soil did not make any difference in the released iron, the data suggests that the mineralogy of the soils changed and suggests what the mineralogy was altered to during the simulated cloud processes.

### 4.3.2 Comparison of Laboratory and Aboard Incubations

Mali soil was used for both laboratory and on board experiments, and the conditions were similar for the experiment that was conducted on the ship where abiotic seawater in the dark was used. The results of these experiments showed quite different dissolved iron concentrations for the processed soils. In general all the dissolved iron values from the laboratory experiment were lower than the concentrations from the on board experiment. A possible explanation could be the different analytical methods used to analyse the dissolved iron in the seawater samples. However, use of CRMs in each case show the accuracy of the methods used, and the non processed Mali soil gave low iron concentrations on both occasions.

The processed soils in the land based laboratory study showed much lower concentrations than experiments using processed soils on board. A possible explanation could be due to the use of fresh seawater during the aboard incubations that could provided with higher concentrations of organic ligands that kept iron dissolved for longer. Another possible explanation is that for the MB samples used for the laboratory experiment the acid treatment was conducted with HCl instead of H<sub>2</sub>SO<sub>4</sub>, so it is not certain if the mineralogy of the soil was altered in a way that provided less labile iron.

### 4.3.3 Comparison with Other Studies

Recent literature reports a wide range of solubility estimates that can be anything between 0.001- 80% of total iron present in soil and there are many diverse methodologies used to derive these estimates. Therefore interpretation of data and comparison with other experiments is a difficult task. Table 4.1 shows similar work on dissolution experiments measuring Fe that is released into water from either aerosols or Saharan soil. On the same table are added the dissolution percentages from our work. The iron dissolution percentage for the laboratory experiments is 0.012% Fe for Mali

soil and 0.0005% for Niger soil (calculated as% of total dust mass not Fe concentration in soil) and for the cruise experiments the average iron dissolution is 0.026% for Mali soil. The present findings seem to be consistent with other studies such as Bonnet et al., (2004) which gives a range of dissolution, according to the particle concentration, of 0.001-1.6% and the parameters in their study (filtered seawater, Saharan dust) are similar to our study.

**Table 4.1 Leachable Percentage (%) of Iron Seawater Solubilities.**

Authors	Type of particles	pH	Amount of particles	Dissolution%
Bonnet and Guieu (2004)	saharan	8	0.01-10mg/L	0.001-1.6
Zhuang et al. (1990)	saharan	8	filter	50
Hsu et al. (2005)	natural aerosol	8.3	filter	1.1
Chen et al. (2006)	aerosol	8	70mg/L	0.003
Baker et al. (2006)	saharan aerosol	8	filter	1.2 (0.5-2.5)
Wagener et al. (2008)	saharan soil	8	5mg/L	0.017
Laboratory exp.	Niger soil	8.1	10mg/L	0.01
Cruise exp.	Mali soil	8.1	10mg/L	0.026

The most interesting finding was that the processed soil samples in all experiments carried out, either laboratory or during the cruise and for both soils Niger and Mali, released initially much higher concentrations of dissolved Fe than the samples of non processed soil.

For the low pH cycled (NSJ and MSJ) samples which have been treated at pH around 2, Spokes and Jickells (1994) report that almost half of the iron present in solution (MQ water) is reduced to Fe (II). However Fe (II) at high pH values was oxidized to Fe (III) which hydrolyzed to form nanoparticles of amorphous Fe (III) oxides. The nanoparticles of amorphous iron oxides (eg. ferrihydrite) are hypothesised to form during the cloud processing. It is suggested in Chapter 3, that these nanoparticles are more soluble than the crystalline iron oxides, which are the most common mineralogical species of iron contained in Saharan soils. This is due to the larger surface and their loose structure (Zhu et al., 1992). The size of these amorphous particles can be very important since nano-sized material can pass through a 0.2  $\mu\text{m}$  filter that is used to measure dissolved pH.

#### 4.3.4 Ligands

Although at seawater pH the solubility of iron (III) is extremely low, several studies (eg. Van den Berg, 1995; Rue and Bruland, 1995; Liu and Millero, 2002; Kraemer, 2004) have revealed that natural strong iron binding ligands which may be released by some phytoplankton or cyanobacteria (Wilhelm and Trick, 1994; Boye and van den Berg, 2000, Witter et al., 2000) enhance the dissolution of iron (hydr)oxides in aquatic systems. Ligands have been demonstrated to be in excess compared to dissolved iron and to form strong iron complexes (Van den Berg, 1995) by strong organic ligands, and Fe in the case of the Western Mediterranean can be up to >99% iron complexed, and this speciation may control the uptake of Fe by microbiota (Wu et al., 2001). Wagener et al., (2008) showed that under natural conditions iron binding ligands affect iron dissolution rates from dust particles when they enter the sea surface. At the same time organic and inorganic ligands present in the seawater form complexes with  $\text{Fe}^{3+}$  and  $\text{Fe}^{2+}$  and keep iron dissolved and these ligands according to studies are the ones controlling iron dissolution and they are the reason for the background level of dissolved iron in the oceans (Rue et al., 1995; Van den Berg, 1995).

An important class of Fe ligands in seawater is the siderophores. Siderophores promote iron oxide dissolution by a direct surface controlled mechanism and by facilitating proton- promoted or other ligand-promoted dissolution mechanisms (Kraemer, 2004). The necessary first step for the siderophore promoted dissolution depends on its adsorption on the mineral. Since we hypothesise that iron nanoparticles were formed in the processed soils, because of the weathering, this means a larger active surface present that could enhance siderophore binding and keep iron into solution. However we have no data on siderophores in our experiments so further study of processed soils and siderophores are essential. In Figure 4.7 is provided a schematic of how siderophores are bound to iron in seawater.

A possible explanation for the higher concentration of dissolved iron for the MB samples observed at the end of the experiment carried out with abiotic seawater in the dark, compared to the MB samples from the other experiments, maybe due to the complexation of iron to ligands. It is suggested, that during the acid treatment of the MB samples amorphous ferrihydrite nanoparticles were formed, as supported by the electron microscopy data and the chemical leaches. These colloidal nanoparticles were probably bound to organic ligands and the iron was kept in solution (Wu et al., 2001). The

proposed mechanism for the removal of iron bound to ligands from the dissolved phase is photochemical degradation. However degradation could not take place because the experiment was performed in the dark, thus iron remained in the dissolved phase. In addition the times of our experiments might not have been enough for colloidal aggregation and settling which would remove more iron from solution.

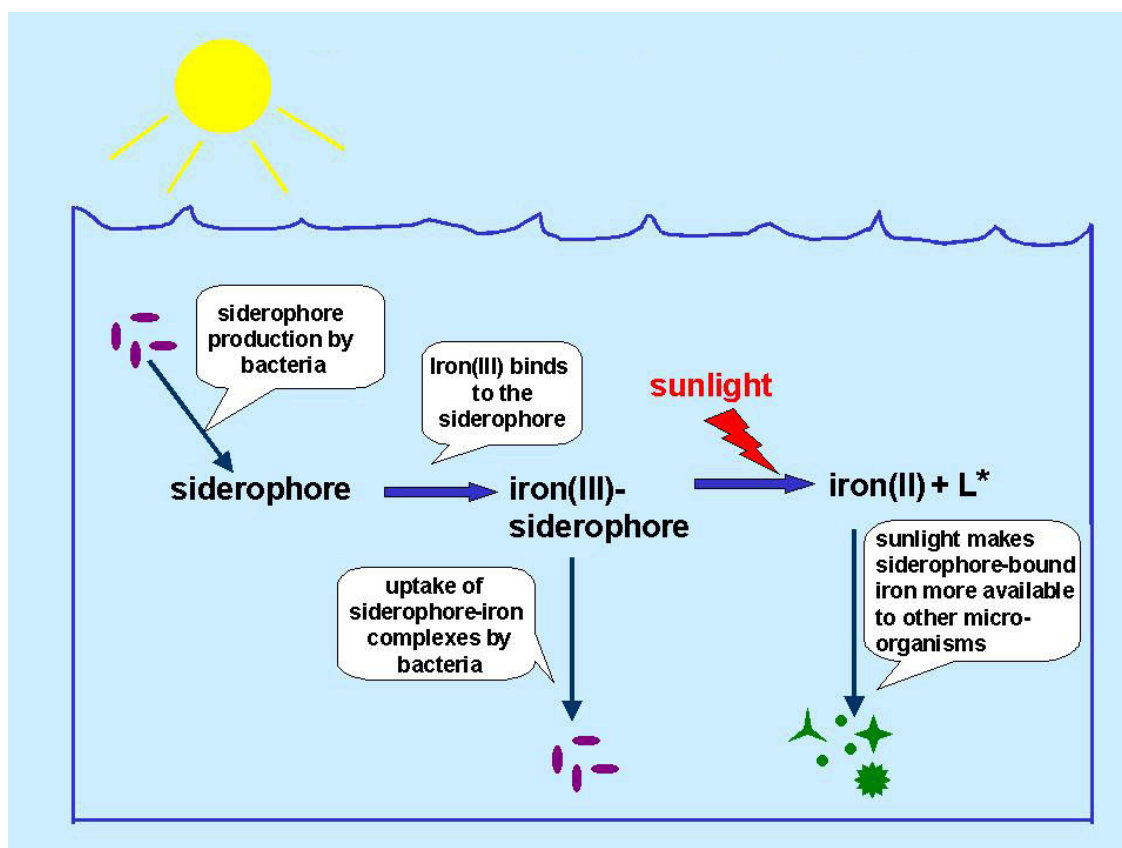


Figure 4.7 Schematic of how siderophores are bound to iron in seawater (<http://www.nsf.gov/od/lpa/news/press/images/fridaygraphicnature.jpg>).

The concentrations of free Fe-binding ligands are 1-2nM (Rue et al., 1995; Vandenberg, 1995; Wu et al., 1995) in the surface waters of the subtropical North Atlantic. However the seawater ligand concentrations during the D326 cruise, the seawater which was used for our onboard experiments, was measured by Dr. Micha Rijkenberg. The results showed that the amount of free ligands in the sub tropical Atlantic seawater was 0.25-0.29nM which seems quite low to account for all the dissolved iron present from our experiments. It is unsure whether the Saharan soils contain any inorganic ligands that play an important role later on in the seawater, or if organic ligands could be released from the atmospheric particles themselves.

Simple functions such as log, exponential, power law and linear were applied to the data set in order to describe the iron dissolution. However, none of these simple functions was satisfactory, probably because a variety of processes were occurring simultaneously during the first hours of the incubation experiments, and the dissolution rate was abrupt compared to the end of the experiment that seemed to move toward equilibrium. Thus, dissolution kinetics possible cannot be explained by a straight forward mechanism but it is rather more complicated as one factor can be important in the beginning of the experiment and other factors could become more important after the course of time. However, in order to be able to make certain assumptions, more experimental points for the beginning of the experiments are needed. Mendez et al (2008) suggests that the type of dust controls the mechanism of dissolution in seawater and our data seem to support this.

Light did not seem to play an important role in the initial release of iron into seawater because the initial sub sampling during our experiments was performed before the seawater solution had been exposed to sunlight. This suggests that other mechanisms more important for the initial times governed the iron dissolution.

However at the end of the experiment, the dissolved iron concentrations are low but had not yet reached the control values, perhaps due to photochemical processes. A conservative estimate of the labile Fe photoreduction rate would be on the order of  $7 \times 10^{-13}$  mol labile Fe/h or  $5.6 \times 10^{-12}$  mol labile Fe/l day for 8h sunlight (Wells et al., 1991) which in this study would equate to around 0.28 nmol DFe in excess of background.

#### 4.3.5 Carbonate

The carbonate content in the soil is important because during cloud processing it can buffer the pH and thus influence the fate of trace metals (Loye-Pilot, 1986). Due to the way samples MSJ and NSJ were processed, by low/high pH cycling we doubt that there was any influence on our results from the carbonate since it was removed in this acidification step.

For the samples MB and NB with their direct acid treatment with HCl or H<sub>2</sub>SO<sub>4</sub> (for the on board experiments) formation of CaCl<sub>2</sub> and CaSO<sub>4</sub> would be expected to be formed. The carbonate present in our samples was 0.28% for the Niger soil and 2.1%

for the Mali soil. The amount of 0.05M HCl added to Mali and Niger soil in the laboratory was soil was 80 $\mu$ L for every acid treated cycle and the amount of 0.025M H<sub>2</sub>SO<sub>4</sub> added to Mali soil for the on board experiments was 20 $\mu$ L. A simple calculation where 2 moles H<sup>+</sup> is needed to neutralize 1 mole CO<sub>3</sub><sup>2-</sup> to CO<sub>2</sub> showed that the carbonate was inadequate to change the pH of the seawater significantly for both for the laboratory and on board experiments.

#### 4.3.6 Removal of Iron from Solution

We postulate that the maximum amount of iron that could be released from the dust particles into the seawater, would be the iron held within the loosely bound fraction and within carbonate and oxide phases in the dust. In this study the maximum iron assumed to become dissolved, if there was no scavenging of iron taking place, is theoretically thought to be the measured hydroxylamine hydrochloride chemical leach, and was found to be 1.2%, 1.8% and 4.5% of the total Fe contained in soil to be released as DFe, for MS, MSJ and MB respectively.

When the aerosol particles enter the seawater, two simultaneous physico-chemical processes take place (Bonnet et al., 2004): dissolution of iron from the aerosol particles, possible complexation by ligands and adsorption of dissolved Fe back on the surfaces of these particles, in addition to more processes which result in the removal of dissolved Fe such as adsorption on container walls, adsorption or uptake into the organisms present, and precipitation of iron oxides.

However, our results show that after 5 days of the experiment, the percentage of dissolved iron decreased to around 0.012% for Mali soil, 0.012% for MSJ and 0.022% for MB which could either mean that iron was removed from solution during the course of the experiment or did not dissolve in the first place.

### *Adsorption of Dissolved Iron on the Bottle Walls*

Iron adsorption on the bottle wall can result in a serious underestimation of aerosol Fe solubility. When the amount of Fe released from the aerosol in the form of Fe(II) exceeds the Fe binding capacity of the ligands present in that seawater (as that may occur at a high aerosol to seawater ratio), the Fe(II) in excess of free organic ligands in the seawater would be oxidized and converted to Fe (III) oxyhydroxide colloids. Some of these colloids could be converted to filterable size particles, whereas others along with dissolved Fe ions could adsorb on the container walls and be removed from the solution, leading to an underestimation of the dissolvable Fe in the aerosol (Wu et al., 1995; Wu et al., 2001).

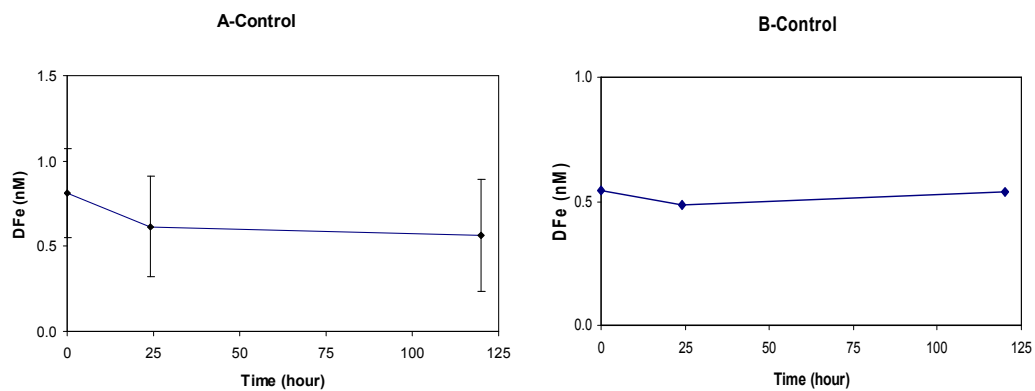


**Figure 4.8** Dissolved Fe concentrations in the control experiments **A** during the cruise, **B** in the laboratory.

In our study, we used polycarbonate bottles for all the dissolution experiments which according to the study by Fischer et al., (2007) are considered the best choice along with the PE bottles. After 70 hours of their experiment around 50% of the originally added iron, adsorbed on the walls of the container (Fischer et al., 2007), which is an important percentage, thus probably we should consider some removal of iron by adsorption on the container walls. However in the present work the experimental controls from both the laboratory and cruise dust addition into seawater experiments showed that the adsorption of iron on the container walls, or contamination of samples by the bottles was not very significant, (Figure 4.8) since the concentration values of iron do not show significant changes over the period of the experiment.

### ***Precipitation***

Under the pH and ionic conditions found in seawater, dissolved Fe (II) is rapidly oxidised within minutes. So  $\text{Fe}^{2+}$  oxidizes to  $\text{Fe}^{3+}$  which given the right pH precipitates as amorphous iron (hydr)oxides (Hove et al., 2008), mainly as amorphous ferrihydrite, which with time will age to more crystalline forms of iron oxides such as goethite and hematite, consistent with the observed removal of dissolved iron from solution (Schwertmann et al., 1983). As the amorphous ferrihydrite aggregate and become more ordered and more crystalline, the particles grow bigger and become less soluble.

### ***Particle Concentration Effect***

The distribution of a metal between its solid and solution phases, in theory, depends only on their relative concentrations (Honeyman et al., 1988). However, experiments have shown that metal solubility does not show this expected behaviour and seems to depend on the absolute particle concentration (Bonnet et al., 2004; Honeyman et al., 1988; Stumm et al., 1992). Aerosols in water, when the particulate loading is high, instead of providing a source through desorption behave as adsorption substrates resulting in the removal of dissolved metals from seawater (Chester et al., 1993). Dissolved iron in seawater, as shown by Zhuang et al. (1990) and later by Bonnet and Guieu (2004) seems to decrease when the total iron added into seawater as desert dust particles is increased. Zhuang et al. (1990) suggest the limit of total iron concentration in seawater to be 300 nmol/ kg before the solubility is controlled through equilibration with a ferric hydroxide solid phase with surface. Bonnet and Guieu (2004) suggest that the percentage of Fe seawater solubility decreases with introduced particle loading following a power law.

In our study a particle concentration of 10 mg/l was used because this amount was necessary to get a measurable effect and it is representative of concentrations of dust in seawater during a heavy dust episode.

### ***Microorganisms***

The results from the biotic light experiment suggest that there was a more rapid removal of iron from the dissolved phase under these conditions compared to the abiotic

experiments. This may be due to uptake into cells by the microorganisms since the seawater is not filtered, or by adsorption on the surface of the bacteria or phytoplankton cells. Several studies have reported ferromanganese oxides coatings on marine bacteria (Cowen et al., 1984); Heldal et al., 1996). The surface of algae provides various types of surface groups on which metal ions can be adsorbed (carboxyl, amino groups, and sulphide groups in proteins at the cell surface; Sigg 1998). Moreover, phytoplanktonic and bacterial exudates would enrich the pool of transparent exopolymeric particles (particles formed abiotically by coagulation of colloidal organic matter and substances exuded by phytoplankton and bacteria) in the microcosms. These particles (1-100 $\mu$ m) also have a large complexing capacity of DFe because of their richness of anionic polysaccharides (Bonnet et al., 2005). Beauvais (2003) showed that these particles can adsorb up to 20nmol of Fe under natural conditions per litre of coastal water. The seawater collected for this experiment was from near the Canary Islands and during the work the number of synecococcus cells was measured to be 5045 cells/ml. Supposing these cyanobacteria to be spheres, with a diameter of 0.8-1.5 $\mu$ m we can estimate the surface area to be between 10.1-26.7mm<sup>2</sup> at the disposal of the iron in the dissolved phase.

#### **4.3.7 Implications for cloud processing**

The results of this study indicate an initial high release of iron into seawater from the processed soils and low initial concentrations from the unprocessed Mali and Niger soil samples. These findings are important because they support the hypothesis that the cloud processing of dust particles will increase iron dissolution. An implication of this is the possibility that during long range transport of aerosol mineral particles in the atmosphere and at relative low pH encountered at ambient humidity or in a cloud solution (Zhu et al. 1993; Spokes et al. 1994; Spokes and Jickells 1996; Siefert et al., 1999; Wu et al., 2001; Wu et al., 2007) soluble Fe and nano-sized amorphous iron particles are formed which are either readily released or the iron nanoparticles are dispersed upon entrance into seawater.

Thus, we suggest that if the dust particles undergo cloud processing by mixing with acidic gases and evaporation and condensation cycling in low pH within the clouds, the metals bound to the solid matrix would change. Supported by the

microscopic data previously presented in Chapter 3 we conclude that amorphous iron nanoparticles and simple iron salts are formed which were quantified by the sequential extractions as easily reducible iron fraction.

#### **4.3.7.1 Wet versus Dry Deposition**

Trace metal solubility is therefore initially influenced by the reactions between aerosol and rainwater and a fraction of the iron already dissolved in water before it is deposited at the surface of the ocean. The dissolved/particulate speciation of the metals is a function of the rain water chemistry, especially the solution pH. However in the dry deposition mode, aerosols reach the sea surface directly without previously having undergone processes that could alter their mineralogy or keep trace metals dissolved in cloudwater if the pH is appropriate.

Guerzoni et al.,(1992) found that approximately 75% of Saharan Dust is deposited with precipitation in the Western Mediterranean. During the summer season the dry deposition of aerosols is higher and during spring and autumn wet deposition is more important. The aerosols in the dry mode are delivered directly to the sea surface by air- sea route and trace metal solubility is constrained by aerosol – seawater reactions (Guerzoni et al., 1996).

### **Manganese**

The leaching experiments for manganese suggest that the content of manganese in the dust depends on the origin of the sample. The Mali soil samples contained a slightly higher percentage of extractable manganese, 0.07%, compared to the Niger soil samples, 0.06%. Thus, the difference in the amount of dissolved manganese released into seawater is probably due to the different amount of total manganese in the parent soils.

The SJ dust samples were initially cycled in MQ water at low pH. The results showed that most manganese was released in the water, leaving only a very small fraction of the manganese to be dissolved in the seawater during the dissolution experiments. Thus it is expected that the leachable manganese will be already

solubilised in raindrops containing dust particles, and enters the seawater column in a dissolved and labile form.

Data on manganese from the dissolution experiments showed that for all types of dust investigated, very rapid solubilisation was observed. Accessible surface sites on the dust allow desorption of the Mn. After around 6 hours a concentration plateau of dissolved manganese was reached and the dissolution rate of manganese did not increase greatly in the course of 5 days. This may be because all the labile manganese has been solubilised and the manganese left in the dust is bound within silicate lattices (Statham et al., 1988), or the seawater has been saturated with manganese with the rest reabsorbing on the dust particles or the walls of the bottle.

Relatively little is known about the dissolution of aerosol manganese in seawater and only the studies made by Statham and Chester (1988) and Guieu et al. (1994) have provided some information about manganese (Saharan dust) dissolution in seawater. Both Statham and Chester (1998) and Guieu et al. (1994) found that 25% of the total Mn goes into solution after less than an hour. In this study the amount of Mn that goes into solution after less than an hour from the non treated Mali soil is similar (22.5%) and seems to derive from the fraction of Mn which is loosely bound as well as carbonate and surface oxide forms. This amount is similar to the loosely bound fraction is 31.2% of the total amount of Mn present in the Mali soil as shown in Chapter 3 where the sequential extractions of the soils are presented.

The processed soils (MB, NB) released more manganese into seawater with the Niger processed soil releasing about 30nM compared to 22nM of the non processed and the Mali processed around 65-70nM compared to 26nM of the non processed soil. There has been no similar study of dissolution experiments using processed soil samples in order to compare the data of the present study. If the soil contained Mn (II) minerals, the seawater would have dissolved all accessible manganese, leaving only Mn found deep within the matrix of the particles unleached. Statham and Chester (1988) suggest that the rapid dissolution of Mn may be due to labile manganese in coatings on the natural particles. Surface oxyhydroxide phases which can readily respond to pH/Eh changes will be more environmentally available than manganese within silicate lattices.

The amount of manganese released to the seawater caused by the acid treated samples MB (MB; which is simulating the repeated encounter of aerosol particles with acids, wetting and drying cycles in the clouds) was around 20nM more than the manganese released from untreated dust, which suggests that the manganese became

more labile after being atmospherically processed. Thus it can be inferred that when mineral particles are incorporated into a cloud in the atmosphere and undergo cycles of evaporation and condensation, the amount of manganese released, when these minerals hit the surface of the sea, will be higher than the amount of manganese that will be released from dry deposition because the manganese will be already dissolved phase during the cloud processes.

The rapid release of manganese was in good agreement with previous studies by Lindberg and Harris (1983) and Statham and Chester (1988). Guieu et al. 1994 suggest that solubilisation of Mn from pollution derived aerosols in seawater is slightly higher than manganese released from mineral aerosols, and consequently Mn may be more exchangeable in character and thus, more soluble. Our data for the processed soil (MB, NB) suggest as the Mn released is around 60nM for our dissolution experiments compared to the ~ 30nM Mn released from the non treated Mali and Niger soil.

Although the amount of released iron into seawater was not connected to the total iron content in the soil, there was a positive relationship between total Mn concentration and dissolved concentration in the seawater. Thus, the greater manganese content of the soil, the higher the release later into seawater. This effect is more obvious when the total Mn concentration introduced into seawater is less than about 5.5 mg/ L as suggested by Guieu et al., (1994). The saturation concentration for Mn should not be higher than 60nmol / L as given in the study of Guieu et al., (1994). The fact that most manganese dissolved from the processed MB sample, which reached a maximum concentration almost from the beginning of the experiments, is probably due to an alteration in the speciation of manganese in the mineral phase during the process of the MB and it is in agreement with the findings of Mendez et al. (2008) which suggest that dissolution is driven by mineral specific solubility.

A likely explanation for the observation that under light conditions the dissolved Mn values from the MS samples are higher than in the dark experiment is photoreduction. For all three experiments polycarbonate bottles were used which allow the light to come through and especially the UV wavelength were photoreduction of manganese is more likely to occur. Sunda et al. (1993) found that the oxidation of manganese is prevented by photoreduction. They concluded that sunlight increased the dissolution rate of manganese oxides 6-70 times higher than rated in the dark. The exact mechanism of photochemical reaction remains unclear (Sunda et al., 1993).

A possible explanation for the slightly smaller amount of net dissolved Mn released during the biotic light experiment compared with the other two experiments may be due to the uptake by the organisms present in the biotic seawater or due to adsorption on the surface of the organisms. However as no manganese was lost from the solution in the controls, substantial uptake on bottle walls does not seem to be occurring.

#### **4.4 Conclusions**

One of the most significant findings to emerge from this study is that the processed soils which have been treated in a way to simulate atmospheric cycling, released more iron and manganese into solution both for the Laboratory experiments and the Cruise experiments. This implies that Saharan dust that reaches the open oceans after a long range transport will contain more reactive iron due to the cloud processing than the Saharan dust which has only a short transit time from the African source desert. Thus, the pathway the dust followed before the deposition of Saharan dust to the open oceans is important. However the dissolved iron released from dust will quickly oxidize and precipitate and probably only the iron bound with ligands will remain dissolved.

The manganese released from the processed soils (MB, NB) is much higher than the manganese released from the non processed soils. The fact that after the MSJ treatment all manganese remained in solution has important implications for rain processing. A large fraction of particulate Mn released would stay in solution if it has previously been atmospherically processed. Thus, when particles hit the sea surface under wet deposition all the manganese will be already soluble.

The amount of iron released is not related to the total amount of iron present in the soil and iron dissolution is more dependent on the iron soil mineralogy. Thus, dust deposition and iron solubility are more important variables to understand than the regional differences in iron amounts in source soils.

For manganese, the origin of the soil is very important and it does not have to be processed in order to release manganese. Dissolved manganese is directly connected to the total manganese present in the soil. So, different soils affect the amount of manganese that will come to solution. This has very important implications when comparing published data.

The DFe concentrations were much lower when the dissolution experiment was conducted in the laboratory, whereas during the aboard seawater dissolution experiments, more iron was found to be released into seawater. In contrast, the amount of dissolved manganese released into seawater either in the laboratory experiments or on board experiments was similar for each soil used.

It seems therefore that the conditions of each experiment e.g., the use of fresh seawater instead of stored one can provide different results. It is not surprising that the DFe laboratory results were different to the DFe on board results since the solubility of iron is dependant on many factors such as ligands, pH, temperature that can not be identically reproduced in both laboratory and cruise experiments. It is important to notify as far as the ligands are concerned, they are considered responsible for retaining iron in solution, however they are quite unstable and they are not found in stored seawater.

The fresh seawater did not seem to influence the release of manganese. The amount of Mn released from soil to seawater, was determined rather by whether the soil had been previously processed or not and if it was of the same origin.

All data from the dissolution experiments manifest rapid initial release of dissolved iron, but always in low concentration levels, that was lost within hours from solution, whereas manganese remained in solution throughout the experiment.

Iron and manganese are both essential nutrients for phytoplankton; however they differ greatly in dissolution kinetics and behaviour in solution. Manganese is much more soluble in seawater than iron. Non treated Saharan soils release around 30-40nM dissolved manganese much more than dissolved Fe which reached values of around 1.5-2nM.

Manganese is more soluble than iron and it has slow oxidation kinetics thus it remains in solution much longer than dissolved iron and it transforms into insoluble forms much slower than iron. Dissolved iron is quickly removed from solution because it is less soluble and given the right conditions quickly oxidizes to more insoluble colloidal forms. These colloidal iron particles aggregate, precipitate and they age into more crystalline iron species thus are removed from the system.

Another difference is that the dissolution of manganese depends on the total manganese concentration of the soil (Guieu et al., 1994, this study). The type of the soil and the quantity and form of manganese content seemed to affect the release of it into the seawater. This is very different to the dissolution of iron that seems to be

independent of the total iron and the iron solubility is affected only by the form of iron minerals associations in the soils.

The use of biotic water in the dissolution experiment provided lower dissolved iron values compared to the abiotic water used for similar experiments. Following the same trend, the released manganese from untreated soil was less when the seawater used was not filtered. However, no change in the dissolved manganese concentrations was observed when processed soil was used.

Biota seems to be important for the dissolved iron as it could act as a substrate for iron removal from solution either by direct intracellular uptake or, adsorption on the cells. The manganese originating from untreated soil seems to be influenced by biota, either by uptake and/or adsorption of manganese by phytoplankton (Rackebrandt, 2009), but when the seawater has been saturated in dissolved manganese, as it did when processed soil was used, the dissolved manganese concentration remained at the same levels.

The seawater experiments performed under light conditions did not show any significant increase in the dissolved iron concentrations, for soils either treated or untreated. Probably photoreduction did not play an important role in iron dissolution at the timescale of the experiments.

Manganese released from treated soils is not dictated by photoreduction but by other mechanisms such as amount of total manganese, minerals containing manganese and how the treatment has influenced those minerals. However, non-treated soils seem to be influenced by photoreduction and release more manganese. In the case of biotic light experiments where the dissolved manganese seemed to be less than in the other two experiments could be due to the fact that photoreduction is competing with other processes including uptake by biota.

## Chapter 5

### Bioassays

#### 5.1 Introduction

Because the North Atlantic waters contain high Fe concentrations around 0.4-0.6nM (Wu et al., 2001), there have been few studies investigating the importance of Fe on primary production in these waters. DFe concentrations in surface waters are highly variable in space and time, due to the episodic dust storms, hydrographic features and biological activities (Blain 2004).

The mechanism by which iron is taken up by algae in the natural system is not yet fully established. However recent data indicates that iron uptake by eukaryotic algae (diatoms) is improved when complexed by protoporphyrins, whereas prokaryotic algae (as exemplified by cyanobacteria) better take up siderophore-bound iron (Hutchins et al., 1999). This is consistent with a mechanism in which the eukaryotic algae use an uptake system based on iron-reduction at the cell surface followed by ionic iron transport.

In this study bioassay experiments were performed using a highly replicated design to investigate the effect of nutrient addition on phytoplankton physiology, growth and nutrient drawdown. The North Atlantic has no permanent HNLC regions. In the permanently stratified oligotrophic subtropical and tropical North Atlantic the availability of macronutrients limits phytoplankton production year round (Graziano et al., 1996; Mills et al., 2004). Conversely, deep winter overturning injects nutrients into surface waters of the central and northern North Atlantic causing transient high nutrient conditions. These high macronutrient inputs result in the development of a marked spring bloom with accumulation of phytoplankton biomass, and significant sequestration of atmospheric CO<sub>2</sub> (Honjo & Manganini, 1993).

Despite the low ratios of Fe to nitrate in upwelled waters in the North Atlantic (Fung et al., 2000; Wu & Boyle, 2002) the spring bloom results in complete removal of nitrate from the mixed layer. The supply of Fe from mineral aerosol of African sources (Gao et al., 2001) is considered to be sufficient to preclude Fe limitation of phytoplankton growth in the North Atlantic.

The aim of our part of the bioassays experiments is to increase our knowledge as to whether chemically reactive iron produced as a result of cloud processing, changes the biological activity in the N. Atlantic.

## **5.2 Description of the Bioassay Experiments**

As with all work involving manipulation of iron availability for phytoplankton populations, strict controls were required to avoid contamination of incubation containers and sampled water. Incubations were performed in 2 l polycarbonate bottles which had passed through a rigorous cleaning process involving a Decon wash and soaking in 50% HCl for 1 week, followed by rinsing then storage with acidified MQ prior to sailing.

The seawater used in the experiments was collected from the underway Fe fish and it was tested for iron contamination in each step of the experiment. The experimental design involved the incubation of 36 bottles in 12 sets of 3 replicates, one set each for control and time zero, one set with  $\text{NH}_4\text{NO}_3$ , P, one set Fe, one set P+Fe, one set N +P, one set P+Fe, one set N+P+Fe, one set MS, one set MSJ and one set MB. The soil was  $2\text{mg soil L}^{-1}$ . All three replicate bottles were sub-sampled after 48 hours.

Sampling of the time-series was routinely performed for chlorophyll, ambient macronutrients (N, P and Si), APA – alkaline Phosphatase activity and PSII characteristics as measured by FRRf but since the data did not show anything interesting they will not be presented. In order to assess contamination, samples were also collected for analysis of total dissolvable iron (TDFe) at the end of the experiments. Each experiment was performed with collaboration of the following people Micha Rijkeberg, measured DFe, Claire Mahhaffey, measured APA, Mark Moore, measured FRRf, Duncan Purdie, measured Chlorophyll A. Eric Achterberg and myself together with the people mentioned above performed each of the experiments.

The map of the locations of the Bioassay experiments is given in Figure 5.1. The sea temperature was around 22°C for Bioassays 1 and 2 and around 24°C and the salinity around 36 except for Bioassay 1 that it was 37.5.

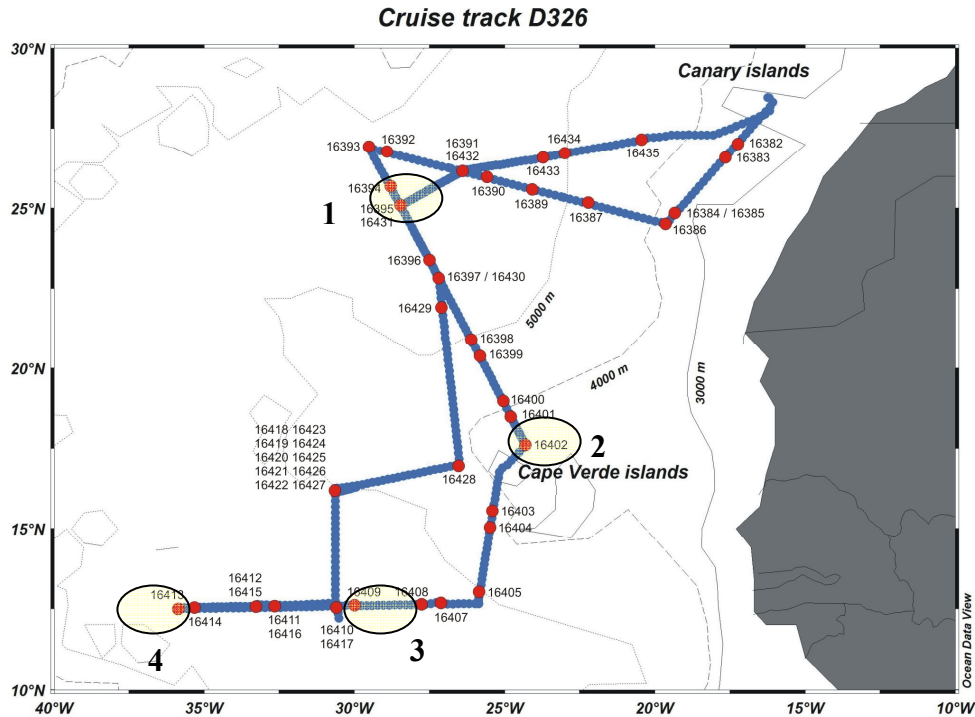
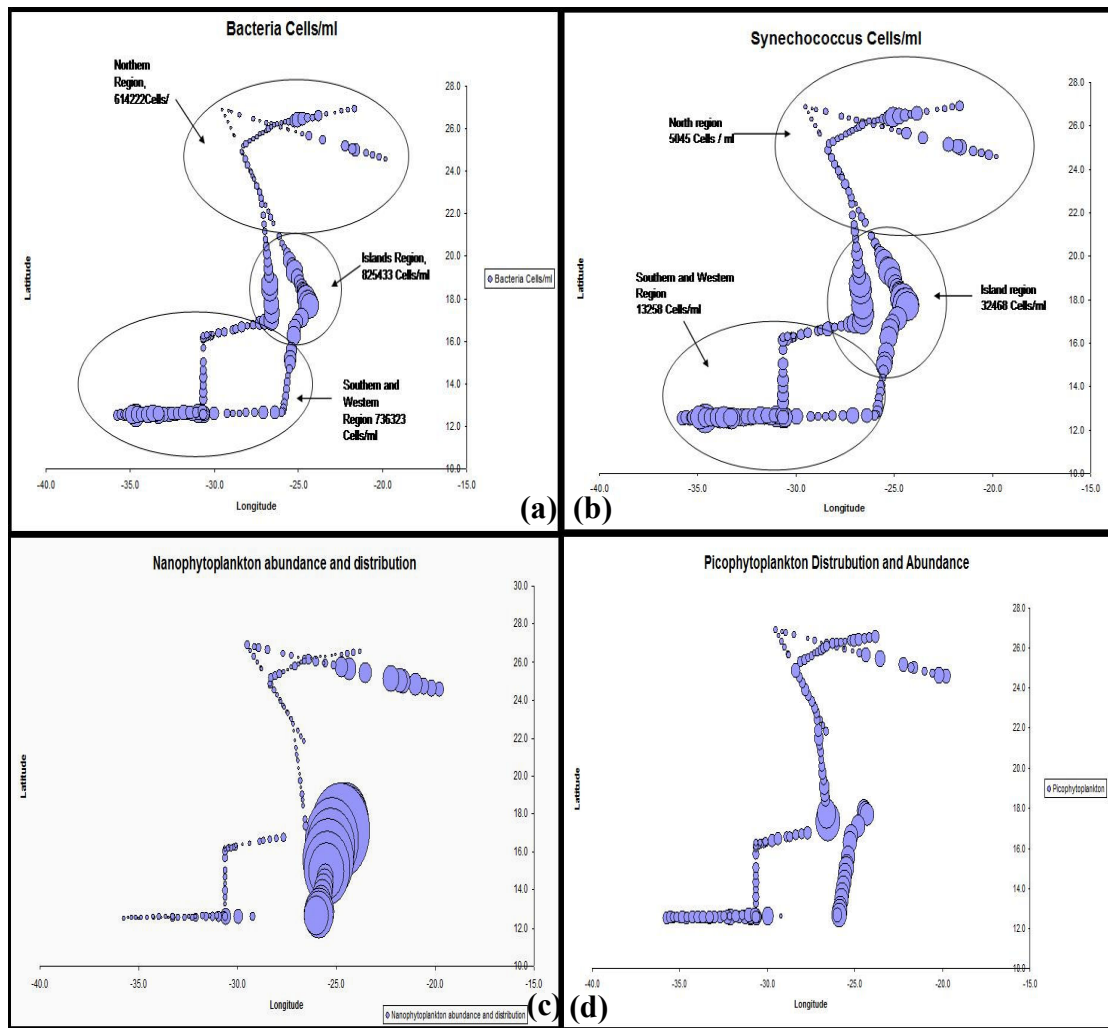


Figure 5.1 Map of the location of the Bioassays 1, 2, 3, and 4

Flow Cytometric Analysis was performed by Ross Holland during the D326 Cruise and 2 protocols run, one for analysis of heterotrophic Bacteria and Cyanobacteria, and one for Pico- and Nanophytoplankton. The results courtesy of Mr Holland are given in Figures 5.2 (a), (b), (c), (d).



**Figure 5.2** Abundance and distribution of (a) heterotrophic bacteria, (b) synechococcus, (c) nanophytoplankton, (d) picophytoplankton

High amount of heterotrophic bacteria was present in this part of the Atlantic with mean abundance of 700000 bacteria/ ml and more specifically between the Canary Islands and Cape Verde and  $1.5 \times 10^6$  close to Cape Verde islands (Figure 5.1(a)). The synechococcus abundance varied between  $<2000$  cells/ml between Tenerife and Cape Verde to  $>70000$  cells/ml close to Cape Verde (Figure 5.2 (b)). The picophytoplankton, class size  $0.2-2 \mu\text{m}$ , varies between 400 Cells/ml between Tenerife and Cape Verde, to 10,000 Cells/ml around Cape Verde (Figure 5.2(c)). The nanophytoplankton abundance varies between  $<100$  in the Southwest and North to 10000 Cells/ml around the Cape Verde Islands (Figure 5.2 (d)).

## 5.3 Results

### 5.3.1 Chlorophyll A

The chlorophyll a measurements from the four experiments are given in Figure 5.3. In the first Bioassay the chlorophyll levels are quite low for all bottles regardless what was added. Compared to the control bottle, the ones that produced more chlorophyll are where N was added, either alone or with other nutrients such as P, Fe. In the case of the MSJ bottles the Mali soil was low pH cycled, and  $\text{HNO}_3$  was used to lower the pH, and thus nitrogen was added to these samples as well as the soluble metal nitrates dissolved from the particles. The other two sets of soil added bottles MS and MB had low chlorophyll values similar to the control bottles.

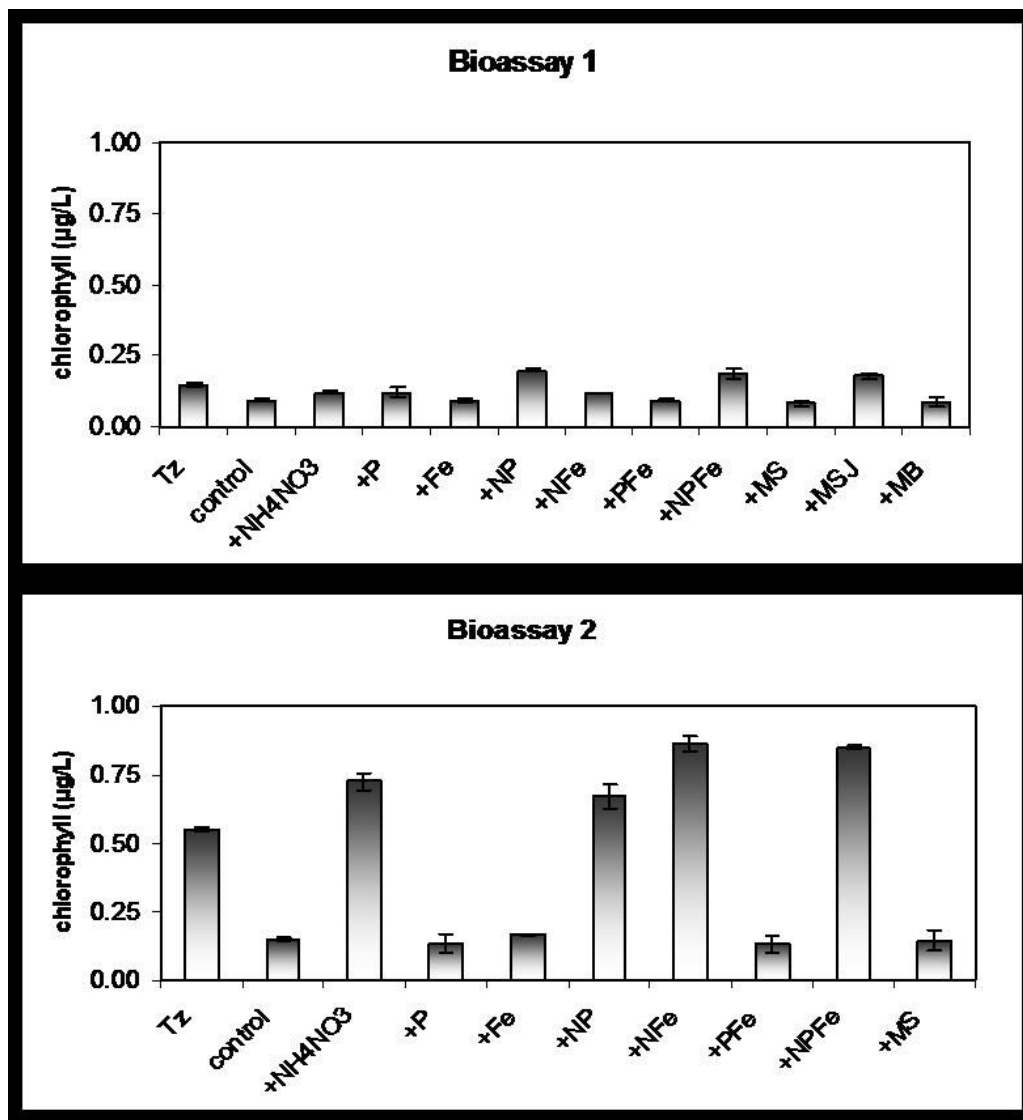


Figure 5.3 Concentration of Chlorophyll (µg/L) in Bioassays 1 and 2 (MS: Mali soil)

In Figure 5.4 the chlorophyll values of the Bioassay 2 are in general higher than Bioassay 1 with some of the highest reaching close to 1  $\mu\text{g/L}$ . Once more the bottles containing N in some form raised the chlorophyll values, giving the highest when N was combined with P and Fe, or just Fe. The value of chlorophyll for the MS and MB added bottles was at the same levels with the control bottles. Tz sample stand for time zero and it was sampled immediately.

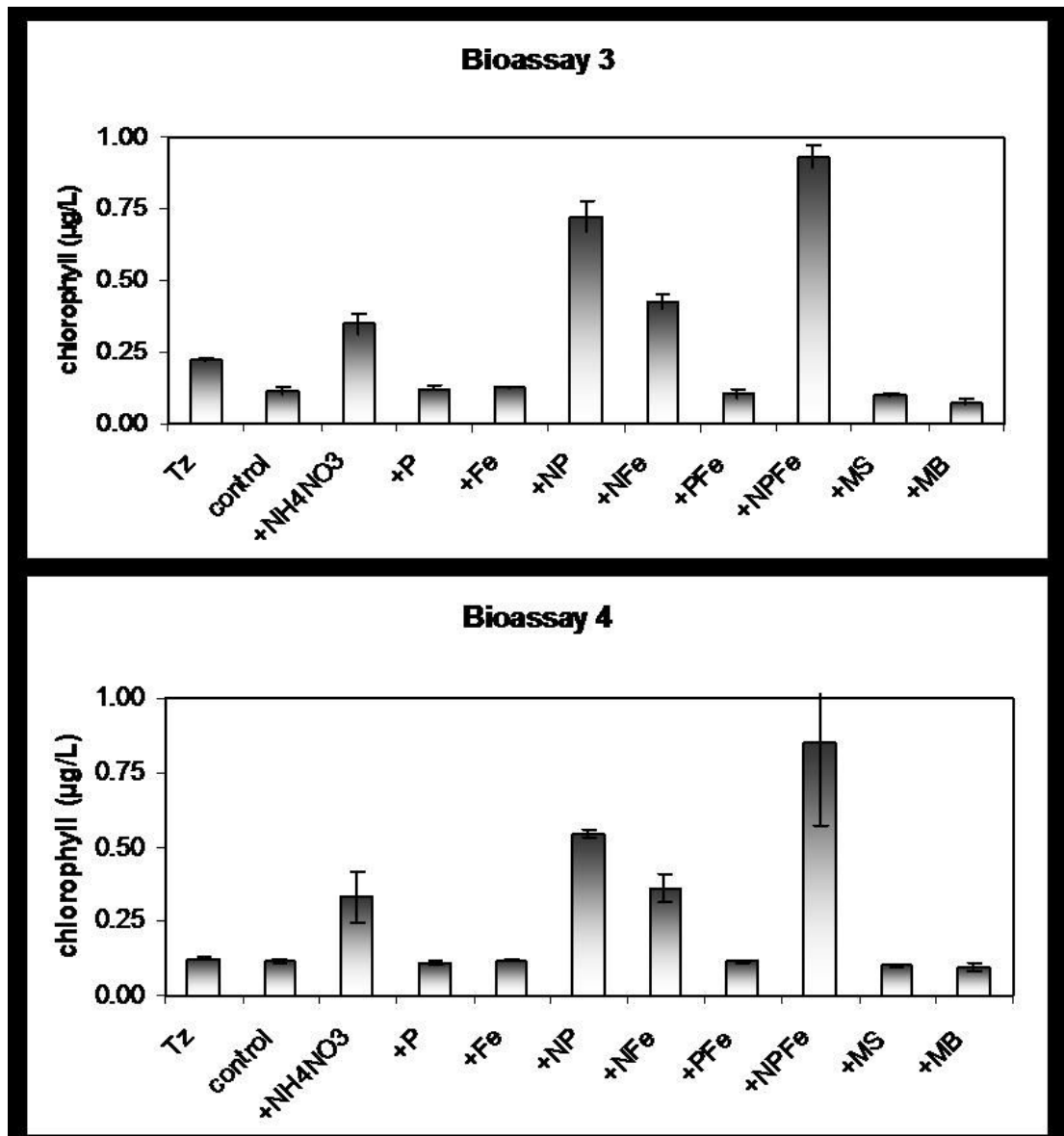


Figure 5.4 Concentration of Chlorophyll ( $\mu\text{g/L}$ ) in Bioassays 3 and 4 (MS: Mali soil, MB: acid treated processed soil)

The same response was seen for Bioassays 3 and 4 where the chlorophyll values are almost at the same level as the control, unless the bottles included N. The confidence level for Bioassay 3 between MS-MB is 99.9% and for Bioassay 4 is 78.2%.

### 5.3.2 Alkaline Phosphatase Activity

The primary means by which marine phytoplankton can convert organic P to bioavailable orthophosphate is induction of alkaline Phosphatase (AP) (Cotner and Wetzel 1991), an enzyme which has broad substrate specificity and hydrolyses ester bonds between phosphate and organic molecules, making organic-P available for cellular assimilation by converting it to phosphate (Cembella et al. 1984). In the study area where the bioassay experiments took place, the seawater contained a high amount of heterotrophic bacteria with a mean value of 700,000cell/ml and considerable smaller amount of nano and pico phytoplankton and synechococcus abundance with mean value 12,000cell/ml.

The nanomolar concentrations of P at the sites where the bioassays took place, were measured by Matt Patey, NOC, and he measured for Bioassay 1 the Phosphorus concentration to be <11nM, for Bioassay 3 6-20nM and Bioassay 4 <10nM. For Bioassay 2, using conventional auto-analyser systems was found to be 100-140 nM.

The alkaline Phosphatase activity –APA was measured by Claire Mahaffey for all sets of bottles for Bioassays 2, 3 and 4 and the results are given at Figure 5.5. Positive response is considered when the value of nmoles P  $\mu\text{g}^{-1}$  Chl  $\text{day}^{-1}$  was higher than the initial APA value which was  $0.17 \pm 0.03$  nmoles P/  $\mu\text{g}$  Chl  $\text{day}^{-1}$ .

In Bioassay 2 (Figure 5.5(a)) the N addition increased the APA value was 1.5 times more than the initial value similar to Fe bottles set around 0.23 and the MS bottles gave an APA positive response 3 times the initial value 0.47.

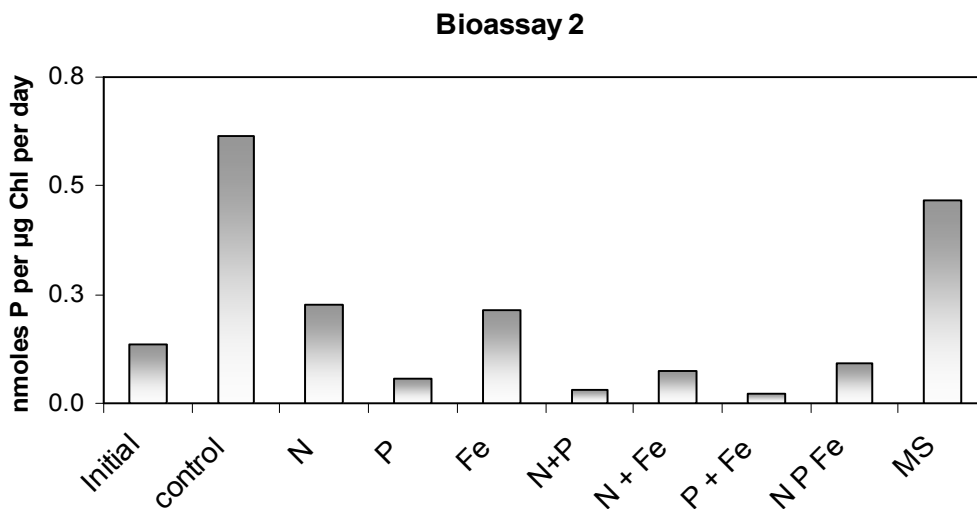
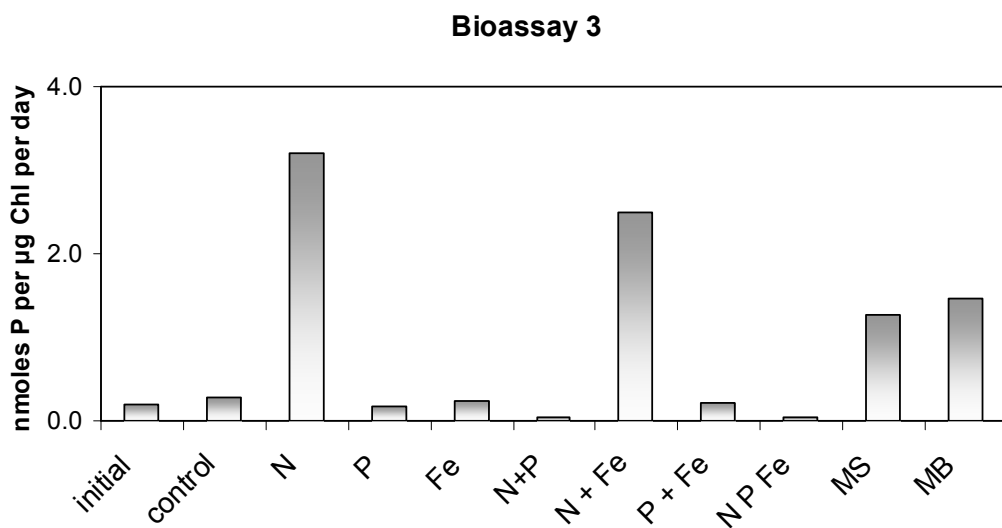


Figure 5.5 (a) Alkaline Phosphatase Activity nmoles P  $\mu\text{g}^{-1}$  Chl  $\text{day}^{-1}$  for Bioassays 2

During this Bioassay, there was a positive response in APA from the control set over the initial value which means that there was contamination during the experiment. However the APA in the other treatments are compared to the initial APA value and since the results from the additions seem coherent with the other two Bioassays, the APA results from Bioassay 2 are thus included.

The APA data from Bioassay 3 (Figure 5.5(b)) showed that the addition of N caused a significant increase in APA to  $3.2 \text{ nmoles P/ } \mu\text{g Chl day}^{-1}$  almost 16 times the initial value. The addition of MS increased the APA six times and the addition of MB increased the APA seven times.



**Figure 5.5 (b) Alkaline Phosphatase Activity  $\text{nmoles P } \mu\text{g}^{-1} \text{ Chl day}^{-1}$  for Bioassays 3**

The results in Bioassay 4 (Figure 5.4 (c)) are similar to the other 2 bioassays. The addition of N and N+Fe increased the APA by a factor of 14 and 11 accordingly. The soil additions also increased the APA however the MS increased APA only 4 times more to the initial seawater value when MB increased it 11 times more. The DFe added in the bottles was  $2 \text{ nM per L}$  of seawater. According to our study the maximum amount of Fe that could be released into seawater from the MS soil is  $1.30 \mu\text{M}$  and from MB soil  $1.35 \mu\text{M}$ . The minimum DFe concentrations are given by the dissolution experiments (Chapter 4) so, the addition of MS soil introduced to the system less than  $1 \text{ nM DFe}$  and less than  $4 \text{ nM}$  the addition of MB soil (biotic light experiment).

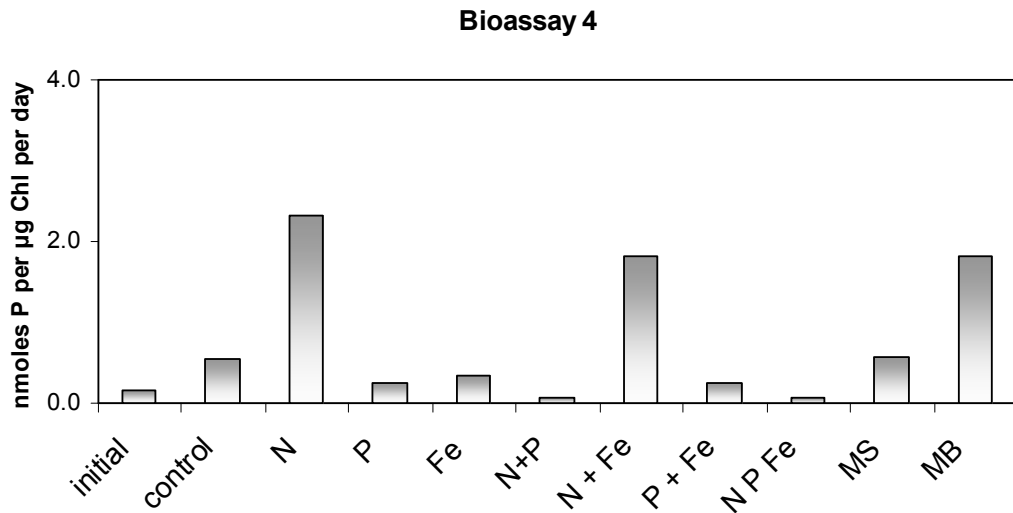


Figure 5.5 (c) Alkaline Phosphatase Activity  $\text{nmoles P } \mu\text{g}^{-1} \text{ Chl day}^{-1}$  for Bioassays 4

## 5.4 Discussion

It is evident from the Chlorophyll *a* measurements that unless N was introduced to the system, no significant change was noticed to the Chlorophyll *a* values. In the case of soil addition, when MSJ (low pH cycled soil) samples were added, the chlorophyll concentration increased as if adding N+P+Fe. This is probably due to the way the MSJ samples were treated, since  $\text{HNO}_3$  was used to lower the pH during the treatment (see Chapter 2) thus, N was introduced to the system and traces of N probably were deposited on the soil. So, the MSJ addition added the nutrients N, and Fe. Because of this effect, MSJ samples were not used for further Bioassays. In all bioassays the chlorophyll values increased only when N was added. When the MB (acid treated soil) sample or MS (non processed) sample were added, the chlorophyll concentration did not increase. Thus, it was concluded that the North Tropical Atlantic was N limited which is in agreement with previous research performed in the same region of the Atlantic (Martin et al., (1993), Fung et al, (2000) and Mills et al. (2006)) that suggested the Tropical Atlantic is nitrogen limited. The addition of Fe to the system had no effect on the primary productivity because the system is not iron limited. This is because this region strongly impacted by Saharan dust input which is a major external source of iron to oceanic surface waters (Jickells et al., 2005; Jickells, 2001). The release of P from Saharan dust is of lower importance since  $5\text{mg L}^{-1}$  of untreated dust might releases

around 25 nM P (Herut et al., 2002; Ridame et al., 2002) and in our study a particle concentration of 2mg/L that was used hence releases less P.

Some background information on alkaline Phosphatase is needed in order to explain the Bioassay APA results. The primary means by which marine phytoplankton can convert organic P to bioavailable orthophosphate is induction of alkaline Phosphatase (AP) (Cotner and Wetzel 1991), an enzyme which has broad substrate specificity and hydrolyses ester bonds between phosphate and organic molecules, making organic-P available for cellular assimilation by converting it to phosphate (Cembella et al.1984). It has been suggested that AP activity is induced by bacteria to hydrolyze organic P molecules to access reduced carbon, P or both (Kirchman et al., 2000; Van Wambeke et al., 2002). Heterotrophic bacteria, in particular, are likely to be P limited as they have higher P requirements than phytoplankton (Cotner et al., 1991; Pomeroy et al., 1995) since they live on DOC, DON, and DOP.

In general, addition of phosphate suppresses alkaline Phosphatase activity, but addition of nitrate, nitrate and iron and dust increases the rates of alkaline Phosphatase activity. This implies that after the N, N+Fe addition, the microbial population was phosphorus limited and therefore needed to produce alkaline Phosphatase to cleave the phosphorus from organic-bound phosphorus.

When untreated soil was added to the seawater there was also a positive response in APA and an even greater APA response when the soil had been previously treated. This positive APA response can be due to microbial population and/or nitrogen fixers that require P. In personal communication with Claire Mahaffey (measured AP activity) she thinks that APA cannot be attributed to nitrogen fixers alone and considering the volumes of incubation, were probably related more to the background microbial population rather than just nitrogen fixers.

However, we suggest that responsible for this positive alkaline Phosphatase response must be an organism that is Fe and P colimited. The processed Saharan soil (MB) contained more chemically reactive Fe than the untreated one, thus it maybe the reason for the higher positive APA response compared to the untreated one. Given that fact we think this group of organisms are responsible for the AP activity are nitrogen fixers. Since the APA of *Trichodesmium* spp. which is abundant in the specific region of the tropical North Atlantic, was not separately measured, it could not be attributed to *Trichodesmium*. The diazotrophic nature of *Trichodesmium* ensures that it is never limited by N and thus other nutrients are important in regulating growth and nitrogen

fixation. Sohm et al (2006) found that DIP concentrations in surface N.Atlantic waters were not sufficient to achieve a growth rate measured of 0.1 per day for *Trichodesmium* colony. Thus, it is suggested that in subtropical and tropical N Atlantic waters *Trichodesmium* does not appear to be able to grow on DIP alone so, P uptake from the DOP pool appears very important to growth (Sohm et al., 2006; Sohm et al., 2008).

Taken together, the results from the Bioassays show that the addition of processed soil, where more reactive Fe is present does not stimulate production since the system is N limited (Mills et al., 2005). However, the processed soil demonstrated a high positive response to alkaline Phosphatase higher than untreated soil that probably means that the nature of Fe added matters to the microbial community. The implication of this is that although this is an area with high mineral deposition thus iron should be in excess, the dust being so near to the source did not have much time to take part in atmospheric processes that could increase the amount of reactive Fe present in the dust. So it is fair to conclude that dust far away from the source that has travelled in the atmosphere for longer will contain more reactive iron and the impact on seawater biota will be higher.

There is a need for further bioassay studies where soil with cloud processed dusts and known processed history, will be added and more parameters will be measured such as  $N_2$  and  $CO_2$  fixation rates along with the chlorophyll a concentrations in order to explain the data more thoroughly.

## Chapter 6

### Conclusions

This thesis investigates the transformation procedures that occur in desert dust particles during their passage through the atmosphere to the ocean as well as providing data to increase our understanding of Fe and Mn released to the ocean.

The data in Chapter 3 illuminate the composition and structure of the Saharan soil and more specifically the Fe-bearing phases in the soil and the phase transformations that occur during cloud processing. It was the first time until recently (Shi et al., 2009) that Saharan soil was artificially atmospherically weathered and then examined by using a combination of microscopy techniques such as scanning electron microscopy and transmission electron microscopy. These techniques indicated formation of iron nanoparticles, and more specifically ferrihydrite particles. The observation above suggests that the amount of reactive iron after simulation processes is increased.

This observation implies that during long range transport of aerosol mineral particles in the atmosphere and at relative low pH encountered at ambient humidity or in a cloud solution (Siefert et al., 1999; Spokes et al., 1996; Spokes et al., 1994; Wu et al., 2007; Wu et al., 2001; Zhu et al., 1993), soluble Fe and nano-sized amorphous iron particles are formed which are either readily dissolved or the iron nano-particles are dispersed upon entrance into seawater. The size of these amorphous particles can be very important since nano-size material can pass through a 0.2  $\mu\text{m}$  filter that is used to separate dissolved Fe. Atmospheric processing can also generate simple iron salts that will readily dissolve on introduction into seawater.

Seawater dissolution experiments were conducted to determine whether solubility of iron and manganese has been altered by simulated cloud processing. The solubility of both iron and manganese increases when the soil particles were subjected to artificial atmospheric weathering. A higher iron release into seawater was clearly shown in all the data from the dissolution experiments, suggesting that there is increase

in the chemically reactive Fe in the processed soil. Manganese was also examined in terms of release from processed and non processed soils to seawater. Processed soils released more manganese into seawater. However the SJ method of simulating cloud processing released all soluble manganese from the soil and as a result the retrieved soil particles did not contain any manganese that could be released later in the seawater dissolution experiments.

These findings indicate that the Fe and Mn solubility of Saharan soils can be strongly influenced by atmospheric processing under low pH regimes and when material has been cycled through clouds during its transport (Baker et al., 2006; Bonnet et al., 2004). This implies that Saharan dust that reaches the open oceans after long range transport will contain more reactive iron due to cloud processing than Saharan dust which has only a short transit time from the African source desert. Thus, deposition of Saharan dust to the open oceans is important but to what extent might be defined by the pathway the dust has followed, before deposition. However the dissolved iron will quickly oxidize and precipitate and probably only the iron bound with ligands will remain dissolved.

The amount of iron released is not directly connected to the total iron content of the soil, but to the iron minerals present. Thus, dissolved iron inputs to the surface ocean relates more to the source regions and their mineralogy rather than the total Fe content in the source soils.

The fact that after the MSJ treatment all Mn remained in solution has important implications for rain processing. A large fraction of particulate Mn would stay in solution if it has been atmospherically processed, thus when particles hit the sea surface under wet deposition all the manganese will be already soluble.

The cloud cycling led to substantial transfer of Mn from particles to surrounding solution and thus it is expected that the leachable manganese in raindrops containing dust particles, will enter the surface seawater in a dissolved and labile form. The relative importance of wet and dry deposition modes and thus the fraction of Mn added to seawater in an already dissolved state will vary from region to region. Guerzoni et al, (1992) found that approximately 75% of Saharan Dust is deposited with precipitation in the Western Mediterranean. During the summer season the dry deposition of aerosols is higher and during spring and autumn wet deposition is more important. The aerosols in the dry mode are delivered directly to the sea surface by air- sea route and trace metal solubility is constrained by aerosol – seawater reactions (Guerzoni et al., 1996).

For manganese in the soils tested, release appears to be directly related to the total manganese present in the soil. Differences in metal release were noted when using fresh seawater as opposed to stored seawater. This was particularly so for experiments where released dissolved Fe and Mn appeared to be taken up by the natural organism populations present.

Limited information regarding the bioavailability of different forms of Fe was one of the driving reasons behind the design of the bioassays experiments performed during the North Atlantic cruise.

In light of results from Chapter 5 that indicate an increase in the Alkaline Phosphatase Activity-APA when dust is added and even higher APA increase when cloud processed dust is added is likely to be due to the response of an organism that is Fe and P co limited. Given that the North Tropical Atlantic is N limited, highlighted by our data in accordance with the work of Mills et al (2005) for the same part of the Atlantic, and because we know that N fixers are Fe and P co limited, it is thus possible that the organisms involved are N fixers. The nature of the Fe added is therefore important to the microbial community.

The impact of iron speciation on phytoplankton dynamics in the marine environment is currently not well understood. Our study highlights the fact that chemically reactive Fe is produced in the dust as a result of cloud processing. This leads to more soluble iron released into seawater. Thus, it is essential to understand that the mineralogy of iron in the dust particles will define the fate of iron in the seawater along with other mechanisms such as organic complexation, light, and the origin of the iron-bearing particles all of which are important for primary production stimulation. Therefore further dissolution experiments are necessary especially in Fe limiting oceanic regions using dust with various mineralogical compositions, collected in source areas and after transport, as well as a closer investigation in the particulate phase of dust. Moreover, further research on how iron-bearing particles originating from industrialised regions of the world should be considered since the worldwide industrialization and increasing anthropogenic emissions could result in an increase in the flux of more soluble iron into the surface ocean.

Lastly it is essential to investigate the biotic activity from the increased iron reactivity, whether the organisms are stimulated and which classes are mostly responding to iron addition. However the key point would be to gain more information

---

regarding the organic complexation and which organic types are important and understand the mechanism behind this complexation process.

## Bibliography

- Aguilar-Islas, A., Wu, J. and Rember, R., 2008. Dissolution of aerosol-derived iron in seawater: The influence of aerosol type, and dissolved iron size fractionation. *Marine Chemistry*, Submitted.
- Andreae, M.O., Charlson, R.J., Bruynseels, F., Storms, H., Vangrieken, R. and Maenhaut, W., 1986. Internal Mixture of Sea Salt, Silicates, and Excess Sulfate in Marine Aerosols. *Science*, 232(4758): 1620-1623.
- Baker, A.R., Jickells, T.D., Witt, M. and Linge, K.L., 2006. Trends in the solubility of iron, aluminium, manganese and phosphorus in aerosol collected over the Atlantic Ocean. *Marine Chemistry*, 98(1): 43-58.
- Barbeau, K., 2006. Photochemistry of organic iron(III) complexing ligands in oceanic systems. *Photochemistry and Photobiology*, 82(6): 1505-1516.
- Barbeau, K., Rue, E.L., Bruland, K.W. and Butler, A., 2001. Photochemical cycling of iron in the surface ocean mediated by microbial iron(III)-binding ligands. *Nature*, 413(6854): 409-413.
- Bates, T.S., Kapustin, V.N., Quinn, P.K., Covert, D.S., Coffman, D.J., Mari, C., Durkee, P.A., De Bruyn, W.J. and Saltzman, E.S., 1998. Processes controlling the distribution of aerosol particles in the lower marine boundary layer during the First Aerosol Characterization Experiment (ACE 1). *Journal of Geophysical Research-Atmospheres*, 103(D13): 16369-16383.
- Bates, T.S., Quinn, P.K., Covert, D.S., Coffman, D.J., Johnson, J.E. and Wiedensohler, A., 2000. Aerosol physical properties and processes in the lower marine boundary layer: a comparison of shipboard sub-micron data from ACE-1 and ACE-2. *Tellus Series B-Chemical and Physical Meteorology*, 52(2): 258-272.
- Biscombe, A., 2004. Factors influencing the seawater solubility of aerosol associated trace metals, University of Plymouth, Plymouth, 251 pp.
- Bonnet, S. and Guieu, C., 2004. Dissolution of atmospheric iron in seawater. *Geophysical Research Letters*, 31(3).
- Bonnet, S. and Guieu, C., 2006. Atmospheric forcing on the annual iron cycle in the western Mediterranean Sea: A 1-year survey. *Journal of Geophysical Research-Oceans*, 111(C9).
- Bowie, A.R., Achterberg, E.P., Croot, P.L., de Baar, H.J.W., Laan, P., Moffett, J.W., Ussher, S. and Worsfold, P.J., 2006. A community-wide intercomparison exercise for the determination of dissolved iron in seawater. *Marine Chemistry*, 98(1): 81-99.
- Boyd, P.W., 2000. A mesoscale phytoplankton bloom in the polar Southern Ocean stimulated by iron fertilization. *Nature*, 407: 695-701.
- Boyd, P.W., 2007. Biogeochemistry - Iron findings. *Nature*, 446(7139): 989-991.
- Boyd, P.W., Jickells, T., Law, C.S., Blain, S., Boyle, E.A., Buesseler, K.O., Coale, K.H., Cullen, J.J., de Baar, H.J.W., Follows, M., Harvey, M., Lancelot, C., Lavoie, M., Owens, N.P.J., Pollard, R., Rivkin, R.B., Sarmiento, J., Schoemann, V., Smetacek, V., Takeda, S., Tsuda, A., Turner, S. and Watson, A.J., 2007. Mesoscale iron enrichment experiments 1993-2005: Synthesis and future directions. *Science*, 315(5812): 612-617.
- Bruland K. W., R.E.L., 2001. Analytical methods for the determination of concentrations and speciation of iron. *The biogeochemistry of iron in seawater*. John Wiley and sons.

- Bruland, K.W., Donat, J.H. and Hutchins, D.H., 1991. *Limnol. Oceanogr.*, 36: 1555-1577.
- Buck, C.S., Landing, W.M., Resing, J.A. and Lebon, G.T., 2006a. Aerosol iron and aluminium solubility in the northwest Pacific Ocean: Results from the 2002 IOC cruise. *Geochemistry Geophysics Geosystems*, 7(4): 1-21.
- Buck, C.S., Landing, W.M., Resing, J.A. and Lebon, G.T., 2006b. Aerosol iron and aluminum solubility in the northwest Pacific Ocean: Results from the 2002 IOC cruise. *Geochemistry Geophysics Geosystems*, 7.
- Buck, C.S., Landing, W.M., Resing, J.A. and Measures, C.I., 2008. The solubility and deposition of aerosol Fe and other trace elements in the North Atlantic Ocean: Observations from the A16N CLIVAR/CO2 repeat hydrography section. *Marine Chemistry*, In Press, Corrected Proof.
- Buck, K.N. and Bruland, K.W., 2007. The physicochemical speciation of dissolved iron in the Bering Sea, Alaska. *Limnology and Oceanography*, 52(5): 1800-1808.
- Chen, Y. and Siefert, R.L., 2004. Seasonal and spatial distributions and dry deposition fluxes of atmospheric total and labile iron over the tropical and subtropical North Atlantic Ocean. *Journal of Geophysical Research-Atmospheres*, 109(D9).
- Chester, R., 1990. *Marine Geochemistry*, London, 698 pp.
- Chester, R., Murphy, K.J.T., Lin, F.J., Berry, A.S., Bradshaw, G.A. and Corcoran, P.A., 1993. Factors controlling the solubilities of trace metals from non-remote aerosols deposited to the sea surface by the "dry" deposition mode. *Marine Chemistry*, 42: 107-126.
- Clegg, S.L. and Brimblecombe, P., 1990. Solubility of Volatile Electrolytes in Multicomponent Solutions with Atmospheric Applications. *Acs Symposium Series*, 416: 58-73.
- Cornell, R.M., U. Schwertmann, 2003. *The iron oxides: Structure, Properties, Reactions, Occurrences and Uses*. Wiley-VCH, Weinheim, 664 pp.
- Cotner, J.B. and Wetzel, R.G., 1991. Bacterial Phosphatases from Different Habitats in a Small, Hardwater Lake. *Microbial Enzymes in Aquatic Environments*: 187-205.
- Cowen, J.P. and Silver, M.W., 1984. The Association of Iron and Manganese with Bacteria on Marine Macroparticulate Material. *Science*, 224(4655): 1340-1342.
- De Baar, H.J.W., 1990. *Mar. Ecol. Prog. Ser.*, 65: 34-44.
- Deguillaume, L., Leriche, M., Desboeufs, K., Mailhot, G., George, C. and Chaumerliac, N., 2005. Transition metals in atmospheric liquid phases: Sources, reactivity, and sensitive parameters. *Chemical Reviews*, 105(9): 3388-3431.
- Desboeufs, K.V., Sofikitis, A., Losno, R., Colin, J.L. and Ausset, P., 2005. Dissolution and solubility of trace metals from natural and anthropogenic aerosol particulate matter. *Chemosphere*, 58(2): 195-203.
- Duce, R.A. and Tindale, N.W., 1991. Atmospheric transport of iron and its deposition in the ocean. *Limnol. Oceanogr.*, 36: 1715-1726.
- Falkowski, P.G., 1997. Evolution of the nitrogen cycle and its influence on the biological sequestration of CO2 in the ocean. *387(6630)*: 272-275.
- Fischer, A.C., Kroon, J.J., Verburg, T.G., Teunissen, T. and Wolterbeek, H.T., 2007. On the relevance of iron adsorption to container materials in small-volume experiments on iron marine chemistry: Fe-55-aided assessment of capacity, affinity and kinetics. *Marine Chemistry*, 107(4): 533-546.
- Fung, I.Y., Meyn, S.K., Tegen, I., Doney, S.C., John, J. and Bishop, J., 2000. Iron supply and demand in the upper ocean (vol 14, pg 281, 2000). *Global Biogeochemical Cycles*, 14(2): 697-700.

- Gao, Y., Kaufman, Y.J., Tanre, D., Kolber, D. and Falkowski, P.G., 2001. Seasonal distributions of aeolian iron fluxes to the global ocean. *Geophysical Research Letters*, 28(1): 29-32.
- Geider, R.J. and LaRoche, J., 1994. *Photosynth. Res.*, 39: 275-301.
- Glaccum, R.A. and Prospero, J.M., 1980. Saharan Aerosols over the Tropical North-Atlantic - Mineralogy. *Marine Geology*, 37(3-4): 295-321.
- Gledhill, M. and van den Berg, C.M.G., 1994. Determination of complexation of iron (III) with natural organic complexing ligands in seawater using cathodic stripping voltammetry. *Marine Chemistry*, 47: 41-54.
- Gledhill, M. and Vandenberg, C.M.G., 1995. Measurement of the Redox Speciation of Iron in Seawater by Catalytic Cathodic Stripping Voltammetry. *Marine Chemistry*, 50(1-4): 51-61.
- Graedel, T.E., Weschler, C.J. and Mandich, M.L., 1985. Influence of transition metal complexes on atmospheric droplet acidity. *Nature*, 317: 240-242
- Guieu, C., Duce, R. and Arimoto, R., 1994. Dissolved Input of Manganese to the Ocean - Aerosol Source. *Journal of Geophysical Research-Atmospheres*, 99(D9): 18789-18800.
- Hand, J.L., Mahowald, N.M., Chen, Y., Siefert, R.L., Luo, C., Subramaniam, A. and Fung, I., 2004. Estimates of atmospheric-processed soluble iron from observations and a global mineral aerosol model: Biogeochemical implications. *Journal of Geophysical Research-Atmospheres*, 109(D17).
- Haygood, M.G. and Holt, P.D., 1993. Aerobactin production by a planktonic marine *Vibrio* sp. *Limnology and Oceanography*, 38(5): 1091-1097.
- Herut, B., Collier, R. and Krom, M.D., 2002. The role of dust in supplying nitrogen and phosphorus to the Southeast Mediterranean. *Limnology and Oceanography*, 47(3): 870-878.
- Honeyman, B.D. and Santschi, P.H., 1988. Metals in Aquatic Systems. *Environmental Science & Technology*, 22(8): 862-871.
- Hong, H. and Kester, D.R., 1986. Redox state of iron in the offshore waters of Peru. *Limnology and Oceanography*, 31(3): 512-524.
- Horsburgh, M.J., Wharton, S.J., Karavolos, M. and Foster, S.J., 2002. Manganese: elemental defence for a life with oxygen? *Trends in Microbiology*, 10(11): 496-501.
- Hove, M., van Hille, R.P. and Lewis, A.E., 2007. Iron solids formed from oxidation precipitation of ferrous sulfate solutions. *Aiche Journal*, 53: 2569-2577.
- Hove, M., van Hille, R.P. and Lewis, A.E., 2008. Mechanisms of formation of iron precipitates from ferrous solutions at high and low pH. *Chemical Engineering Science*, 63(6): 1626-1635.
- Hutchins, D.A., Witter, A.E., Butler, A. and Luther, G.W., 1999. Competition among marine phytoplankton for different chelated iron species. *Nature*, 400(6747): 858-861.
- Jambor, J.L. and Dutrizac, J.E., 1998. Occurrence and constitution of natural and synthetic ferrihydrite, a widespread iron oxyhydroxide. *Chemical Reviews*, 98(7): 2549-2585.
- Jickells, T.D., An, Z.S., Andersen, K.K., Baker, A.R., Bergametti, G., Brooks, N., Cao, J.J., Boyd, P.W., Duce, R.A., Hunter, K.A., Kawahata, H., Kubilay, N., laRoche, J., Liss, P.S., Mahowald, N., Prospero, J.M., Ridgwell, A.J., Tegen, I. and Torres, R., 2005. Global iron connections between desert dust, ocean biogeochemistry, and climate. *Science*, 308(5718): 67-71.
- Jickells, T.D. and Spokes, L.J., 2001. *The Biogeochemistry of Iron in Seawater*.

- Jickells, T.D.a.S., L.J., 2001. Atmospheric Iron Inputs to the Oceans in The Biogeochemistry of Iron in Seawater 85-121. SCOR/IUPAC. J. Wiley.
- Johnson, K.S., Chavez, F.P., Elrod, V.A., Fitzwater, S.E., Pennington, J.T., Buck, K.R. and Walz, P.M., 2001. The annual cycle of iron and the biological response in central California coastal waters. *Geophysical Research Letters*, 28(7): 1247-1250.
- Johnson, K.S., Coale, K.H., Elrod, V.A. and Tindale, N.W., 1994. Iron photochemistry in seawater from the Equatorial Pacific. *Marine Chemistry*, 46: 319-334.
- Journet, E., Desboeufs, K.V., Caquineau, S. and Colin, J.L., 2008. Mineralogy as a critical factor of dust iron solubility. *Geophysical Research Letters*, 35(7).
- Kernen, N., Kidd, M.J., Penner-Hahn, J.E. and Pakrasi, H.B., 2002. A light-dependent mechanism for massive accumulation of manganese in the photosynthetic bacterium *Synechocystis* sp. PCC 6803. *Biochemistry*, 41(50): 15085-15092.
- Kessick, M.A. and Morgan, J.J., 1975. Mechanism of Autoxidation of Manganese in Aqueous-Solution. *Environmental Science & Technology*, 9(2): 157-159.
- Kirchman, D.L., Meon, B., Cottrell, M.T., Hutchins, D.A., Weeks, D. and Bruland, K.W., 2000. Carbon versus iron limitation of bacterial growth in the California upwelling regime. *Limnology and Oceanography*, 45(8): 1681-1688.
- Koçak, M., Kubilay, N., Herut, B. and Nimmo, M., 2007. Trace metal solid state speciation in aerosols of the Northern Levantine Basin, East Mediterranean. *Journal of Atmospheric Chemistry*, 56: 239-257.
- Koretsky, C.M., Sverjensky, D.A., Salisbury, J.W. and Daria, D.M., 1997. Detection of surface hydroxyl species on quartz, gamma-alumina, and feldspars using diffuse reflectance infrared spectroscopy. *Geochimica Et Cosmochimica Acta*, 61(11): 2193-2210.
- Kraemer, S.M., 2004. Iron oxide dissolution and solubility in the presence of siderophores. *Aquatic Sciences*, 66(1): 3-18.
- Lampitt, R.S., Achterberg, E.P., Anderson, T.R., Hughes, J.A., Iglesias-Rodriguez, M.D., Kelly-Gerreyn, B.A., Lucas, M., Popova, E.E., Sanders, R., Shepherd, J.G., Smythe-Wright, D. and Yool, A., 2008. Ocean fertilization: a potential means of geoengineering?, pp. 3919-3945.
- Liu, X.W. and Millero, F.J., 1999. The solubility of iron hydroxide in sodium chloride solutions. *Geochimica Et Cosmochimica Acta*, 63(19-20): 3487-3497.
- Lohan, M.C., Aguilar-Islas, A.M. and Bruland, K.W., 2006. Direct determination of iron in acidified (pH 1.7) seawater samples by flow injection analysis with catalytic spectrophotometric detection: Application and intercomparison. *Limnology and Oceanography-Methods*, 4: 164-171.
- Lohan, M.C., Aguilar-Islas, A.M., Franks, R.P. and Bruland, K.W., 2005. Determination of iron and copper in seawater at pH 1.7 with a new commercially available chelating resin, NTA Superflow. *Analytica Chimica Acta*, 530(1): 121-129.
- Loye-Pilot, M., D., Martin M., Morelli J., 1986. influence of the saharan dust on the rain acidity. *Nature*(321): 427-428.
- Mackie, D.S., Boyd, P.W., Hunter, K.A. and McTainsh, G.H., 2005. Simulating the cloud processing of iron in Australian dust: pH and dust concentration. *Geophysical Research Letters*, 32(6).
- Mahowald, N., 1999. Dust sources and deposition during the last glacial maximum and current climate: a comparison of model results with paleodata from ice cores and marine sediments. *J. Geophys. Res.*, 104: 15895-15916.

- Mahowald, N.M., Baker, A.R., Bergametti, G., Brooks, N., Duce, R.A., Jickells, T.D., Kubilay, N., Prospero, J.M. and Tegen, I., 2005. Atmospheric global dust cycle and iron inputs to the ocean. *Global Biogeochemical Cycles*, 19(4).
- Maldonado, M.T. and Price, N.M., 1996. Influence of N substrate on Fe requirements of marine centric diatoms. *Marine Ecology-Progress Series*, 141(1-3): 161-172.
- Maldonado, M.T. and Price, N.M., 1999. Utilization of iron bound to strong organic ligands by plankton communities in the subarctic Pacific Ocean. *Deep-Sea Research II*, 46: 2447-2473.
- Martin, J.H., 1990. Glacial-interglacial CO<sub>2</sub> change; the iron hypothesis. *Paleoceanography*, 5: 1-13.
- Martin, J.H., 1994. Testing the iron hypothesis in ecosystems of the equatorial Pacific Ocean. *Nature*, 371: 123-129.
- Martin, J.H. and Fitzwater, S.E., 1988. Iron deficiency limits phytoplankton growth in the north-east Pacific subarctic. *Nature*, 331: 341-343.
- Martin, J.H., Gordon, R.M., Fitzwater, S. and Broenkow, W.W., 1989. Vertex: phytoplankton/iron studies in the Gulf of Alaska. *Deep Sea Res.*, 36: 649-680.
- Measures, C.I., Yuan, J. and Resing, J.A., 1995. Determination of Iron in Seawater by Flow Injection-Analysis Using in-Line Preconcentration and Spectrophotometric Detection. *Marine Chemistry*, 50(1-4): 3-12.
- Mehra, O.P., Jackson, M.L., 1960. Iron oxide removal from soils and clays by a dithionite-citrate system buffered with sodium bicarbonate, Seventh National Conference on Clays and clay minerals S.N.
- Mendez, J., Guieu, Cecile, and Adkins, Jess, 2008. Atmospheric input of manganese and iron next term to the ocean: Seawater dissolution experiments with Saharan and North American dusts. *Marine Chemistry*.
- Millero, F.J., 1998. Solubility of Fe(III) in seawater. *Earth and Planetary Science Letters*, 154(1-4): 323-329.
- Mills, M.M., Ridame, C., Davey, M., La Roche, J. and Geider, R.J., 2005. Iron and phosphorus co-limit nitrogen fixation in the eastern tropical North Atlantic. 435(7039): 232.
- Moffett, J.W., 2001. Chapter 8. Transformations among different forms of iron in the ocean. In: Turner D.R. and Hunter K.A. (Editor), *The biogeochemistry of iron in seawater*. Wiley J. and Sons, Ltd, Baltimore, pp. 343-372.
- Morel, F.M.M., 1994. *Nature*, 369: 740-742.
- Morel, F.M.M. and Hering, J.G., 1993. *Principles and Applications of Aquatic Chemistry*. John Wiley & Sons, Inc., New York.
- O'Sullivan, D.W., Hanson, A.K., Miller, W.L. and Kester, D.R., 1991. Measurement of Fe(II) in surface water of the equatorial Pacific. *Limnology and Oceanography*, 36(8): 1727-1741.
- Pehkonen, S.O., Siefert, R., Erel, Y., Webb, S. and Hoffmann, M.R., 1993. Photoreduction of Iron Oxyhydroxides in the Presence of Important Atmospheric Organic-Compounds. *Environmental Science & Technology*, 27(10): 2056-2062.
- Planquette, H., Statham, P.J., Fones, G.R., Charette, M.A., Moore, C.M., Salter, I., Nedelec, F.H., Taylor, S.L., French, M., Baker, A.R., Mahowald, N. and Jickells, T.D., 2007. Dissolved iron in the vicinity of the Crozet Islands, Southern Ocean. *Deep-Sea Research Part II-Topical Studies in Oceanography*, 54(18-20): 1999-2019.

- Pomeroy, L.R., Sheldon, J.E., Sheldon, W.M. and Peters, F., 1995. Limits to Growth and Respiration of Bacterioplankton in the Gulf-of-Mexico. *Marine Ecology-Progress Series*, 117(1-3): 259-268.
- Poulton, S.W. and Canfield, D.E., 2005. Development of a sequential extraction procedure for iron: implications for iron partitioning in continentally derived particulates. *Chemical Geology*, 214(3-4): 209-221.
- Pruppacher, H.R. and Jaenicke, R., 1995. The Processing of Water-Vapor and Aerosols by Atmospheric Clouds, a Global Estimate. *Atmospheric Research*, 38(1-4): 283-295.
- Rackebandt, S., 2009. Manganese depletion by phytoplankton: a model study, IBIT - Universitätsbibliothek, Oldenburg.
- Ridame, C. and Guieu, C., 2002. Saharan input of phosphate to the oligotrophic water of the open western Mediterranean Sea. *Limnology and Oceanography*, 47(3): 856-869.
- Rosenfeld, D., Rudich, Y. and Lahav, R., 2001. Desert dust suppressing precipitation: A possible desertification feedback loop. *Proceedings of the National Academy of Sciences of the United States of America*, 98(11): 5975-5980.
- Rue, E.L. and Bruland, K.W., 1995. Complexation of Iron(II) by Natural Organic-Ligands in the Central North Pacific as Determined by a New Competitive Ligand Equilibration Adsorptive Cathodic Stripping Voltammetric Method. *Marine Chemistry*, 50(1-4): 117-138.
- Schwertmann, U., Friedl, J. and Stanjek, H., 1999. From Fe(III) ions to ferrihydrite and then to hematite. *Journal of Colloid and Interface Science*, 209(1): 215-223.
- Schwertmann, U. and Murad, E., 1983. Effect of Ph on the Formation of Goethite and Hematite from Ferrihydrite. *Clays and Clay Minerals*, 31(4): 277-284.
- Sedwick, P.N., Sholkovitz, E.R. and Church, T.M., 2007. Impact of anthropogenic combustion emissions on the fractional solubility of aerosol iron: Evidence from the Sargasso Sea. *Geochemistry Geophysics Geosystems*, 8(10): 1-21.
- Seguret, M., 2009. Dissolution of aerosol Fe in seawater with FI-CL, university of plymouth, Plymouth.
- Shi, T., Sun, Y. and Falkowski, P.G., 2007. Effects of iron limitation on the expression of metabolic genes in the marine cyanobacterium *Trichodesmium erythraeum* IMS101. *Environmental Microbiology*, 9(12): 2945-2956.
- Shi, Z., Krom, M.D., Bonneville, S., Baker, A.R., Jickells, T.D. and Benning, L.G., 2009. Formation of Iron Nanoparticles and Increase in Iron Reactivity in Mineral Dust during Simulated Cloud Processing. *Environmental Science & Technology*, 43(17): 6592-6596.
- Shiller, A.M., 1997. Manganese in surface waters of the Atlantic Ocean. *Geophysical Research Letters*, 24(12): 1495-1498.
- Siefert, R.L., Johansen, A.M. and Hoffmann, M.R., 1999. Chemical characterization of ambient aerosol collected during the southwest monsoon and intermonsoon seasons over the Arabian Sea: Labile-Fe(II) and other trace metals. *Journal of Geophysical Research-Atmospheres*, 104(D3): 3511-3526.
- Sohm, J.A. and Capone, D.G., 2006. Phosphorus dynamics of the tropical and subtropical North Atlantic: *Trichodesmium* spp. versus bulk plankton. *Marine Ecology-Progress Series*, 317: 21-28.
- Sohm, J.A., Mahaffey, C. and Capone, D.G., 2008. Assessment of relative phosphorus limitation of *Trichodesmium* spp. in the North Pacific, North Atlantic, and the north coast of Australia. *Limnology and Oceanography*, 53(6): 2495-2502.

- Spokes, L.J. and Jickells, T., 1996. Factors controlling the solubility of aerosol trace metals in the atmosphere and on mixing into seawater *Aquatic Geochemistry*, Volume 1(Number 4 ): 355-374.
- Spokes, L.J., Jickells, T.D. and Lim, B., 1994. Solubilization of Aerosol Trace-Metals by Cloud Processing - a Laboratory Study. *Geochimica Et Cosmochimica Acta*, 58(15): 3281-3287.
- Statham, P.J. and Burton, J.D., 1986. Dissolved manganese in the North Atlantic Ocean, 0-35°N. *Earth and Planetary Science Letters*, 79(1-2): 55-65.
- Statham, P.J. and Chester, R., 1988. Dissolution of Manganese from Marine Atmospheric Particulates into Seawater and Rainwater. *Geochimica Et Cosmochimica Acta*, 52(10): 2433-2437.
- Stumm, W. and Morgan, J.J., 1981. *Aquatic Chemistry*.
- Stumm, W. and Morgan, J.J., 1996. *Aquatic Chemistry*. Wiley-Interscience, New York.
- Stumm, W. and Sulzberger, B., 1992. The Cycling of Iron in Natural Environments - Considerations Based on Laboratory Studies of Heterogeneous Redox Processes. *Geochimica Et Cosmochimica Acta*, 56(8): 3233-3257.
- Stuut, J.-B., Smalley, I. and O'Hara-Dhand, K., 2009. Aeolian dust in Europe: African sources and European deposits. *Quaternary International*, 198(1-2): 234-245.
- Sulzberger, B. and Laubscher, H., 1995. Reactivity of Various Types of Iron(Iii) (Hydr)Oxides Towards Light-Induced Dissolution. *Marine Chemistry*, 50(1-4): 103-115.
- Sulzberger, B., Suter, D., Siffert, C., Banwart, S. and Stumm, W., 1989. Dissolution of Fe(Iii)(Hydr)Oxides in Natural-Waters - Laboratory Assessment on the Kinetics Controlled by Surface Coordination. *Marine Chemistry*, 28(1-3): 127-144.
- Sunda, W. and Huntsman, S., 2003. Effect of pH, light, and temperature on Fe-EDTA chelation and Fe hydrolysis in seawater. *Marine Chemistry*, 84(1-2): 35-47.
- Sunda, W.G. and Huntsman, S.A., 1997. Interrelated influence of iron, light and cell size on marine phytoplankton growth. *Nature*, 390(6658): 389-392.
- Sunda, W.G., Huntsman, S.A. and Harvey, G.R., 1993. Photo-Reduction of Manganese Oxides in Seawater and Its Geochemical and Biological Implications. *Nature*, 301(5897): 234-236.
- Suter, D., Banwart, S. and Stumm, W., 1991. Dissolution of Hydrous Iron(Iii) Oxides by Reductive Mechanisms. *Langmuir*, 7(4): 809-813.
- Timmermans, K.R., Gerringa, L.J.A., de Baar, H.J.W., van der Wagt, B., Veldhuis, M.J.W., de Jong, J.T.M., Croot, P.L. and Boye, M., 2001a. Growth rates of large and small Southern Ocean diatoms in relation to availability of iron in natural seawater. *Limnology and Oceanography*, 46(2): 260-266.
- Turner, D. and Hunter, K., 2001. *The Biogeochemistry of Iron in Seawater*. Series on Analytical and Physical Chemistry of Environmental Systems, 396 pp.
- Tyrrell, T., 1999. The relative influences of nitrogen and phosphorus on oceanic primary production. *Nature*, 400(6744): 525-531.
- Usher, C.R., Michel, A.E. and Grassian, V.H., 2003. Reactions on mineral dust. *Chemical Reviews*, 103(12): 4883-4939.
- Van den Berg, C.M.G., 1995. Evidence for Organic Complexation of Iron in Seawater. *Marine Chemistry*, 50(1-4): 139-157.
- Van Wambeke, F., Christaki, U., Giannokourou, A., Moutin, T. and Souvemerzoglou, K., 2002. Longitudinal and vertical trends of bacterial limitation by phosphorus and carbon in the Mediterranean Sea. *Microbial Ecology*, 43(1): 119-133.

- Waite, T.D., 2001. Chapter 7: Thermodynamics of the iron system in seawater. In: Turner D.R. and Hunter K.A. (Editor), *The biogeochemistry of iron in seawater*. Wiley J. and Sons, Ltd, Baltimore, pp. 291-342.
- Warneck, P., 1999. The relative importance of various pathways for the oxidation of sulfur dioxide and nitrogen dioxide in sunlit continental fair weather clouds. *Physical Chemistry Chemical Physics*, 1(24): 5471-5483.
- Wells, M.L. and Mayer, L.M., 1991. The Photoconversion of Colloidal Iron Oxyhydroxides in Seawater. *Deep-Sea Research Part a-Oceanographic Research Papers*, 38(11): 1379-1395.
- Wu, J. and Luther, G.W., 1995. Complexation of Fe(III) by natural organic ligands in the Northwest Atlantic Ocean by a competitive ligand equilibration method and a kinetic approach. *Mar. Chem.*, 50: 159-178.
- Wu, J., Rember, R. and Cahill, C., 2007. Dissolution of aerosol iron in the surface waters of the North Pacific and North Atlantic oceans as determined by a semicontinuous flow-through reactor method. *Global Biogeochemical Cycles*, 21.
- Wu, J.F., Boyle, E., Sunda, W. and Wen, L.S., 2001. Soluble and colloidal iron in the oligotrophic North Atlantic and North Pacific. *Science*, 293(5531): 847-849.
- Zhu, X., Prospero, J.M., Savoie, D.L., Millero, F.J., Zika, R.G. and Saltzman, E.S., 1993. Photoreduction of Iron(III) in Marine Mineral Aerosol Solutions. *Journal of Geophysical Research-Atmospheres*, 98(D5): 9039-9046.
- Zhu, X.R., Prospero, J.M. and Millero, F.J., 1997. Diel variability of soluble Fe (II) and soluble total Fe in North African dust in the trade winds at Barbados. *Journal of Geophysical Research*, 102(D17): 21,297-21,305.
- Zhu, X.R., Prospero, J.M., Millero, F.J., Savoie, D.L. and Brass, G.W., 1992. The Solubility of Ferric Ion in Marine Mineral Aerosol Solutions at Ambient Relative Humidities. *Marine Chemistry*, 38(1-2): 91-107.
- Zhuang, G.S., Yi, Z., Duce, R.A. and Brown, P.R., 1992. Link between Iron and Sulfur Cycles Suggested by Detection of Fe(II) in Remote Marine Aerosols. *Nature*, 355(6360): 537-539.
- Zinder, B., Furrer, G. and Stumm, W., 1986. The Coordination Chemistry of Weathering .2. Dissolution of Fe(III) Oxides. *Geochimica Et Cosmochimica Acta*, 50(9): 1861-1869.
- Zuo, Y.G. and Hoigne, J., 1994. Photochemical Decomposition of Oxalic, Glyoxalic and Pyruvic-Acid Catalyzed by Iron in Atmospheric Waters. *Atmospheric Environment*, 28(7): 1231-1239.
- Zuo, Y.G. and Hoigne, J., 1992. Formation of Hydrogen-Peroxide and Depletion of Oxalic-Acid in Atmospheric Water by Photolysis of Iron(III) Oxalato Complexes. *Environmental Science & Technology*, 26(5): 1014-1022.

